Dissertation

Physiological importance of phospholipid biogenesis in *Toxoplasma gondii*

zur Erlangung des akademischen Grades
doctor rerum naturalium
(Dr. rer. nat.)
im Fach Biologie

eingereicht an der

Lebenswissenschaftlichen Fakultät
der Humboldt-Universität zu Berlin

von

M. Sc. Bingjian Ren

Präsidentin der Humboldt-Universität zu Berlin
Prof. Dr.-Ing. Dr. Sabine Kunst

Dekan der Lebenswissenschaftlichen Fakultät
Prof. Dr. Bernhard Grimm

Gutachter: 1. PD. Dr. Nishith Gupta
2. Prof. a. D. Dr. Richard Lucius
3. Prof. Dr. Jos Brouwers

eingereicht am: 02.08.2019

Datum der mündlichen Verteidigung: 24.10.2019

Abstract

Toxoplasma gondii is an obligate intracellular parasite that causes Toxoplasmosis in human and livestock. Phospholipid biosynthesis is crucial for the successful intracellular survival and replication of the parasites, as the phospholipids have important roles in the biogenesis of membrane organelles, signal transduction and other cellular processes. Here, we dissected the physiological importance of two pathways accounting for the synthesis of PtdEtn and PtdIns.

We demonstrated the presence of a novel PtdIns synthase (PIS) in *T.gondii* termed *Tg*PIS, expressing a functional enzyme with a catalytically vital CDP-alcohol phosphotransferase motif, which resides exclusively in the Golgi body. The parasite imports *myo*-inositol from milieu, and co-utilizes *de novo*-synthesized CDP-diacylglycerol to produce PtdIns. An auxin-inducible conditional repression of *Tg*PIS abrogated the lytic cycle of the parasite in mammalian cells due to defects in the replication, motility and egress. Lipidomic profiling of the PIS mutant demonstrated selective reduction of certain PtdIns and PtdThr species, whereas selected PtdGro, PtdSer and BMP species were increased, which suggested a tight inter-regulation and homeostasis of anionic phospholipids to maintain the membrane integrity.

In addition, we identified an ethanolamine cytidyltransferase (*Tg*ECT), the rate-limiting enzyme of Kennedy pathway, which is localized in the cytosol. The enzyme is clearly essential for the lytic cycle as its genetic ablation was not feasible, and auxin-meditated conditional knockdown severely impaired the parasite growth in plaque assays. Similarly, lipidomic analysis of the mutant identified an important role in the biogenesis of selected species of PtdEtn, PtdSer and PtdThr. Moreover, we discovered that *Tg*ECT is required for the generation of ethanolamine-phosphory ceramide (EPC), a rare sphingolipid present only a limited number of organisms. Our further work indicated the presence of an insect-like EPC synthase in the parasite which remains to be characterized.

Keyword: Apicomplexan, Toxoplasma, Phospholipid

Zusammenfassung

Toxoplasma gondii ist ein obligater intrazellulärer Parasit, der bei Menschen und Nutztieren Toxoplasmose verursacht. Die Phospholipid-Biosynthese ist entscheidend für das erfolgreiche intrazelluläre Überleben und die Replikation des Parasiten, da sie eine wichtige Rolle bei der Biogenese von Membranorganellen, der Signal- transduktion und anderen zellulären Prozessen spielt. Hier untersuchten wir die physiologische Bedeutung von zwei Synthesewegen, die für PtdEtn und PtdIns verantwortlich sind.

Wir zeigen das Vorhandensein einer neuartigen PtdIns-Synthase (PIS) in *T. gondii*, die als *Tg*PIS bezeichnet wird und ein funktionelles Enzym mit einem katalytisch wichtigen CDP-Alkohol-Phosphotransferase-Motiv codiert, das sich ausschließlich im Golgi-Apparat befindet. Der Parasit importiert Myoinosit aus dem Milieu und verwendet es zusammen mit de novo synthetisiertem CDP-Diacylglycerin, um PtdIns zu produzieren. Eine durch Auxin induzierbare bedingte Unterdrückung von *Tg*PIS schaltet den Lysezyklus des Parasiten aufgrund von Defekten in der Replikation, Motilität und Austritt in Säugetierzellen aus. Das Lipidom-Profiling der PIS-Mutante zeigt eine selektive Reduktion bestimmter PtdIns- und PtdThr-Spezies, wohingegen ausgewählte PtdGro-, PtdSer- und BMP-Spezies erhöht sind, was auf eine enge Interregulation und Homöostase von anionischen Phospholipiden zur Aufrechterhaltung der Membranintegrität hindeutet. Zusätzlich identifizierten wir eine Ethanolamin-Cytidyltransferase (*Tg*ECT), das geschwindigkeitsbestimmende Enzym des Kennedy-Signalwegs, das im Cytosol lokalisiert ist. Das Enzym ist eindeutig für den Lysezyklus essentiell, da seine genetische Ablation nicht durchführbar ist und der durch Auxin meditierte bedingte Abbau des Proteins das Parasitenwachstum in Plaqueassays stark beeinträchtigt. Die Lipidomanalyse der Mutante identifizierte eine wichtige Rolle bei der Biogenese ausgewählter Arten von PtdEtn, PtdSer und PtdThr. Darüber hinaus haben wir festgestellt, dass *Tg*ECT für die Erzeugung von Ethanolamin-Phosphor-Ceramid (EPC) erforderlich ist, einem seltenen Sphingolipid, das nur eine begrenzte Anzahl von Organismen enthalten. Unsere weitere Arbeit wies auf das Vorhandensein einer insektenähnlichen EPC-Synthase im Parasiten hin, die noch charakterisiert werden muss.

Schlüsselwörter: Apikomplexan,Toxoplasma, Phospholipid

Figure Content

List of Abbreviations

Phospholipid and other metabolics	
CDP-DAG	cytidine diphosphate-diacylglycerol
CL	cardiolipin
DAG	diacylglycerol
EPC	ethanolamine phosphorylceramide
Glyecerol-3P	glycerol 3-phosphate
GPI	glycosylphosphatidylinositol
IPC	inositol phosphorylceramide
Lyso-PtdOH	lysophosphatidic acid
PIP	phosphatidylinositol phosphate
PtdCho	phosphatidylcholine
PtdEtn	phosphatidylethanolamine
PtdGro	phosphatidylglycerol
PtdOH	phosphatidic acid
PtdIns	phosphatidylinositol
PtdSer	phosphatidylserine
PtdThr	phosphatidylthreonine
SM	sphingomyelin

Enzymes in carbon or phospholipid metabolism	
ACS	acetyl-CoA synthase
CDS	cytidine diphosphate-diacylglycerol synthase
CK	choline kinase
CCT	choline cytidylyltransferase
CPT	choline phosphotransferase
DGK	diacylglycerol kinase
EK	ethanolamine kinase
ECT	ethanolamine cytidylyltransferase
EPT	ethanolamine phosphotransferase
EPCS	ethanolamine phosphorylceramide synthase

Subcellular structure and localization markers	
DG	dense granule
ER	endoplasmic reticulum
GAP45	glideosome-associated protein 45
GRA1	dense granule protein 1
HSP90	heat shock protein 90
PV	parasitophorous vacuole
SAG1	surface antigen 1
SERCA	sarco/endoplasmic reticulum Ca2+-ATPase

Selection markers/drugs	
DHFRTS	dihydrofolate reductase-thymidylate synthase
FUDR	5-Fluoro-2'-deoxyuridine
HXGPRT	hypoxanthine-xanthine-guanine phosphoribosyltransferase
MPA	mycophenolic acid
UPRT	uracil phosphoribosyltransferase

Buffers and Culture medias	
BSA	bovine serum albumin fraction V
DMEM	Dulbecco's modified eagle media
DMSO	dimethyl sulfoxide
FBS	fetal bovine serum
HBSS	Hank's balanced salt solution
PBS	phosphat buffered saline

Reference genes for qRT-PCR	
EFA	elongation factor A
GT1	glucose transporter 1
TubA	tubulin A

Terms and drugs for genetic manipulation	
aTc	anhydrotetracycline

FAE	fatty acid elongase
FAS	fatty acid synthase
G3PAT	glycerol 3-phosphate acyltransferase
PAP	phosphatidic acid phosphatase
PIS	phosphatidylinositol synthase
PSD	phosphatidylserine decarboxylase
PSS	phosphatidylserine synthase
PTS	phosphatidylthreonine synthase
AID	auxin-induced degron
DD	destabilization domain
GOI	gene of interest
IAA	indole-3-acetic acid

Others

HPLC	high-performance liquid chromatography
MS	mass spectrometry

1. Introduction

1.1 Protozoan parasites

1.1.1 Diversity of parasites

The kingdom protozoa comprise more than 40,000 known single-cell extant species, of which about 25,000 occur as free-living, while the remaining have adapted to a parasitic lifestyle[1]. The latter group includes at least 6,000 apicomplexan, 2,500 ciliate, 1,800 flagellate, and 250 amoebae species. These eukaryotic pathogens have acquired countless niches dispersed across the tree of life. Just human and livestock alone serve as hosts to a startling number of parasites with many protists among them. Parasites belonging to two phyla, namely apicomplexa and kinetoplastida, account for a majority of infections **(Figure.1)**. *Plasmodium*, *Toxoplasma*, *Eimeria*, *Sarcocystis*, *Cryptosporidium*, *Theileria*, *Babesia*, *Trypanosoma*, *Leishmania* and *Cryptobia* are some of the notorious genera to name but a few. Then there are many other rather unappreciated genera, whose recognition is limited merely to the taxonomy books[2]. Collectively, all these parasites impose a significant burden on human and animal healthcare as well as on food industry. Not only do they affect the infected hosts by altering growth, behavior, nutritional status, reproductive abilities and mortality, but also shape our ecosystem by swaying trophic interactions, food webs and biodiversity[3,4].

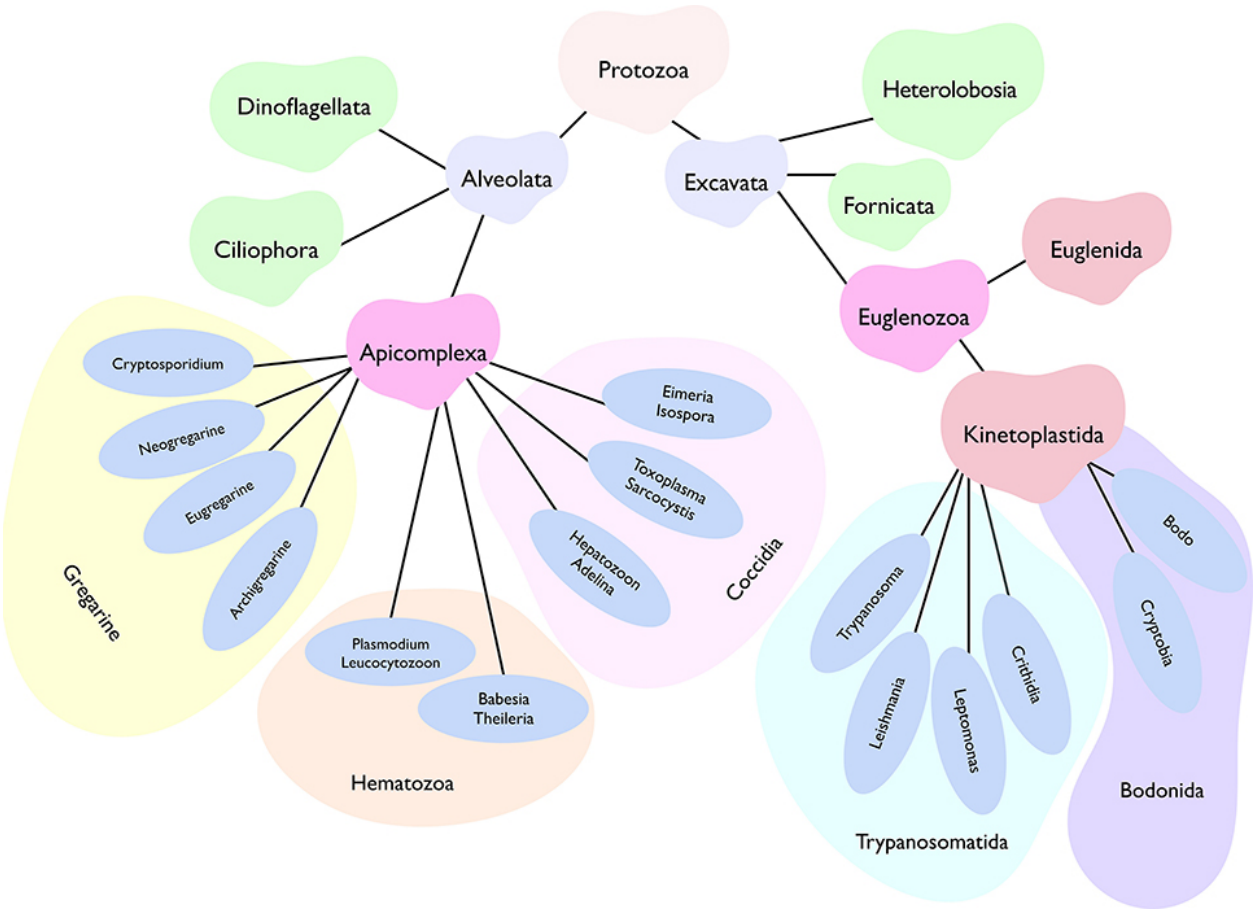

Figure.1: Abridged phylogenetic tree depicting main super-phyla of the kingdom protozoa, namely alveolata and excavata. Two of the all shown phyla, apicomplexa, and kinetoplastida, comprise a vast majority of human and animal pathogens. Only the selected genera representing each class are displayed. While most apicomplexans (except for gregarines) favor an intracellular lifestyle, kinetoplastids prefer an extracellular life (barring certain stages of *T. cruzi* and *Leishmania*). Besides, apicomplexan parasites exhibit well-defined asexual as well as sexual reproduction, whereas the latter phase is not yet known in most kinetoplastids. Individual genera or even species have evolved a notably distinct lifecycle in specific host organisms, which often involves a perpetual inter-host transmission in nature.

Because of the clinical, socioeconomic, and ecological relevance, some species of parasite have caught more interest than the rest. For example, *Toxoplasma* and *Plasmodium* that belong to phylum apicomplexa, have witnessed a rapid research advancement, particularly in the last two decades[5-8].

From a technological perspective, parasites can be categorized into either model or non-model parasites. There are well-studied genera such as *Toxoplasma* or *Plasmoidum.* However, the rest of them have been minimally engineered and studied, despite the fact

that they could provide sufficient complementary biological insights. For instance, *Cryptosporidium* with <4000 genes has a highly abbreviated genome, and inhabits an extra-cytosolic (epicellular) vacuole as opposed to intracellular residence of mainstream apicomplexans[9]. *Eimeria* species completing their lifecycle in one host can illuminate the sexual development of coccidians[10], which remains heavily understudied[11]. Equally, *Sarcocystis* resides freely in the host cytosol[12], *Babesia* mimics many features of cerebral malaria in human[13] and *Theileria* exerts a cancer-like phenotype to infected lymphocytes[14]. These apicomplexans have therefore potential to reveal exclusive developmental aspects[15,16]. This work focused on *T. gondii*, one representative species of the apicomplexan parasites.

1.1.2 *Toxoplasma gondii*

T. gondii is the only known species under genus *Toxoplasma*, which is among the most wide-spread parasites of the phylum apicomplexa. *T. gondii* is seen as one of the most successful pathogens due to its capacity to invade and replicate in almost all warm-blood animals. During its asexual lifecycle in the intermediate host, *T. gondii* can switch between two reversible asexual stages, tachyzoites and bradyzoites, resulting in acute and chronic infections[17,18] **(Figure.2)**, respectively. As the causative parasite of Toxoplasamosis, *T. gondii* imposes a great danger to people whose immune system is weakened or impaired, by causing severe tissue necrosis through fast replication[19]. Further, the chronic infection of *T. gondii* can cause certain behavior changes in infected individuals, sometimes leading to neurological disorders[20].

Tachyzoite stage of *T. gondii* is the most well-studied developmental phase. A typical tachyzoite lytic cycle can be marked by several critical steps: invasion of the host cell, intracellular replication, and egress from the host **(Figure.2)**. Though *T. gondii* does not have flagellum, the parasites developed unique action mode for movement called gliding motility, which is driven by actin/myosin protein. These hallmark steps of the lytic cycle have been adapted for measuring the growth fitness of the parasite in *T. gondii* study.

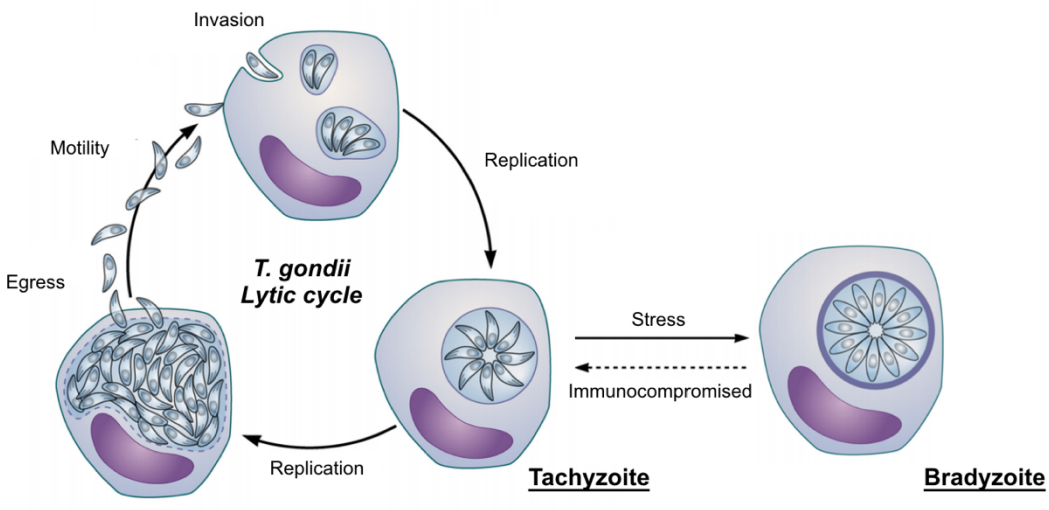

Figure.2: Intracellular reproduction and development of *T. gondii*. A lytic cycle of *T. gondii* tachyzoite consists of four critical steps: invasion, replication, egress and gliding motility, which are used as parameters for evaluating the overall growth fitness of tachyzoites. When facing environmental stress, tachyzoites can quickly develop to bradyzoites which are protected by thick cyst well. When the host becomes immunocompromised, bradyzoite cysts can convert again to fast-proliferation tachyzoites. *The figure is modified from Zhang et.al*[21].

Successful survival and reproduction of *T. gondii* rely on the production of parasitophorous vacuole (PV), which is formed immediately after the invasion of the host cell. The PV is crucial for the follow-up intracellular replication of the parasite. After establishing a suitable inner-environment for its reproduction, *T. gondii* modulates host cell transcriptomes[22], interrupts host signaling pathways[23,24], changes the fate of its host to avoid the apoptosis[23], and evades the immune response[25,26]. In addition, the parasites salvage nutrients from the host and recruit organelles to its PV[27,28]. Though the role of recruited endoplasmic reticulum (ER) and mitochondria is still ambiguous[29], it is assumed that the organelle recruitment is needed for an optimal intracellular replication of the parasite.

1.1.3 Genetic manipulation of *T. gondii*

The genetic manipulation of *T. gondii* is established thanks to a well annotated genome and the discovery of a wide range of selection-markers that can be used for drug selection to make desired mutants[30]. A “parental” strain of *T. gondii* with deleted *ku80* gene has been developed with the enhanced homology recombination, resulting in efficient gene endogenous tagging and deletion[31]. However, the “classical” way **(Figure.3)** of genetic manipulation is limited to certain genetic backgrounds where *ku80* is deleted[31].

In 2014, the state-of-art clustered regularly interspaced short palindromic repeats (CRSIPR) based gene editing was introduced to *T. gondii,* providing an improved strategy for genetic manipulation in the parasite, particularly for strains such as type I GT1 or type III CTG, in which genetic manipulation is hard to achieve due to the activity of *ku80* [32,33]. “CRISPR scissors” create a double strand break (DSB) at the desired locus that can be repaired either by non-homologous end joining (NHEJ) or homology-directed repair (HDR) approaches, which has simplified the gene editing process. In addition, large-scale genomic manipulation by multiple-site editing has become possible by CRISPR.

One remaining challenge for gene editing in *T. gondii* is the manipulation of genes that are crucial for the lytic cycle. A variety of conditional silencing systems have been developed to meet the requirement **(Figure.4)**. The strategies can be classified as conditional manipulation at genome level, at transcription level and at translational level. For the conditional gene deletion at genome level, an improved system based on Cre-loxP has been developed[34]. The DiCre system is based on site-specific recombination using dimerizable Cre-recombinase[35]. Cre catalyses the excision of DNA region by recognition of a 34 bp loxP sequence. Two inactive subunits of Cre, FRB and FKBP are co-expressed in RH strain, loxP-sequences are introduced to the up- and down-stream of genomic region to be deleted. The two splited parts of Cre can be fused by rapamycin, resulting in the reconstitution of functional Cre and the excision of the loxP-marked region. Thus, the

deletion of gene of interest (GOI) will only happen when rapamycin is added to the culture medium.

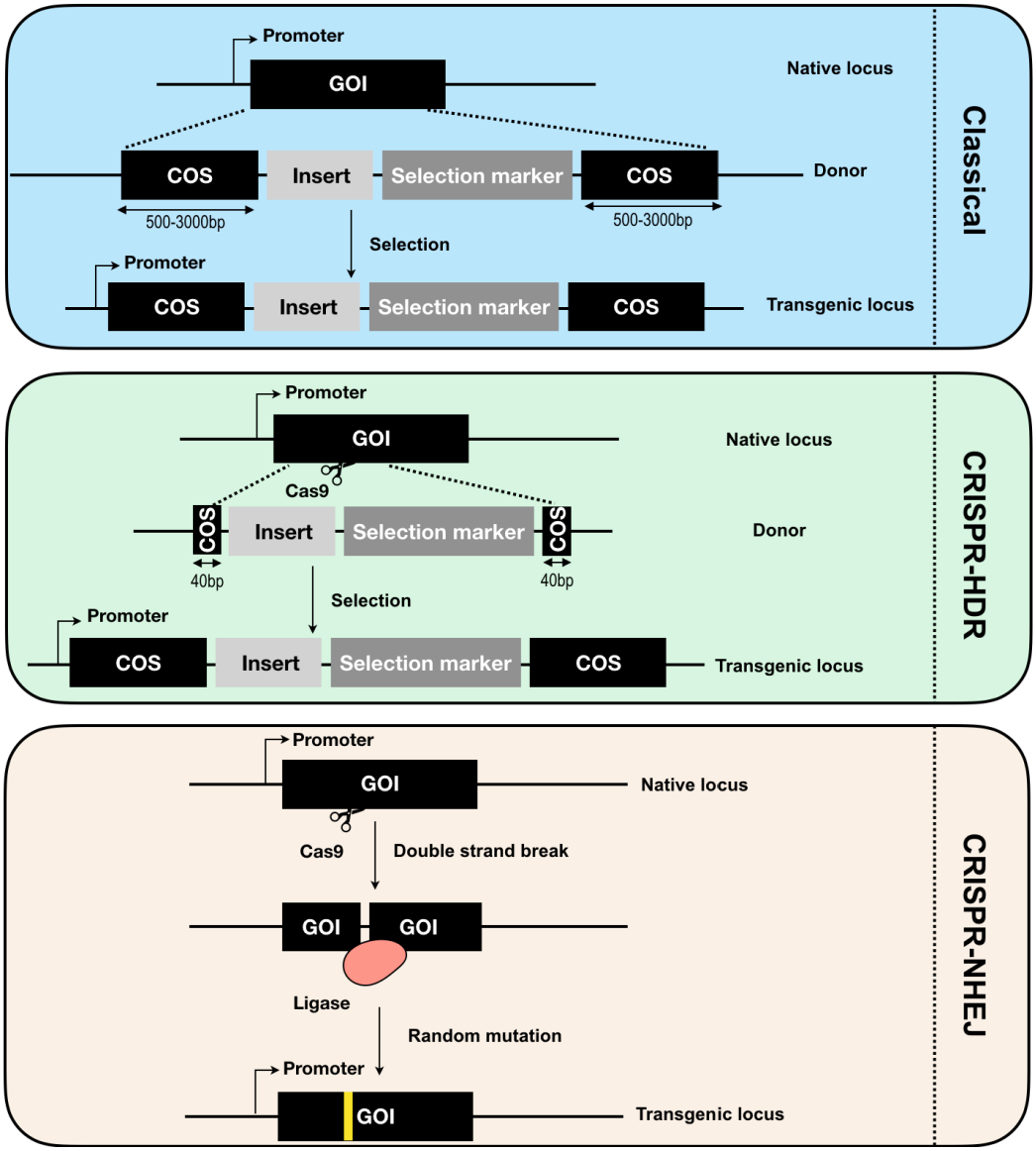

Figure.3: Comparison of classical strategy for genetic manipulation of *T. gondii* with CRISPR-based gene editing tools. Genetic manipulation based on "classical" homology recombination requires at least 500 bp homology arms up and downstream of desired gene of interest (GOI) to drive the gene insertion, while in CRISPR-HDR method the homology arms can be shortened up to 40 bp. The "insert" shown in figure can be an epitope tagging or a functional motif depending on the purpose of gene manipulation. For applications that only aim to interrupt the function of GOI, CRISPR-NHEJ method offers a simplified tool for creating mutant by introducing random mutations at the desired locus thus triggering gene mutagenesis. No donor DNA fragment is supplied in such

cases. *COS: crossover sequence, GOI: gene of interest, NHEJ: non-homologous end joining, HDR: homology-directed repair*

At transcription level, tetracycline-regulated system has been established[36]. By swaping the native promoter of GOI with a tetracycline-regulatable repressor (TetR), the transcription of selected gene can be shut off by the addition of anhydrotetracycline (aTc). The most popular strategies used for making conditional mutants by regulating their protein translation are destabilizing domain (DD) system[37] and auxin-inducible degron (AID) system[38]. In both cases a functional motif (DD or AID) will be inserted to the GOI to enable further operation. The DD motif destabilized the expressed protein to trigger further degradation, which can be reversed by adding ligand Shield1. In contrast, AID motif is required for the formation of a protein complex that can be detected and degraded by proteasome in presence of indole-3-acetic acid (IAA). Development of these conditional systems paves the way for the study focusing on genes that are crucial for the lytic cycle of *T. gondii.*

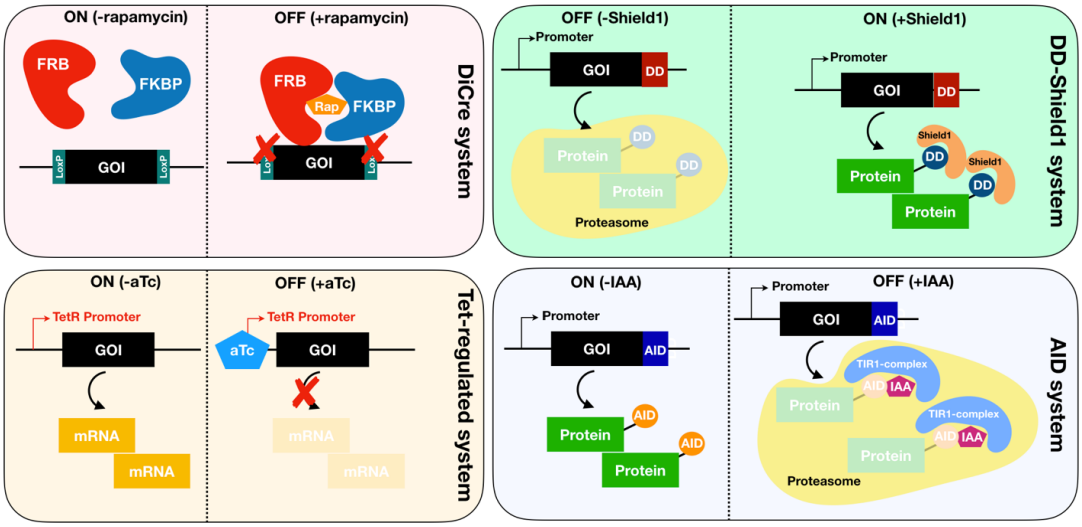

Figure.4: Major conditional gene knockdown systems in *T. gondii.* Functional Cre-recombinase is reconstituted in presence of the ligand rapamycin, resulting in the cleavage of loxP-sites on genome. In tetracycline-regulated system, the promoter region of GOI is replaced by TetR promoter. Addition of aTc leads to transcription repression of mRNA. DD-Shield1 and AID-systems regulate the gene expression at translational level, in both cases functional domain (DD or AID) must be tagged to the GOI. The tagging of DD motif destabilizes target protein. The process can be blocked by addition of Shield1 ligand as a “protector” to the GOI. Auxin-induced degron, however, works the opposite. Ectopic expression of *Tir1* gene is needed to form TIR-1 complex, which could recognize

AID motif in the presence of IAA, leading to the degradation of the tagged protein. *aTc: anhydrotetracycline, AID: auxin-inducible degron, DD: destabilizing domain, IAA: indole-3-acetic acid, GOI: gene of interest.*

1.2 Physiological importance and biogenesis of phospholipid

1.2.1 Phospholipid biogenesis in *T. gondii*

Lipids are essential compounds required for all organisms. Different types of lipid are involved in multiple cellular processes ranging from nutrient supply to signal transduction. In *T. gondii,* the major phospholipids consist of 8 glycerophospholipid classes that could be detected *via* mass spectrometry during the tachyzoite stage of the parasite, including phosphatidic acid (PtdOH), phosphatidylcholine (PtdCho), phosphatidylethanolamine (PtdEtn), phosphatidylinositol (PtdIns), phosphatidylglycerol (PtdGro), phosphatidylserine (PtdSer), phosphatidylthreonine (PtdThr) and cardiolipin (CL) and 2 species of sphingoipid namely sphingomyelin (SM) and ethanolamine phosphorylceramide (EPC)[39].

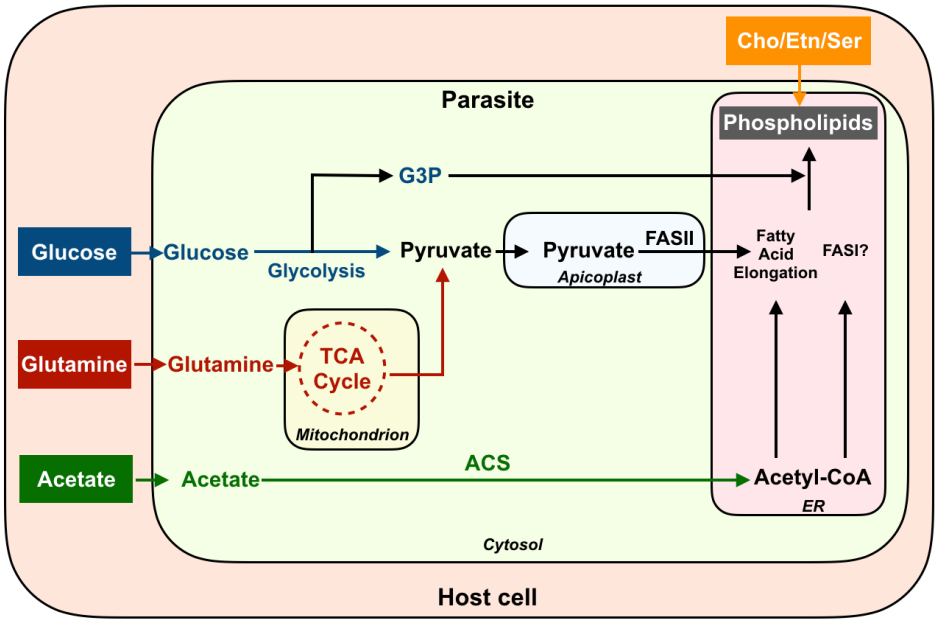

Figure.5: Metabolic cooperation of glucose, glutamine and acetate to facilitate phospholipid synthesis. Glucose and glutamine imported from host cell can be converted to pyruvate through glycolysis or TCA cycle and further used for the fatty acid elongation by FASII dependent pathway, while acetate is used for synthesis of acetyl-CoA and further catalyzed by either elongase or FASI to assemble acyl chain. One important precursor for phospholipid synthesis, G3P, is also produced through glycolysis from glucose. The amino acids used for certain phospholipid synthesis are salvaged from host. *ER: endoplasmatic reticulum, G3P: glycerol-3-phosphate, TCA: tricarboxylic acid, ACS: acetyl-CoA synthase, FAS: fatty acid synthase. Cho: choline, Etn: Ethanolamine, Ser: Serine*. *The figure is modified from Figure 8 in article published by Nitzsche R et. al*[40].

The biogenesis of phospholipid depends on robust carbon metabolism. Glucose, glutamate and acetate[40,41] are three major carbon sources supporting the phospholipid synthesis by formation of the required precursors **(Figure.5)**. Through glycolysis or tricarboxylic acid (TCA) cycle, glucose and glutamate can be converted to pyruvate, and later used for the synthesis of carbon backbone for phospholipid biogenesis. The reaction is catalyzed by type II fatty acid synthase (FASII)[42]. Acetate is used for the synthesis of acetyl-CoA by acetyl-CoA synthase (ACS), further involved in acyl chain assembly in type I fatty acid synthase (FASI) or/and elongase dependent manner[43,44]. The last step for the precursor synthesis is the assembly of PtdOH or lyso-PtdOH by glycerol 3-phosphate acyltransferase (*Tg*G3PAT2)[45] which could further be converted to diacylglycerol (DAG) or cytidine diphosphate diacylglycerol (CDP-DAG), and used to drive the synthesis of phospholipids.

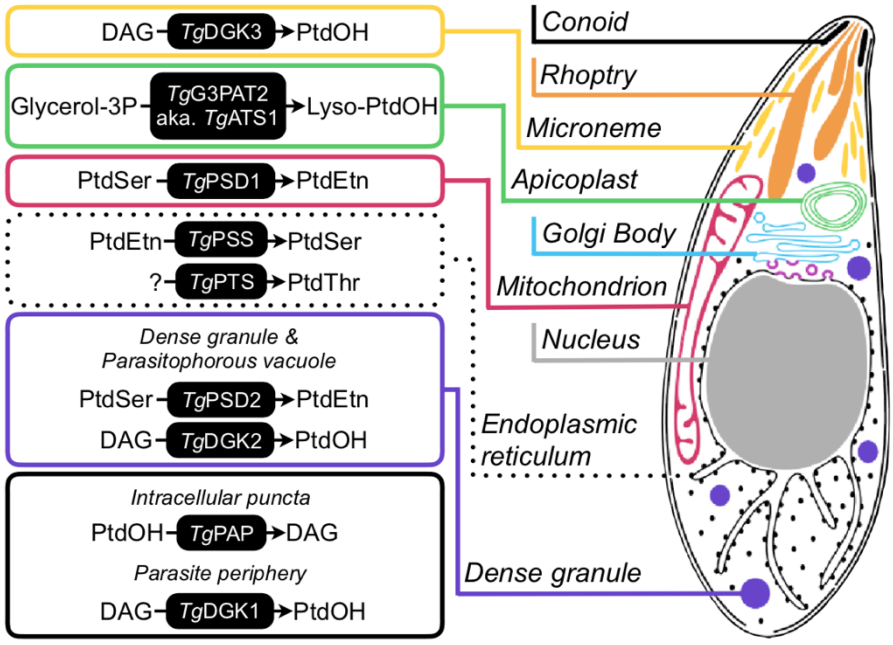

Figure.6: Phospholipid biogenesis with corresponding enzymes identified in *T. gondii*. Enzymes identified from past research that are involved in the synthesis of some major phospholipids (PtdEtn, PtdSer, PtdThr) and their precursors (PtdOH, Lyso-PtdOH, DAG) are shown. *DAG: diacylglycerol, DGK: diacylglycerol kinase, G3PAT/ATS: glycerol 3-phosphate acyltransferase, Glycerol-3P: glycerol 3-phosphate, Lyso-PtdOH: lysophosphatidic acid, PAP: phosphatidic acid phosphatase, PSD: phosphatidylserine decarboxylase, PSS: phosphatidylserine synthase, PtdEtn: phosphatidylethanolamine, PtdOH: phosphatidic acid, PtdSer: phosphatidylserine, PtdThr: phosphatidylthreonine, PTS: phosphatidylthreonine synthase. The figure is obtained from Kong, P (PhD thesis).*

Previous work done by several members of our group have revealed pathways accounting for the biogenesis of several phospholipids **(Figure.6)**. Autonomous synthesis of PtdSer, PtdEtn, and PtdCho has been identified[46] and the *de novo* synthesis of PtdCho has been found likely to be essential[47]. PtdEtn biogenesis was detected as plausible. In addition to the *de novo* synthesis, while PtdSer could contribute as precursor to the synthesis of PtdEtn by PtdSer decarbonxylases (PSDs)[48,49]. Later, it was shown that the synthesis of PtdSer is through a base-exchange type PtdSer synthase (PSS) from PtdEtn[50]. Interestingly, one coccidian specific phospholipid, PtdThr, was found to be synthesized by *T. gondii via* PtdThr synthase (PTS). PtdThr has only been detected in *T. gondii* and *E. falciformis*[39,51], and was shown to be involved in controlling the calcium homeostasis of the parasite[51,52]. It is not known yet what is the precursor used for PtdThr biogenesis.

1.2.2 Physiological importance and biogenesis of PtdEtn

Following PtdCho, PtdEtn is the second abundant glycerophospholipid in eukaryotic cells, while in prokaryotic cells, PtdEtn is the most enriched phospholipid. In most protozoan parasites, PtdEtn comprises 10%-20% of the total lipid phosphorus with an exception of *Plasmodium*, in which a relatively higher content of PtdEtn (35%-45%) can be identified[39,53-56]. PtdEtn is enriched in membrane derived organelles and crucial for several processes, such as membrane fusion, fission, budding or cytokinesis[57] by increasing membrane curvature[58]. The conical shape of the head-group of PtdEtn makes the inner layer of plasma membrane easier for protein binding[59-61]. Moreover, PtdEtn metabolism is required for important cellular processes, such as signaling transduction and autophagy[62].

Synthesis of PtdEtn can occur either *via de novo* synthesis starting from ethanolamine by a three-step reaction termed Kennedy pathway[63] **(Figure.7)**, or *via* decarboxylation of PtdSer[64]. In *T. brucei,* all three enzymes involving in PtdEtn *de novo* synthesis were identified and experimentally tested[65]. Interruption of the three enzymes resulted in several defects, such as changing in mitochondrial morphology, formation of multinucleate cells and impaired growth, suggesting that the Kennedy pathway is required for parasite growth[65,66]. Similar to *T. brucei,* enzymes involving in CDP-ethanolamine branch of Kennedy pathway were also located on the genome of *Leishmania* and *T. cruzi*[67,68]*,* indicating that the occurrence of the *de novo* synthesis of PtdEtn in other kinetoplastid species. The alternative pathway accounting for PtdEtn biogenesis *via* decarboxylation of PtdSer was also identified in kinetoplastids, however, it was reported that in *T. brucei* the reaction was unable to rescue the blocked PtdEtn synthesis *via* Kennedy pathway[69].

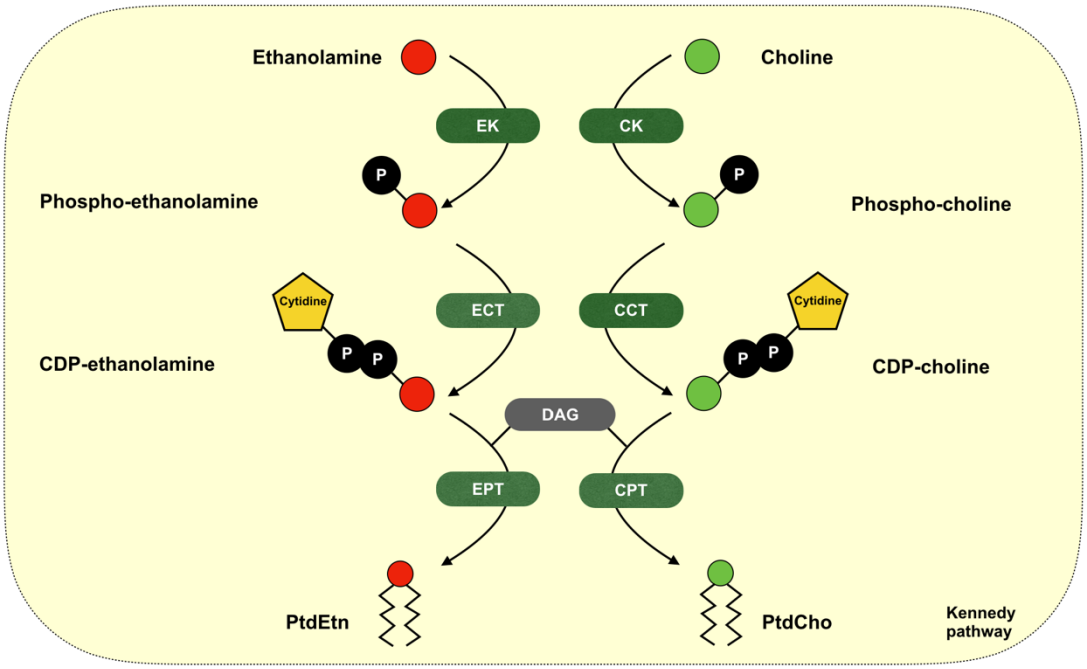

Figure.7: *De novo* synthesis of PtdCho and PtdEtn through Kennedy pathway. The synthesis of PtdCho and PtdEtn starts with ethanolamine or choline in the cytosol, which further gets phosphorylated by EK or CK, and is converted to CDP-ethanolamine or CDP-choline by ECT or CCT. The last step takes place at ER using CDP-choline/ethanolamine and DAG as precursors to produce PtdCho or PtdEtn by EPT or CPT. *EK/CK: ethanolamine/choline kinase, ECT/CCT: ethanolamine/choline cytidylyltransferase, EPT/CPT: ethanolamine/choline phosphotransferase, DAG: diacylglycerol.*

In apicomplexa, enzymes driving CDP-ethanolamine branch of Kennedy pathway have been identified in several species of *Plasmodium* and *T. gondii*. The alternative pathway *via* decaboxylation of PtdSer was also characterized, with one PSD in *Plasmodium*[70] and two PSDs in *T. gondii*[48,49] identified. Attempts to delete the genes that are required for the *de novo* synthesis of PtdEtn in *P. berghei* failed[71], indicating the CDP-ethanolamine branch of Kennedy pathway is likely to be essential for the parasite survival. In *T. gondii*, two functional kinases (*Tg*CK and *Tg*EK) that can catalyze the reaction from ethanolamine to phospho-ethanolamine have been studied, while the *Tg*CK that can mediate the phosphorylation of both choline and ethanolamine was found essential[47]. Together with that neither of the identified PSDs has been shown essential for the lytic cycle of *T. gondii*, it

can be assumed that CDP-ethanolamine branch of Kennedy pathway for PtdEtn synthesis is likely to be crucial as well.

The second step of the Kennedy pathway driven by ethanolamine cytidylyltransferase (ECT) is considered as the rate-limiting step. Only one functional ECT has been identified so far in majority of eukaryotic species[72]. The activity of ECT is strictly controlled. One conserved domain of ECT has been identified locating at the upstream of the open reading frame (ORF), which provides binding sites for transcription factors such as NFκB, C/EBP, NF-Y and EGR1 and thereby allows for the transcriptional regulation of ECT[73]. Post-translational regulation of ECT was also reported, the activity of ECT can be regulated by protein kinase C (PKC) as a response to the cell growth and nutrient supply status[74]. Phosphorylation status of several residues in the catalytic center impacts on its conformational structure and thus controls CDP-ethanolamine synthesis.

1.2.3 Physiological importance and biogenesis of PtdIns

As one of the major lipid classes, PtdIns is yet-another primary constituent of the parasite membranes, accounting for 5-10% of the total glycerophospholipids in the protozoan parasites[54,75-77]. Metabolism of PtdIns derivatives has drawn notable attention due to their crucial roles in the parasite pathogenesis and potential as targets for drug, vaccine, or diagnosis[78-86]. One group of the well-characterized PtdIns-derived metabolites includes various forms of PtdIns phosphate (PIP), which are considered as essential signaling mediators involved in apicoplast homeostasis (*Toxoplasma*)[87,88], protein export (*Plasmodium*)[89,90], gliding motility and egress (*Plasmodium*)[91,92], endocytosis (*Trypanosoma*)[93,94] and autophagy (*Plasmodium* and *Trypanosoma*)[95,96]. Apart from PIPs as stated, another important class of PtdIns derivatives is glycosylphosphatidylinositol (GPI), providing membrane anchor to glycoproteins. Several GPI-anchored surface proteins have been implicated in modulation of the host's immune response[97-99] and the

parasite survival[100,101]. A vital requirement of PtdIns and its downstream metabolites for the infection and pathogenesis of the protozoan parasites necessitates understanding the mechanism of PtdIns biogenesis.

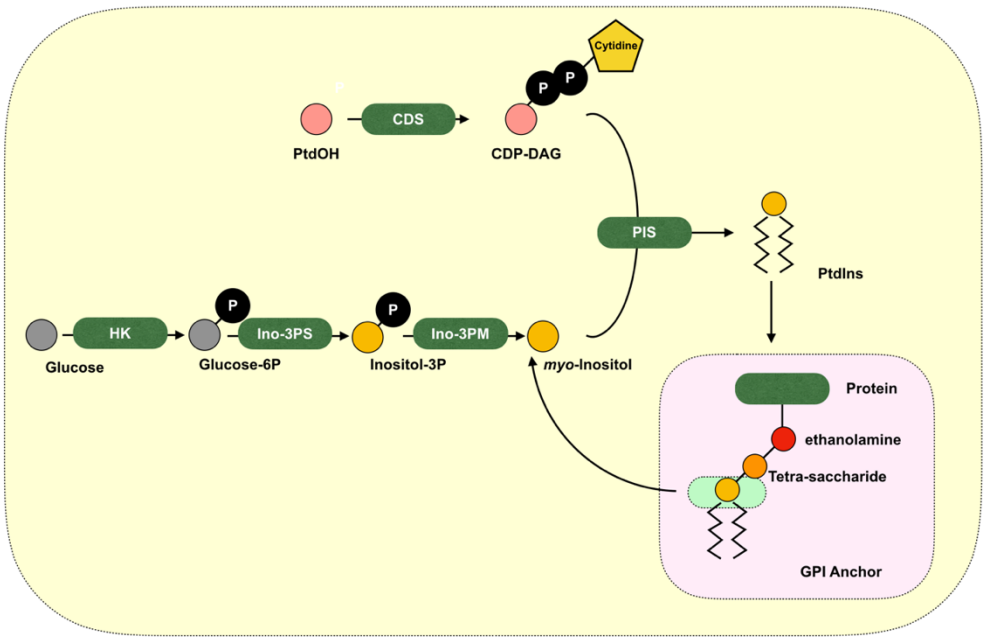

Figure.8: Biogenesis of PtdIns in eukaryotic cell. CDP-DAG is synthesized by CDS from PtdOH while the generation of *myo*-inositol is completed *via* a three-step reaction. Glucose is turned into Glucose-6P by HK, and further converted to inositol-3P by inositol-3PS, and finally used for the synthesis of *myo*-inositol by insoitol-3PM. The inositol head of GPI which is produced from PtdIns can be recycled as precursor for PtdIns generation. *PtdOH: phosphatic acid, CDP-DAG: CDP-diacylglycerol, Glucose-6P: Glucose-6-phosphate, Inositol-3P: inositol-3-phosphate, GPI: glycosylphosphatidylinositol, CDS: cytidine diphosphate-diacylglycerol synthase, HK: hexokinase, Ino-3PS: inositol-3-phosphate synthase, Ino-3PM: inositol-3-monophosphatase, PIS: phosphatidylinositol synthase.*

Synthesis of PtdIns is catalyzed by PtdIns synthase (PIS), which co-utilizes CDP-diacylglycerol (CDP-DAG) and *myo*-inositol[102] **(Figure.8)**. Thus far only one protozoan PIS, isolated from the kinetoplastid parasite, *Trypanosoma brucei*, has been studied in details. *Tb*PIS localizes in both ER and Golgi bodies in the bloodstream forms of *T. brucei*[103], generating two distinct PtdIns pools in the two organelles. In ER, the *de novo* synthesized *myo*-inositol is utilized to produce PtdIns, which subsequently drives GPI metabolism. On the other hand, PtdIns production in the Golgi network employs exogenous (host-derived)

myo-inositol, and this pool of lipid is used for the biogenesis of inositol phosphorylceramide (IPC)[104,105]. Among intracellular parasites, the presence of PIS has been reported in *Plasmodium*, *Toxoplasma* and *Eimeria* species[106-108], however the biochemical characterization and physiological importance of the enzyme have not been investigated yet.

1.3 Objective of the study

The fast proliferation of *T. gondii* tachyzoites suggests a great need for efficient phospholipid biogenesis for the construction of plasma membrane and membrane derived organelles. This work focused on the biogenesis and physiological importance of two major classes of phospholipids: PtdEtn and PtdIns.

For PtdEtn, we aimed to dissect the role of CDP-ethanolamine branch of Kennedy pathway in PtdEtn biogenesis and lytic cycle by identifying the rate-limiting enzyme *Tg*ECT. For PtdIns, we focused on the enzyme *Tg*PIS, which accounts for the biogenesis of PtdIns in eukaryotes. For both assays genetic manipulation of the target genes was conducted followed by in-depth phenotyping to reveal their roles during the lytic cycle of *T. gondii.* Eventually, the mutants were collected for lipidomic analysis to reveal the role of these key enzymes in the biogenesis of PtdEtn and PtdIns. Last but not least, we attempted to summarize a hypothetical model demonstrating the physiological importance of both selected enzymes and the corresponding phospholipids based on the experiment results.

2. Material and Method

2.1 Materials

2.1.1 Biological Materials

2.1.1.1 Organism

Description	Source
E. coli XL1Blue Strain	Stratagene (Heidelberg, Germany)
T. gondii tachyzoites	
- RH*Δku80Δhxgprt*-Tati	Vern Carruthers (University of Michigan)
- *RHΔku80Δhxgprt*-TIR1	David Sibley (University of Washington)
- *RHΔku80Δhxgprt*-diCre	Markus Meissner (University of Munich)
- *Δtgcds1r*	Pengfei Kong (Humboldt University of Berlin)
- *Δtgpisr*	Pengfei Kong (Humboldt University of Berlin)
- *Tg*PIS-3'UTR$_{Floxed}$	Pengfei Kong (Humboldt University of Berlin)
Human Foreskin Fibroblasts (HFF)	Cell Lines Service (Eppelheim, Germany)

2.1.1.2 Vectors

Description	Source
pTKO-HXGPRT	John Boothroyd (Stanford University)
pNTP3	Isabelle Coppens (John Hopkins University)
pTUB-mAID-3HA-HXGPRT	David Sibley (University of Washington)
pLinker-AID-HA-DHFR-TS	David Sibley (University of Washington)
pTETO7SAG1-UPKO	modified from pNTP3
pQE-60	Qiagen (Hilden,Germany)
pU6-Universal	Sebastian Lourido (Whitehead Institute)

2.1.1.3 Antibodies

Name	Dilution	Source
α-HA (mouse)	1:10000	Sigma-Aldrich (St. Louis, MO)
α-HA (rabbit)	1:1000	Sigma-Aldrich (St. Louis, MO)
α-*Tg*GAP45 (rabbit)	1:10000	Dominique Soldati-Favre (University ıeva)
α-*Tg*HSP90 (rabbit)	1:1000	Sergio O.Angel (Chascomús, Prov. ɔs Aires, Argentina)
α-*Tg*SERCA (rabbit)	1:200	Friendbio (Wuhan, China)
α-*Tg*SAG1(mouse)	1:10000	Thermo-Fisher (Waltham, MA)
α-mouse IgG Alexa Fluor 488 (goat)	1:3000	Life Technologies (Waltham, MA)
α-mouse IgG Alexa Fluor 594 (goat)	1:3000	Life Technologies (Waltham, MA)
α-rabbit IgG Alexa Fluor 488 (goat)	1:3000	Life Technologies (Waltham, MA)
α-rabbit IgG Alexa Fluor 594 (goat)	1:3000	Life Technologies (Waltham, MA)
α-mouse IgG IRDye 800CW (goat)	1:10000	LI-COR Biosciences (Lincoln, NE)
α-rabbit IgG IRDye 680RD (goat)	1:10000	LI-COR Biosciences (Lincoln, NE)

2.1.1.4 Enzymes

Description	Source
DreamTaq polymerase	Fermentas (Waltham, MA)
Q5 polymerase	New England Biolabs (Ipswich,
Restriction endonucleases	New England Biolabs (Ipswich,
Proteinase K	Sigma-Aldrich (St. Louis, MO)
T4 ligase	Life Technologies (Waltham, MA)

2.1.1.5 Primers

Name	Sequence
Preparing gRNAs required for CRISPR/Cas9 recognition	
pU6-*Tg*ECT-HA-AID-F	AAGTTGAATGGATTGATGGACGCGGG
pU6-*Tg*ECT-HA-AID-R	AAAACCCGCGTCCATCAATCCATTCA
pU6-*Tg*PIS-3HA-mAID-F	AAGTTGAGGCAAGACTGTTTTTCAGG
pU6-*Tg*PIS-3HA-mAID-R	AAAACCTGAAAAACAGTCTTGCCTCA
pU6-*Tg*EPCS-HA-AID-F	AAGTTGGAGGAACTCTGCACACTGGG
pU6-*Tg*EPCS-HA-AID-R	AAAACCCAGTGTGCAGAGTTCCTCCA
Amplifying donor fragment for CRISPR-Based Homology-Direct-Repair(HDR)	
*Tg*ECT-AID-DHFRTS-F	CGAACAAGAGCAGGGACAGATGGTGTCTCTGA CAGAACTCATGGGCAGTGTCGAGCTG
*Tg*ECT-AID-DHFRTS-R	AAACGGAGAGAACCAAAACTTGACAAAGTCGC GTATCACGTGTCACTGTAGCCTGCCAGA
*Tg*PIS-mAID-3HA-F	GCGCTTGGTTGCGTGCGACATTTTTGGTGCGC CCTCGTCGGCTAGCAAGGGCTCGGGCTCGAC CCAGC
*Tg*PIS-mAID-3HA-R	GAGAACTTGTGGCTGCTCTCAGGGTAGGTCTC CCCAGAGGATAGGGCGAATTGGAGCTCC
*Tg*EPCS-AID-DHFRTS-F	CCGAAGAAACGGCACCTGCCGGGCGCAGCGG AAAACCGAGATGGGCAGTGTCGAGCTG
*Tg*EPCS-AID-DHFRTS-R	ATGCAGCCGAACTCTTTTGGGTTGTCCAACCTC TCTGGAGGACTGTAGCCTGCCAGA
Screening for CRSIPR-guided AID-insertional taging	
*Tg*ECT-AID-DHFRTS-Scr-F	GTGTTGCTGTCTTTGCATGCAG
*Tg*ECT-AID-DHFRTS-Scr-R	TGTCACTGTAGCCTGCCAGA
*Tg*PIS-mAID-3HA-Scr-F	CTGACGAATCTCCTCCAAG
*Tg*PIS-mAID-3HA-Scr-R	GGAGCTCCAATTCGCCCTAT
*Tg*EPCS-AID-DHFRTS-Scr-F	TACATGTGGTGGCCTGT
*Tg*EPCS-AID-DHFRTS-Scr-R	TTGTCAATGCCATCTTTCCTG
Ectopic expression of *Tg*PIS$^{49-258}$ in *T. gondii*	

*Tg*PIS$^{49\text{-}258}$-F (NcoI)	CTCATCCCATGGTTTTCCTCTACGTGCCAA
*Tg*PIS-HA-R (PacI)	CTCATCTTAATTAATCAAGCGTAATCTGGAACATCGTA TGGGTACGACGAGGGCGCACCAAA
Functional expression of *Tg*PIS and its mutants (*E. coli* M15 strain)	
*Tg*PIS-QE-F (BglII)	CTCATCAGATCTATGGCGGGGACTTCTGCAAG
*Tg*PIS-QE-R (BglII)	CTCATCAGATCTCGACGAGGGCGCACCAAA
*Tg*PIS$^{49\text{-}258}$-QE-F (BglII)	CTCATCAGATCTATGGTTTTCCTCTACGTGCCAAACA
*Tg*PIS^{D91A}-F	GCCGCAGTCGATGGCG
*Tg*PIS^{D91A}-R	CAGGCATTGCGATGTAACA
*Tg*PIS^{D94A}-F	GCTGGCGCTGCCGC
*Tg*PIS^{D94A}-R	GACTGCGTCCAGGCATTG
*Tg*PIS^{Q103G}-F	GGAGTTTCCATTGTCGGCG
*Tg*PIS^{Q103G}-R	GCCCAGACGGCGTG
*Tg*PIS$^{D112A/Q113G}$-F	GCCGGAGTTGTCGACCGG
*Tg*PIS$^{D112A/Q113G}$-R	GAGACAGGCGCCGACA
*Tg*PIS$^{D116A/R117G}$-F	GCCGGGCTTTCAACATGTCT
*Tg*PIS$^{D116A/R117G}$-R	GACAACTTGGTCGAGACAGG
Making the *Δtgpisr* strain (RH*Δku80*-TaTi strain)	
*Tg*PIS-F (NcoI)	CTCATCCCATGGCGGGGACTTCTGCAAGCCG
*Tg*PIS-HA-R (PacI)	CTCATCTTAATTAATCAAGCGTAATCTGGAACATCGTA TGGGTACGACGAGGGCGCACCAAA
*Tg*PIS-5'UTR-F (ApaI)	CTCATCGGGCCCCGAAGTCTTACTCGTCCAGAAAA
*Tg*PIS-5'UTR-R (ApaI)	CTCATCGGGCCCGCTGTTAGAACGACGCACAC
*Tg*PIS-3'UTR-F (XhoI)	CTCATCCTCGAGTATCCGAGCTGTCGCTGTC
*Tg*PIS-3'UTR-R (XbaI)	CTCATCTCTAGAATCTGCACGAAGTTCGGC
*Tg*PIS-5'Scr-F	TCGACACGTATACGCAAACC
*Tg*PIS-5'Scr-R	ACGATGCGATTGGGATATATC
*Tg*PIS-3'Scr-F	TCAGGTTCATCATGCCGTC
*Tg*PIS-3'Scr-R	TTGCTTAAATCGTGGCAGTG
Making the *Tg*PIS-3'UTR$_{Floxed}$ and *Tg*PIS-3'UTR$_{Excised}$ strains (RH*Δku80*-diCre strain)	
*Tg*PIS-3'IT-F1	TACTTCCAATCCAATTTAATGCTTCTCTTCCGTACTCGATGG

*Tg*PIS-3'IT-R1	TCCTCCACTTCCAATTTTAGCCGACGAGGGCGCACCAAA
*Tg*PIS-3'IT-Scr-F	GGTTCTTCATGTGCCTTCTTCT
*Tg*PIS-3'IT-Scr-R	CATGATTACGCCAAGCTCG
Making the *Tg*PIS-HA_{Floxed} and *Δtgpis*-$HA_{Excised}$ strains (RH*Δku80Δhxgprt* strain)	
*Tg*PIS-Cre-F (EcoRI)	CTCATCGAATTCCGACAAAATGGCGGGGACTTCTGC
*Tg*PIS-HA-R (PacI)	CTCATCTTAATTAATCAAGCGTAATCTGGAACATCGTATGGGTACGACGAGGGCGCACCAAA
*Tg*PIS-5'UTR-Cre-F (ApaI)	CTCATCGGGCCCATGGCCAACAGCTCAGCT
*Tg*PIS-5'UTR-Cre-R (EcoRI)	CTCATCGAATTCTATAACTTCGTATAATGTATGCTATACGAAGTTATGAGCCGCTTTTCTTTTTGC
*Tg*PIS-3'UTR-Cre-F (SacI)	CTCATCGAGCTCGGTCGCTTTTCTCGTGAAGA
*Tg*PIS-3'UTR-Cre-R (SacI)	CTCATCGAGCTCTTGTGCGAACTAGACGTATGACTT
*Tg*PIS-HA_{Floxed}-5'Scr-F	CTCGATATGGGGAACCCAA
*Tg*PIS-HA_{Floxed}-5'Scr-R	CAGATGAACTTCAGGGTCAGC
*Tg*PIS-HA_{Floxed}-3'Scr-F	CTACGACTTCAACGAGATGTTCC
*Tg*PIS-HA_{Floxed}-3'Scr-R	GTCCAGTGTTCAGGACATTGAGT
*Tg*PIS-ORF-Scr-F	GTCAGATTCTGACCTTTCTCATGA
*Tg*PIS-ORF-Scr-R	GAACGGTAGTAGACGGAGAGAATG
qPCR of *Tg*PIS	
*Tg*PIS-qPCR-F	CAAACATCATTGGATACGTTCG
*Tg*PIS-qPCR-R	TGTTGAAAGCCGGTCGAC
*Tg*EfA-qPCR-F	AGTCGACCACTACCGGACAC
*Tg*EfA-qPCR-R	CTCGGCCTTCAGTTTATCCA
*Tg*TubA-qPCR-F	AGGATGCTGCGAACAACTTC
*Tg*TubA-qPCR-R	TCAAGAAACCCTGGAGACCA
*Tg*GT1-qPCR-F	GGCTATTTTGGCACCTTTCA
*Tg*GT1-qPCR-R	AACGGGAAGACAAACCACAG

2.1.2 Chemical Materials

2.1.2.1 Chemical Reagents

Name	Source
Acetic Acid	Carl Roth (Karlsruhe, Germany)
ATP	Sigma-Aldrich (St. Louis, MO)
Agarose	Biozym (Hessisch Oldendorf, Germany)
Ampicillin	Carl Roth (Karlsruhe, Germany)
Anhydrotetracycline (aTc)	IBA Lifesciences (Goettingen, Germany)
Bovine serum albumin fraction V (BSA)	Applichem (Darmstadt, Germany)
Chloroform	Carl Roth (Karlsruhe, Germany)
Crystal violet	Sigma-Aldrich (St. Louis, MO)
Dimethyl sulfoxide (DMSO)	Sigma-Aldrich (St. Louis, MO)
DNA ladder (1 kb)	Fermentas (Waltham, MA)
Distilled water (HPLC-purified)	Carl Roth (Karlsruhe, Germany)
dNTP-Mix (100 mM)	Fermentas (Waltham, MA)
Dulbecco's modified eagle media (DMEM)	PAN-Biotech (Aidenbach, Germany)
Fetal bovine serum (FBS)	PAN-Biotech (Aidenbach, Germany)
Fluoromount-G/DAPI	SouthernBiotech (Birmingham, AL)
Glycerol	Applichem (Darmstadt, Germany)
Hank's balanced salt solution (HBSS)	PAA (Linz, Austria)
Indole-3-acetic acid	Sigma-Aldrich (St. Louis, MO)
Isopropanol	Applichem (Darmstadt, Germany)
L-glutamine (100x stock)	PAN-Biotech (Aidenbach, Germany)
Methanol	Carl Roth (Karlsruhe, Germany)

MEM non-essential amino acids (100x stock)	PAN-Biotech (Aidenbach, Germany)
Mycophenolic acid (MPA)	Applichem (Darmstadt, Germany)
Natural and synthetic lipids	Avanti Polar Lipids (Alabaster, AL)
Paraformaldehyde	Merck (Darmstadt, Germany)
Penicillin/Streptomycin (100x stock)	PAN-Biotech (Aidenbach, Germany)
Phosphat buffered saline (PBS)	PAN-Biotech (Aidenbach, Germany)
Protein marker (prestained)	Fermentas (Waltham, MA)
Pyrimethamine	AK Scientific (Union City, CA)
Rotiphorese gel 30 (Acrylamide)	Carl Roth (Karlsruhe, Germany)
Sodium pyruvate (100x stock)	PAN-Biotech (Aidenbach, Germany)
Tris-HCl	Promega (Fitchburg, WI)
Triton-x100	Biowest (Riverside, MO)
Trizol	Life Technologies (Waltham, MA)
Trypsin/EDTA	Biowest (Riverside, MO)

2.1.2.2 Commercial Kits

Name	**Source**
First-strand cDNA synthesis kit	Life Technologies (Waltham, MA)
Genomic DNA preparation kit	Analytik Jena (Jena, Germany)
InnuPREP DOUBLEpure kit	Analytik Jena (Jena, Germany)
InnuPREP plasmid mini kit	Analytik Jena (Jena, Germany)
PureLink RNA mini kit	Life Technologies (Waltham, MA)

2.1.2.3 Instruments

Instruments	Source
Camera system (E.A.S.Y. RH)	Herolab (Wiesloch Germany)
Cell counting chamber (Neubauer-improved)	Carl Roth, (Karlsruhe, Germany)
Centrifuges (5417R, 5424, 5810R)	Eppendorf, (Hamburg, Germany)
Cryo container (Nalgene, Mr. Frosty)	Thermo Fisher Scientific (Waltham, MA)
Electric pipetting aid (Accu-jet Pro)	Brand (Wertheim, Germany)
Electrophoresis Power Supply (EPS 200/300)	Pharmacia Biotech (Uppsala, Sweden)
Electroporator (Amaxa Nucleofector)	Lonza (Basel, Switzerland)
Gel electrophoresis system (Easy Phor)	Biozym (Hessisch Oldendorf, Germany)
Ice machine (ZBE 110-35)	Ziegra (Isernhagen, Germany)
Incubator- CO_2 (HERACELL 150i)	Thermo Fisher Scientific (Waltham, MA)
Incubators (SE200-400)	Memmert (Schwabach, Germany)
Infrared imaging system (Odyssey FC)	LI-COR Biosciences (Lincoln, NE)
Microscope-fluorescence (Axio Image.Z2)	Zeiss (Oberkochen, Germany)
Microscope-inverted (LABOVERT)	Leica (Wetzlar, Germany)
Microscope-light optical (DM750)	Leica (Wetzlar, Germany)
Microwave (M805 Typ KOR-6115)	Alaska (Düsseldorf, Germany)
SDS-PAGE electrophoresis system (Hoefer™ Mighty Small™ II)	Hoefer (Holliston, MA)
Multichannel pipette (Transferpipette® -8/-12) (50-200 µl)	Brand (Wertheim, Germany)
NanoDrop® spectral photometer (ND-1000)	Peqlab (Darmstadt, Germany)
PCR Cycler	Analytik Jena (Jena, Germany)
PerfectBlue™ 'Semi-Dry' blotter (SEDEC M)	Peqlab (Darmstadt, Germany)

Photometer (BioPhotometer)	Eppendorf, (Hamburg, Germany)
Pipettes	Eppendorf, (Hamburg, Germany)
Precision scale (PCB 1000-2)	Kern & Sohn (Balingen, Germany)
Precision scale (BP 110 S)	Sartorius (Göttingen, Germany)
Safety work benches (HERA safe)	Heraeus Instruments (Hanau, Germany)
Shaking incubator (Innova 4000)	Eppendorf (Hamburg, Germany)
Steam-sterilizer (VARIOKLAV)	Thermo Fisher Scientific (Waltham, MA)
UV-transilluminator (UVT-20 M/W)	Herolab, Germany
Thermoshaker (Thermomixer comfort/ 5436)	Herolab (Wiesloch, Germany)
Waterbath (WB-4MS)	Biosan (Riga, Latvia)
Waterbath (U 3/8)	Julabo (Seelbach, Germany)

2.1.2.4 Plastic ware and disposables

Items	**Source**
Cell culture dishes (60x15 mm)	Sarstedt (Nümbrecht, Germany)
Cell culture flasks (T25, T75, T175, T300)	Sarstedt (Nümbrecht, Germany)
Cell culture plate (6, 24, 96 well)	Sarstedt (Nümbrecht, Germany)
Cell scraper (30 cm)	TPP (Trasadingen, Switzerland)
Centrifugal filters (0.22-µm, Corning Costar Spin-X)	Sigma-Aldrich (St. Louis, MO)
Cryotube preservation tubes (2 ml)	Greiner Bio One (Kremsmünster, Austria)
Electroporation cuvettes (2 mm)	Peqlab (Darmstadt, Germany)
Falcon Tubes (15 ml/ 50 ml), CELLSTAR™	Greiner Bio One (Kremsmünster, Austria)
Filter (5 µm), Millex® syringe-compatible	Merck Millipore (Billerica, MA)
Filter sterilizer (0.22 µm)	Schleicher Schuell (München, Germany)
Filter tubes (Amicon Ultra-0.5 ml)	Merck Millipore (Billerica, MA)
Glass slides, microscopic (76x26 mm)	Carl Roth (Karlsruhe, Germany)

Gloves	Sempermed (Vienna, Austria)
Microtube (8x0.2 ml)	Biozym (Hessisch Oldendorf, Germany)
Microtube lid (8x0.2 ml)	Biozym (Hessisch Oldendorf, Germany)
Ni-NTA columns for protein purification (Novex)	Thermo Fisher Scientific (Waltham, MA)
Nitrocellulose transfer membrane	Applichem (Darmstadt, Germany)
Parafilm	Bemis Company (Neenah, WI)
PCR-tube-stripes (0.2 ml)	Biozym (Hessisch Oldendorf, Germany)
Pipette-pasteur	A. Hartenstein (Würzburg, Germany)
Pipette tips (10 µl, 20 µl, 200 µl, 1ml)	Sarstedt (Nümbrecht, Germany)
Reaction tubes (0.2 ml, 0.5 ml, 1.5 ml, 2 ml)	Sarstedt (Nümbrecht, Germany)
RNAase free barrier tips (10 – 1,000 µl)	Biozym (Hessisch Oldendorf, Germany)
Serological pipettes, sterile (5 ml, 10 ml, 25 ml)	Sarstedt (Nümbrecht, Germany)
UV-cuvettes	Carl Roth (Karlsruhe, Germany)
Whatman paper (3 MM)	A. Hartenstein (Würzburg, Germany)

2.1.2.5 Software and Online tools

Identification of candidates for study was done by using EuPathDB (www.eupathdb.org) and ToxoDB (www.toxodb.org). Prediction of conserved domain was done by using InterProScan (https://www.ebi.ac.uk/interpro/search/sequence-search). Sequence alignment was done by using CLC Sequence Viewer (http://www.clcbio.com/products/clc-sequence-viewer). Data processing, significant test and plotting were done by either Microsoft Excel or Graphpad Prism (https://www.graphpad.com/scientific-software/prism). Analysis of plaque images for plaque assay was done by ImageJ (https://imagej.nih.gov/ij). Heatmap for lipidomic analysis of *Tg*PIS was drawn by Qlucore (https://qlucore.com). Data presentation and scheme making were done by Mac Keynote.

2.1.2.6 Buffer and media

For HFF/*T. gondii* culture

D10 Medium (For *T. gondii*/HFF culture)		Cytomix (For *T. gondii* transfection)		Freezer Stocker Buffer	
DMEM	500 ml	KCl	120 mM	DMSO	10%
iFBS	50 ml	HEPES(pH7.6)	25 mM	iFBS	90%
200mM L-Glutamin	5.5 ml	$MgCl_2$	5 mM		
penicillin/streptomycin (100x);	5.5 ml	EDTA	2 mM		
sodium pyruvate	5.5 ml	$CaCl_2$	0.15 mM		
MEM non-essential amino acids (100x stock)	5.5 ml	K_2HPO_4/KH_2PO_4(pH7.6)	10 mM		
		Adjusted to pH 7.6 and filter-sterilized with 0.22 μM filter			

For *E.coli* culture

LB Medium		SOC Medium	
Trypton	10 g	Trypton	20 g
Yeast extract	5 g	Yeast extract	5 g
NaCl	10 g	NaCl	0.5 g
H_2O	1 L	KCl	0.186 g
*Optional(For plates) Agar	15 g	H_2O	1 L

Autoclaving and stored in room temperature.	Autoclaving, and then added filter -sterilized
	$MgCl_2$ 0.952 g
	Glucose 3.603 g

For *E.coli* transformation

TFB-I buffer		TFB-II buffer	
KoAC	30 mM	NaMOPS	10 mM
$MnCl_2$	50 mM	RbCl	10 mM
RbCl	100 mM	$CaCl_2$	75 mM
Glycerol	15%	Adjusted to pH 5.8 and filter-sterilized with 0.22 μM filter, stored at 4 °C	
Adjusted to pH 5.8 and filter-sterilized with 0.22 μM filter, stored at 4 °C			

For SDS-PAGE gel preparation

5% - Stacking		10% - Resolving	
30% acrylamide	0.33 ml	30% acrylamide	1.67 ml
1 M Tris-HCl (pH6.8)	0.25 ml	1.5 M Tris-HCl (pH8.8)	0.25 ml
10% SDS	20 μl	10% SDS	50 μl
10% APS	20 μl	10% APS	50 μl
TEMED	10 μl	TEMED	5 μl
H_2O	1.4 ml	H_2O	1.93 ml
SDS-PAGE Running		Wet-Blot Transfer	

Glycin	3 g	Glycin	3 g
Tris-Base	14.4 g	Tris-Base	14.4 g
SDS	1 g	Methanol	200 ml
Dissolved in 1 L H_2O			
TBS Buffer (10x)		TBS-T Buffer	
500mM Tris-HCl (pH7.6)	1.25 M	1x TBS Buffer	99.8%
1.5M NaCl	0.5%	Tween 20	0.2%

2.2 Method

2.2.1 *T. gondii* and host cell culture

Tachyzoites of *T. gondii* were propagated by serial passage in HFF monolayers at a MOI=1. HFFs were cultured in D10 medium in a humidified incubator (5% CO_2, 37 °C). Cells were harvested by trypsinization and grown to confluence in flasks, dishes or plates as needed. For all assays, parasites were mechanically released from late-stage cultures and used immediately. Briefly, parasitized cells (40-42 h post infection) were scraped in fresh medium and squirted through 23- and 27-gauge syringes to obtain extracellular tachyzoites, which were either used directly for transfection and phenotyping assays, or stored at -80 °C for lipid extraction, as described below.

2.2.2 Molecular cloning

2.2.2.1 Parasites DNA/RNA preparation

RNA was isolated from freshly purified tachyzoites of *T. gondii* using TRIzol-extraction method and subsequently reverse-transcribed into first-strand cDNA. The gDNA was isolated using the genomic DNA preparation kit.

2.2.2.2 PCR

DNA amplicons for vector construction or transfection were amplified using Q5-HiFi-Polymerase, 5 ng of plasmid or 50-200 ng of cDNA were used as template. The gradient PCR or colony PCR was done using DreamTaq polymerase. For colony PCR, *E. coli* colonies were resuspended in 20 µl sterilized H_2O and 5 µl of the suspension was used as template. All the DNA samples were separated by 1% agarose gel and visualized by RotiSafe DNA staining dye at 85-130 V in TAE running buffer for 20-45 minutes. Samples were purified with innuPREP DOUBLEpure kit.

2.2.2.3 DNA ligation and digestion

The digestion of PCR products and vector were performed using corresponding restriction enzymes from NEB. The usage of enzyme was 1 unit/µg for PCR products and 3 unit/µg for vector. The ligation of DNA fragments was done with T4 ligase. Reaction mix consisted of a molar ratio of 3:1/5:1/7:1 (f mol insert: f mol vector) and was placed in room temperature for 1 h or in 4 °C overnight before transformation into *E. coli.*

2.2.2.4 *E. coli* transformation

XL1-Blue *E. coli* competent cells were always prepared before the transformation. Briefly, the bacteria cells were inoculated in 5 ml SOB medium (with 12.5 µg/ml tetracycline) at 37 °C shaker overnight, and then diluted into 200 ml with the same medium. The competent cells were harvested by centrifuging for 10 minutes at 1,000 g, 4°C. The pellet was washed with TFB-I buffer, resuspended in 6.4 ml TFB-II buffer, and then aliquoted into a volume of 110 µl (for one transformation) or 220 µl, frozen in liquid nitrogen and stored in -80 °C.

For the transformation, *E. coli* competent cells were thawed on ice for 5 minutes, then added DNA samples needed to be transformed. The cells were incubated another 30 minutes on ice, and placed in 42 °C water bath for 45 s. After chilling on ice again for 5 more minutes, 1 ml SOC medium was added to the tube, following by inoculating at 37 °C for 1 h and plated on LB-agar-ampicillin. The *E. coli* was cultured overnight at 37° C incubator, and harvested for further purpose.

2.2.2.5 Plasmid isolation

For plasmid isolation from small volume culture (<10 ml), innuPREP plasmid mini kit was used. Large-scale DNA isolation was done by using PureLink HiPure plasmid midiprep kit. Purified plasmid samples were stored at -20 °C before use.

2.2.3 Protein assays

2.2.3.1 Protein expression in *E. coli*

The bacterial strains were cultured in M9 minimal medium containing ampicillin (100 mg/L) and kanamycin (50 mg/L). Protein expression was induced overnight at 25 °C by adding 1 mM Isopropyl β-D-1-thiogalactopyranoside (IPTG) to the cultures between OD_{600} of 0.4-0.6 (grown at 37 °C),

2.2.3.2 Western Blot

Fresh extracellular parasites (1.5×10^7) were washed twice with PBS, pelleted (400 g, 10 min, 4 °C), resuspended in the protein-loading buffer and subjected to denaturing gel electrophoresis. Proteins were resolved by 12% SDS-PAGE and transferred to a nitrocellulose membrane (85 V, 90 min). The membrane was treated with 4% skimmed dry milk suspended in Tris-buffered saline and 0.2% Tween 20 (overnight, 4 °C), incubated

with anti-HA and anti-*Tg*HSP90 antibodies (2 h at room temperature), washed 3 times for 5 min each, and then incubated with IR dyes-conjugated secondary antibodies (680RD and 800CW) for 1 h at room temperature. Proteins were visualized using a Li-COR imaging system.

2.2.4 Transgenic parasites construction

For generating the transgenic strains, the respective constructs (10 µg) were transfected into freshly released tachyzoites of specific strains (~10^7 parasites) suspended in filter-sterile Cytomix using a Amexa (Program T-016). Transfected parasites were selected for resistance to a drug corresponding to the selection marker encoded by transfected plasmid. The drug-resistant transgenic parasites were cloned by limiting dilution, and individual clones were screened by PCR and/or immunofluorescence assays.

2.2.5 Immunofluorescent assay (IFA)

Parasitized HFFs cultured on glass coverslips were washed with PBS 20-24 h post infection, fixed with 4% paraformaldehyde for 10 min, and neutralized with 0.1 M glycine in PBS for 5 min. Cells were permeabilized with 0.2% Triton X-100 in PBS for 20 min and treated with 2% bovine serum albumin in 0.2% Triton X-100 in PBS for 20 min. Samples were stained with primary antibodies for 1 h, as shown in figures. Cells were washed three times with 0.2% Triton X-100 in PBS and then stained with Alexa488/594-conjugated antibodies for 45 min. Following three additional washings with PBS, samples were mounted in Fluoromount G and DAPI mix and stored at 4 °C. Imaging was done by an epifluorescence fluorescence microscope (ApoTome, Zeiss, Jena, Germany).

2.2.6 Lytic cycle assays

Standard phenotyping methods were used to determine the impact of genetic manipulation on the lytic cycle of tachyzoites *in vitro*. Plaque assays were performed by infecting HFF cells in 6-well plates (100-200 tachyzoites/well). Infected cells were incubated unperturbed

for 7 days followed by fixation with ice-cold methanol and staining with crystal violet (5%). Plaques were imaged and scored for their sizes and numbers using the ImageJ software.

For invasion assays, confluent HFFs cultured on coverslips placed in 24-well plates were infected with tachyzoites (MOI=10) for 1 h. Cultures were stained with α-*Tg*SAG1 antibody prior to detergent permeabilization (to visualize noninvaded parasites). Cells were washed 3x with PBS, permeabilized with 0.2% triton X-100 in PBS for 20 min and then stained with α-*Tg*GAP45 antibody (to recognize invaded parasites). The percentages of invaded (intracellular) parasites were determined to compare the invasion efficiency across strains.

To measure the gliding motility, $4x10^5$ parasites suspended in Hank's balanced salt solution (HBSS) were incubated first to let them settle (15 min, RT) and glide (15 min, 37 °C) onto 0.01% BSA-coated coverslips. Samples were then stained with α-*Tg*SAG1 and Alexa488 antibodies, as mentioned above. Motile fraction was counted on the microscope, and trail lengths were quantified by ImageJ software. To test the natural egress, host cell monolayers on coverslips were infected with MOI=1 for 40 and 64 h. Similarly, induced egress in response to Zaprinast treatment (500 µM) was monitored for 30 min in early cultures (MOI=1, 24 h post-infection). In both cases, cells were subsequently fixed with 4% PFA (15 min), neutralized by 0.1 M glycine/PBS (5 min), and blocked in 3% BSA/PBS (30 min). Egressed vacuoles were immunostained with α-*Tg*SAG1 antibody prior to detergent permeabilization. Cultures were washed 3 times with PBS, permeabilized with 0.2% triton X 100/PBS (20 min) followed by staining with α-*Tg*GAP45 antibody to visualize the intact vacuoles. Samples were washed and stained with Alexa488 and Alexa594-conjugated antibodies. The egress was calculated as the ratio of lysed to total vacuoles.

2.2.7 Lipid analysis

2.2.7.1 Lipid extraction and thin layer chromatography

Cell pellets were suspended in 5.8 ml of methanol:water (2:0.9, v/v) followed by sequential addition of chloroform (2 ml), 0.2 M KCl (1.8 ml) and chloroform (2 ml), each accompanied with vigorous vortex-mixing. The aqueous (upper) phase was removed from the biphasic system, and the chloroform (lower) phase was washed twice with methanol:KCl (0.2 M):chloroform (1:0.9:0.1, v/v). Lipids obtained from the radiolabeled parasites or recombinant bacteria were backwashed three times, each with 2.1 ml of methanol:PBS:chloroform (1:0.9:0.15, v/v). The lower chloroform phase containing lipids was recovered, dried by N_2 stream, and then resuspended in 50-100 µl of chloroform:methanol (9:1, v/v). Phospholipids were resolved by one-dimensional TLC on silica H plates developed either in a solvent comprising chloroform:methanol:2-propanol:KCl (0.25%):triethylamine (90:28:75:18:54, v/v), or chloroform/ethanol:water:triethylamine (30:35:7:35, v/v). Alternatively, lipids were separated by two-dimensional TLC on silica 60 plates developed first in chloroform:methanol:NH_4OH (65:35:5, v/v), and then in chloroform:acetic acid:methanol:water (75:25:5:2.2, v/v). Phospholipids were visualized by staining with iodine vapor, or by spraying 0.2% (w/v) anilino-1-naphthalene sulfonic acid followed by exposure to ultraviolet light, or by autoradiography using X-ray film. Lipids were identified based on their co-migration with authentic standards.

2.2.7.2 Lipidomic analysis

Pellets of purified parasites (1-2x10^7) were suspended in 0.8 ml PBS and subjected to lipid extraction according to Bligh and Dyer[78]. Lipid extracts were dried under nitrogen, dissolved in 100 µL of chloroform/methanol (1:1), and injected (10 µL) into a hydrophilic interaction liquid chromatography column (2.6 µm HILIC 100 Å, 50x4.6 mm, Phenomenex, Torrance, CA). Lipid classes were separated by gradient elution on an Infinity II 1290 UPLC (Agilent, Santa Clara, CA, USA) at a constant flow rate (1 ml/min). ACN/acetone (9:1, v/v) was used as solvent A, while solvent B consisted of a mixture of ACN/H_2O (7:3, v/v) and 10 mM ammonium formate. Both solvents contained 0.1% formic acid. Gradient elution was done as follows (time in min, % B): (0, 0), (1, 50), (3, 50), (3.1, 100), (4, 100). No re-equilibration

of the column was necessary between successive samples. The column effluent was connected to a heated electrospray ionization (hESI) source of an Orbitrap Fusion mass spectrometer operated at -3,600 V in the negative ionization mode. Temperatures for the vaporizer and ion transfer tube were 275 °C and 380 °C, respectively. Full scan measurements (MS1) in the mass range from 450 to 1,150 amu were collected at a resolution of 120,000. Parallelized data-dependent MS2 experiments were done with HCD fragmentation set at 30 V, using the dual stage linear ion trap to generate up to 30 spectra per second. Data processing was done using the R, and was based on the packages including 'XCMS' for peak recognition and integration, 'pcaMethods' and 'statistics' for statistical analysis. Lipids were quantified by calculating response factors for individual lipid classes using authentic standards.

2.2.8 Statistic analysis

All data shown in graphs were presented as the mean with S.E. from at least three independent assays using representative parasite clones, unless specified otherwise. Statistical analyses were performed using the GraphPad Prism program (v7, Prism Software Inc., La Jolla, CA). Significance was tested by unpaired two-tailed Student's t test with equal variances (*$p<0.05$, **$p<0.01$, ***$p<0.001$).

3. Results

3.1 PtdIns biogenesis in *T. gondii*

3.1.1 *T. gondii* can synthesize PtdIns by co-utilizing *myo*-inositol and CDP-DAG

To investigate whether the parasite can import and utilize exogenous inositol for PtdIns biogenesis, we incubated fresh extracellular tachyzoites with [^{3}H]-*myo*-inositol. Parasites exhibited a time-dependent incorporation of *myo*-inositol into lipids, which was nearly linear during the first 4 h of incubation and then gradually decelerated afterwards **(Figure.9A)**. Separation of total lipids from radiolabeled tachyzoites by thin layer chromatography (TLC) revealed that among key phospholipids, only PtdIns was labeled with [^{3}H]-*myo*-inositol **(Figure.9B)**. In similar assays using saturating amount of *myo*-inositol (0.5 mM), we observed a significant surge in PtdIns synthesis **(Figure.9C)**, confirming a substrate-dependence of the reaction. Likewise, addition of CDP-DAG as a co-substrate further stimulated the synthesis of PtdIns under low as well as high inositol conditions. We also estimated the maximal rates of PtdIns synthesis by extracellular tachyzoites of the RH strain, which was about 0.25 nmol/h for an aliquot of 10^8 cells. The rate of lipid synthesis is circa 20% of the amount needed for a cell doubling based upon a content of 8 nmol PtdIns/10^8 cells. Collectively, the data demonstrate that host-free tachyzoites are competent in synthesizing PtdIns using inositol and CDP-DAG as co-substrates. However, their synthetic capacity in extracellular environment cannot fulfil the actual demand of lipid harbored by the parasite.

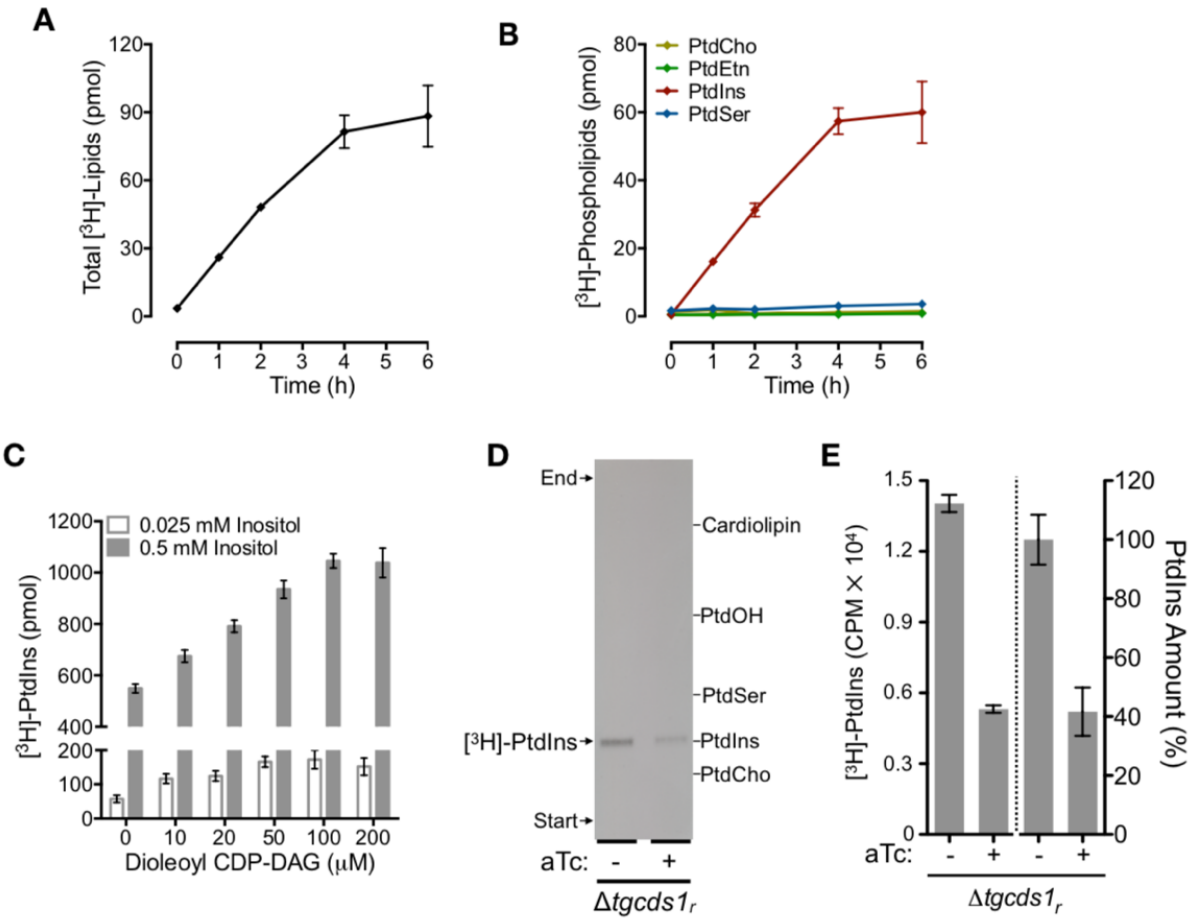

Figure.9: Extracellular tachyzoites of *Toxoplasma gondii* can generate PtdIns co-utilizing *myo*-inositol and CDP-diacylglycerol. (A-C) Radioactive labeling of purified tachyzoites of the RH strain with *myo*-inositol. Fresh parasites (10^8/reaction) were incubated with [^{3}H]-*myo*-inositol (10 µCi, 0.025 mM) at 37 °C for the indicated periods in the labeling medium, immediately followed by lipid extraction. Incorporation of radiotracer was quantified in total lipids **(A)** and major phospholipid classes resolved by thin layer chromatography **(B)**. A conversion of CPM counts scored by liquid scintillation counter into absolute amounts was achieved using the formula (X CPM = Y pmol) derived from the reference measurements of the original substrate preparation. The panel **(C)** shows the same assay as depicted in **(A)** and **(B)** except for that CDP-DAG and *myo*-inositol were included at the specified concentrations (assay duration, 4 h). **(D)** Autoradiogram showing TLC-resolved lipids from radiolabeled tachyzoites of the *Δtgcds1r* strain under on (-aTc) and off (+aTc) conditions. The *Δtgcds1r* strain was precultured in aTc (1 µM) for two passages (96 h) prior to setting up assays. Fresh parasites ($5x10^7$/reaction) were labeled with [^{3}H]-*myo*-inositol (10 µCi, 0.5 mM) for 4 h at 37 °C. Lipids were separated by TLC, and visualized by X-ray detection at -80 °C for 40 h. **(E)** Quantification of PtdIns labeling and amount in the *Δtgcds1r* mutant. The left Y-axis shows the mean scintillation

counts in TLC-scraped PtdIns bands from the panel **(D)**. The right Y-axis illustrates the steady-state amount of PtdIns in the mutant in the absence or presence of aTc. The data in panel **(A-C)** and panel **(E)** represent the mean with S.E. from three independent assays. The underlying data was generated by Nishith Gupta and Pengfei Kong.

Notably, increased supply of CDP-DAG up to 0.2 mM led to accentuated biogenesis of PtdIns, albeit the dose-dependence of lipid synthesis on CDP-DAG was not as proportionate as observed with *myo*-inositol **(Figure.9C)**. In other words, a 20-fold increase in *myo*-inositol (from 0.025 to 0.5 mM) caused a 10x higher PtdIns synthesis, whereas a 20-fold increase in exogenous CDP-DAG (from 10 to 200 µM) yielded only a 2x additional labeling. We therefore tested the notion whether the parasite may depend on *de novo*-produced CDP-DAG for PtdIns biogenesis **(Figure.9D-E)**. We performed [^{3}H]-*myo*-inositol labeling of a regulatable mutant of CDP-DAG synthase 1 (*Δtgcds1r*), in which the synthesis of lipid precursor can be repressed by anhydrotetracycline (aTc). Indeed, the knockdown of *Tg*CDS1 caused a strong reduction in [^{3}H]-*myo*-inositol incorporation into PtdIns **(Figure.9D-E)**. Consistently, the steady-state amount of PtdIns was also reduced to the same extent in the *Δtgcds1r* mutant. Together, these results show that tachyzoites are competent in synthesizing PtdIns by co-utilizing external *myo*-inositol and endogenous CDP-DAG.

3.1.2 *T. gondii* encodes a functional PtdIns synthase in the Golgi-complex

Our bioinformatic search of the *T. gondii* database identified only one potential PtdIns synthase gene, termed *Tg*PIS (*Tg*GT1_207710). The open reading frame of *Tg*PIS encodes for 258 residues, and contains 4 transmembrane regions and a typical CDP-alcohol phosphotransferase domain with signature motifs ($DX_2DGX_2ARX_{8/9}GX_3DX_3D$) **(Figure.10A)**. The functional motifs are conserved in CDP-alcohol phosphotransferase-type enzymes. Besides, we identified two amino acids, Glutamine (103Q) and Arginine (117R) that are present only in PIS sequences **(Appendix.1A and Table S1)**. Next, we

expressed recombinant *Tg*PIS-6xHis in *E. coli*, which lacks the native PIS activity, and thus is well suited for functional analysis of PIS. The catalytic activity of *Tg*PIS was assessed in the presence of different concentrations of *myo*-inositol **(Figure.10D-E)**. TLC analysis of the bacterial strain harboring the empty vector (negative control, N.C.) showed no detectable PtdIns synthesis as expected, whereas the expression of *Tg*PIS-6xHis led to a significant production of PtdIns in a *myo*-inositol-dependent manner **(Figure.10B-C)**. We also generated mutants with site-mutations or deletion of conserved residues, and examined them in *E. coli* **(Appendix.1)**. Only the *Tg*PIS isoform with 103Q-G mutation could still produce PtdIns, however with a notably reduced efficiency, whereas all other mutations abolished the catalysis **(Appendix.1B-C)**, revealing the functional importance of the residues predicted by our bioinformatic analysis.

To examine the subcellular localization, we expressed *Tg*PIS-HA under the control of the endogenous promoter and found it exclusively in the Golgi network, as determined by co-localization with a known organelle marker *Tg*ERD2 tagged with a C-terminal Ty1 epitope **(Figure.10B)**. The alignment of *Tg*PIS with homologs from other organisms also revealed a prolonged N-terminal extension in *Tg*PIS **(Figure.10A)**. To resolve its importance, we ectopically expressed a mutant lacking the specified extension (*Tg*PIS$_{49\text{-}258}$-HA). A single copy of the expression cassette directed by the *pTETO7SAG1* promoter was inserted at the uracil phosphoribosyltransferase (UPRT) locus by double homologous recombination **(Figure.10C)**. *Tg*PIS$_{49\text{-}258}$-HA was targeted to the Golgi network, as judged by its co-localization with *Tg*ERD2-Ty1 in immunofluorescence assay. We also performed functional expression of the truncated *Tg*PIS$_{49\text{-}258}$-6xHis in *E. coli*, but observed only a minor reduction in PtdIns synthesis **(Figure.10D-E)**. These results demonstrate that *Tg*PIS is a catalytically active enzyme with vital signature residues. Moreover, the protein localizes in the parasite Golgi, and its prolonged N-terminus is dispensable for the subcellular localization and catalytic activity.

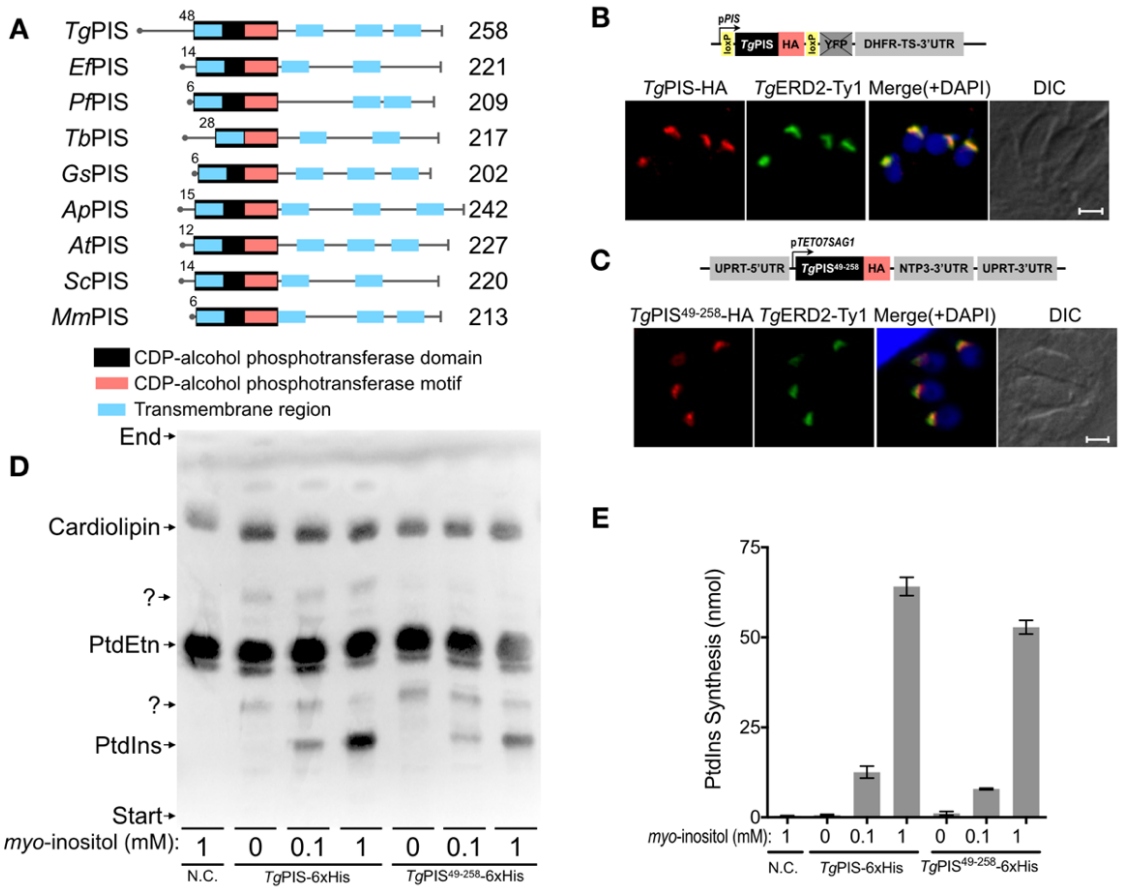

Figure.10: Tachyzoite express a functional PtdIns synthase in the Golgi complex. (A) The primary structures of *Tg*PIS and selected orthologs from different organisms. CDP-alcohol phosphotransferase domains and transmembrane regions were predicted by Simple Modular Architecture Research Tool and transmembrane hidden Markov model. The numbers indicate the size of the N-termini, and the length of full-length proteins. *Ef, Eimeria falciformis; Pf, Plasmodium falciparum; Tb, Trypanosoma brucei; Gs, Galdieria sulphuraria; Ap, Auxenochlorella protothecoides; At, Arabidopsis thaliana; Sc, Saccharomyces cerevisiae; Mm, Mus musculus*. **(B-C)** Immunofluorescence images of transgenic tachyzoites expressing either *Tg*PIS-HA or *Tg*PIS$_{49\text{-}258}$-HA. The truncated isoform lacking the extended N-terminal region was regulated by *pTETO7SAG1* promoter and NTP3-3'UTR. The *Tg*PIS$_{49\text{-}258}$-HA expression cassette was inserted at the UPRT locus by homologous recombination and negative selection with FUdR. Stable transgenic parasites with either of the PIS-HA variants were transfected with a plasmid expressing *Tg*ERD2-Ty1 for co-localization studies. Immunostaining was performed 24 h post-infection using α-HA/Alexa594 (red) and α-Ty1/Alexa488 (green) antibodies. The parasite nuclei were stained with DAPI (blue). Scale bars, 2 µ; DIC, differential interference contrast. **(D)** TLC-resolved lipid profile of *E. coli* strains harboring pQE60 (N.C., negative control), *pQE60-TgPIS-6xHis*, or *pQE60-TgPIS$_{49\text{-}258}$-6xHis* constructs. Expression was induced by 1 mM IPTG, and cultures were supplemented with *myo*-inositol. Lipids were visualized by staining with 8-anilino-1-naphthalenesulfonic acid followed by UV detection. **(E)** Lipid-phosphorous quantification of TLC bands corresponding to PtdIns in panel **D**. Graph shows the mean values with S.E. from 3 different assays. The underlying data were generated by Fatima Heider and Pengfei Kong.

3.1.3 PtdIns synthase is essential for the lytic cycle of *T. gondii*

To investigate the physiological importance of *Tg*PIS in the tachyzoite stage of *T. gondii*, we attempted to delete the *Tg*PIS locus by double homologous recombination. However, the gene was refractory to deletion, suggesting a vital requirement of this enzyme during the lytic cycle, which prevented us from obtaining viable parasites after transgenic selection. To confirm the premise, we implemented the Cre-mediated gene-swap strategy[34] to ablate the *Tg*PIS gene. In this regard, the *Tg*PIS locus was first replaced by a cassette comprising the loxP-flanked (floxed) ORF of *Tg*PIS with a C-terminal HA tag (*Tg*PIS-HA), followed by yellow fluorescence protein (YFP), DHFR-TS-3'UTR and HXGPRT selection marker **(Appendix.2A)**. The method enabled us to get a viable strain (*Tg*PIS-HA_{Floxed}), as confirmed by genomic PCR of clonal transgenic parasites **(Appendix.2B)**. Transfection of the *Tg*PIS-HA_{Floxed} strain with the *pSAG1-Cre* plasmid expressing Cre recombinase (regulated by the *Tg*SAG1 elements) induced excision of floxed *Tg*PIS-HA, repositioning YFP under the control of the *Tg*PIS promoter that resulted in fluorescing *Δtgpis*-$HA_{Excised}$ mutant **(Appendix.2A)**. The mutant could not be drug-selected because it was not feasible to generate a clonal knockout strain. Nevertheless, it allowed us to investigate the effect of genetic ablation on the parasite growth by scoring the progression of the YFP-positive *Δtgpis*-$HA_{Excised}$ strain up to 10 days of transfection **(Appendix.2C-E)**. Indeed, parasites without *Tg*PIS-HA signal but showing YFP expression had much smaller vacuoles, and *vice versa* **(Appendix.2C-D)**. The YFP-positive vacuoles disappeared from mixed parasite culture within 7-10 days **(Appendix.2E)**, confirming the essential nature of *Tg*PIS during the lytic cycle.

Because a *Tg*PIS deletion mutant could not be generated, conditional mutagenesis was implemented. We deployed two established methods based on tetracycline-induced repression[109] and rapamycin-induced U1 snRNP-mediated silencing of transcript[110]. To construct a tetracycline-regulatable strain *(Δtgpisr*), we inserted an extra copy of *Tg*PIS (*Tg*PIS-HA) governed by the *pTETO7SAG1* promoter at the UPRT locus in the RH*Δku80*-

TaTi strain **(Appendix.3A)**, and subsequently replaced the native PIS locus by chloramphenicol acetyltransferase selection marker[111] **(Appendix.3A)**. Crossover-specific PCR screening confirmed the occurrence of 5'- and 3'-homologous recombination events in the mutant **(Appendix.3B)**. RT-PCR showed that the level of *Tg*PIS transcript in the *Δtgpisr* strain was induced 8-fold due to ectopic overexpression when compared to the parental strain **(Appendix.3C)**. Nonetheless, the treatment of the mutant with aTc resulted in 7-fold transcriptional repression, which was well reflected in the protein level by immunofluorescence and immunoblot analyses **(Appendix.3D-E)**. Surprisingly, even though *Tg*PIS-HA was no longer detectable in the *Δtgpisr* strain treated with aTc for 4 days, its growth was only minimally affected (28% reduction) in plaque assays **(Appendix.4)**. Given the essential nature of *Tg*PIS, the data signify that a residual protein expression is sufficient to confer a normal growth to *T. gondii*.

Our inability to achieve a predicted phenotype in the aTc-regulatable mutant prompted us to engineer another strain (*Tg*PIS-3'UTR$_{Floxed}$ mutant) by 3'-insertional tagging of the *Tg*PIS gene with loxP-flanked *Tg*SAG1-3'UTR and HXGPRT, followed by four U1 sites in the RH*Δku80*-diCre strain **(Appendix.5A)**. The clonal mutant can be then treated with rapamycin to activate diCre recombinase for excising the floxed sequence **(Appendix.5A)**. The eventual *Tg*PIS-3'UTR$_{Excised}$ strain lacks a functional 3'UTR and has 4xU1 recognition sites placed at the terminal exon of the *Tg*PIS gene, which induces the degradation of *Tg*PIS pre-mRNA. As strategized, the events of integration and deletion of the floxed sequence at the *Tg*PIS locus were endorsed by genomic PCR **(Appendix.5B)**. The replacement of the endogenous *Tg*PIS-3'UTR by *Tg*SAG1-3'UTR in the *Tg*PIS-3'UTR$_{Floxed}$ strain exerted only a minimal effect in plaque assays with plaque size and number reduced by 8% and 22%, respectively **(Appendix.5C-E)**. In contrast, degradation of *Tg*PIS pre-mRNA in the *Tg*PIS-3'UTR$_{Excised}$ mutant caused severe defects in the plaque formation, which were reduced by 73% and 80% in the size and number when compared to the parental strain. Notably however, the parasite mutant adapted quickly, almost regaining the parental phenotype within 2-3 weeks, yet again impeding the follow-up phenotyping. On

the other hand, both conditional mutants revealed an exceptional resilience of tachyzoites to a transcriptional knockdown of PtdIns synthesis.

3.1.4 Auxin-induced proteasomal degradation of *Tg*PIS is lethal to tachyzoites

Next we resorted to engineering a workable conditional mutant of *Tg*PIS, which would enable us to do in-depth phenotyping and biochemical assays. We therefore deployed the auxin-inducible degradation (AID) system to make a conditional mutant allowing a translational control of protein stability[112]. A CRISPR/Cas9 construct expressing a guide RNA targeting to the 3'UTR region of the *Tg*PIS gene (*pU6-TgPIS*$_{sgRNA}$*-Cas9*) was co-transfected with a PCR-amplified homology-directed-repair template containing a minimal functional AID motif (mAID), 3x HA tag, GRA1-3'UTR and HXGPRT selection cassette to allow recombination-mediated epitope tagging of the native locus by positive selection **(Figure.11A)**. Successful mAID-HA-tagging of PIS was confirmed by screening PCR **(Figure.11B)**, and immunoblot analysis revealed an expected size of about 35-kDa **(Figure.11C)**. As reckoned, the HA signal was no longer detectable after 1 day of auxin exposure **(Figure.11C-D)**. In plaque assays, we observed a severe impairment of the parasite growth following the hormone-mediated depletion of PIS. The plaque size was reduced down to 10% when the *Tg*PIS-mAID-3xHA mutant was treated with 500 µM auxin **(Figure.11E-F)**. Consistently, the parasite growth was ceased after 3-4 passages in regular cultures. The data confirm a physiologically vital role of *Tg*PIS for the lytic cycle of tachyzoites.

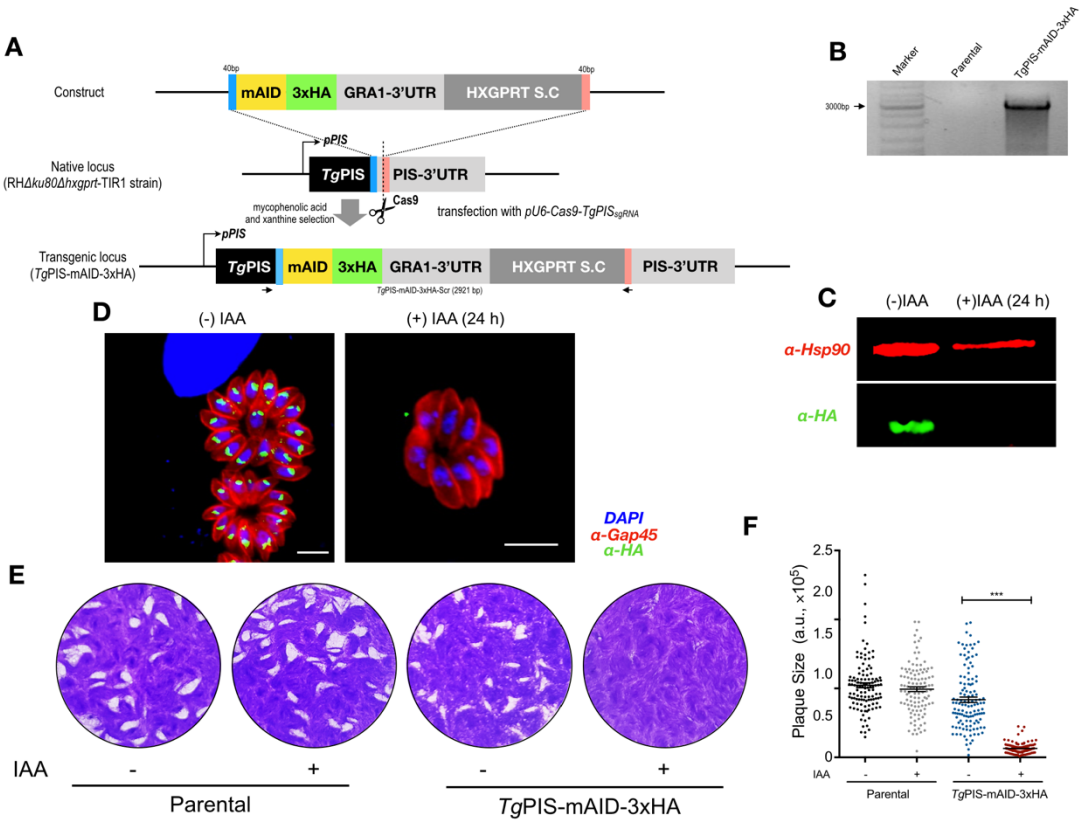

Figure.11: Auxin-induced degradation of *Tg*PIS blights the lytic cycle of tachyzoites. (A) Scheme showing the Cas9-assisted 3'-genomic tagging of *Tg*PIS with a minimal auxin-inducible degron (mAID) and 3x HA epitope. Indicated amplicon (mAID-3xHA-GRA1-3'UTR-HXGPRT) flanked with short (40 bp) crossover sequence (COS) was co-transfected with a *pU6-TgPIS*$_{sgRNA}$*-Cas9* vector (expressing Cas9 and guide RNA) into the RHΔ*ku80Δhxgprt*-TIR1 strain, and drug-selected for the HXGPRT selection cassette (S.C.). The ensuing *Tg*PIS-mAID-3xHA strain expressed C-terminally epitope-tagged *Tg*PIS, enabling its conditional knockdown by auxin treatment. **(B)** PCR confirming the event of 3'-insertional tagging in the *Tg*PIS-mAID-3xHA strain. Primers used for the genomic PCR-screening at the *Tg*PIS locus are marked as arrows in panel **(A)**. **(C)** Western blot imaging show the auxin-dependent degradation of *Tg*PIS after 24 h treatment. Proteins extracted from 10^7 freshly harvested parasites were used for the analysis. α-HA was used to visualize *Tg*PIS (Green), while α-*Tg*HSP90 (Red) was used as loading control. **(D)** Immunofluorescence images showing the dependence of *Tg*PIS expression on auxin in the *Tg*PIS-mAID-3xHA mutant. Parasites were cultured with 500 µM IAA (indole-3-acetic acid) for 24 h, and stained with α-HA and α-*Tg*GAP45 antibodies to visualize *Tg*PIS in the Golgi network (green), and *Tg*GAP45 in the inner membrane complex located just underneath the plasma membrane (red), respectively. DAPI was utilized to highlight the parasite and host-cell nuclei. **(E-F)** Plaque assays showing growth fitness of the *Tg*PIS-mAID-3xHA and parental strains. Crystal violet-stained images **(E)** revealed plaques formed by successive lytic cycles of the indicated strains in the absence or presence of IAA (500 µM). The plaque area, depicted as arbitrary units (a. u.), was measured by ImageJ software. A total of 150-200 plaques for each strain were scored from 3 assays. Size of individual plaques was presented as the dot graph (mean ± S.E.; ***, $p<0.001$).

3.1.5 Depletion of PIS impairs the parasite replication, egress and motility

The auxin-regulated *Tg*PIS-mAID-3xHA mutant enabled additional phenotyping, which permitted us to evaluate individual events of the lytic cycle such as, replication, egress, invasion and gliding motility. Indeed, as shown above using the *Δtgpis*-$HA_{Excised}$ mutant **(Appendix.4)**, we recorded a significant defect in the intracellular replication rate of the auxin-treated *Tg*PIS-mAID-3xHA strain when compared to the parental strain **(Figure.12A)**. A minor impairment in the cell division of the mutant was also observed even under untreated condition that can be attributed to mAID-3xHA tagging and GRA1-3'UTR. Interestingly, the *Tg*PIS-mAID-3xHA mutant also exhibited a defect in egress in normal cultures (-IAA), which was radically accentuated upon inclusion of hormone **(Figure.12B)**. To test whether a curtailed egress may be caused by slow replication, we examined induced egress in response to activation of cGMP signaling by Zaprinast, a phosphodiesterase inhibitor[113]. Certainly, we recorded a notable retrieval in egress of the auxin-treated mutant; however, the defect was still evident **(Figure.12C)**. Unlike natural and induced egress, we did not score any apparent reduction in the invasion efficiency of the mutant irrespective of auxin **(Figure.12D)**. Both events are driven by calcium-dependent activation of gliding motility immediately following the completion of replication[114]. Our appraisal of the parasite motility demonstrated only a modest (but significant and well correlated to induced egress) reduction in the motile fraction and trail length of the mutant after auxin exposure **(Figure.12D)**. Hence, the data advocate a need of *Tg*PIS for efficient cell division and motility-dependent egress.

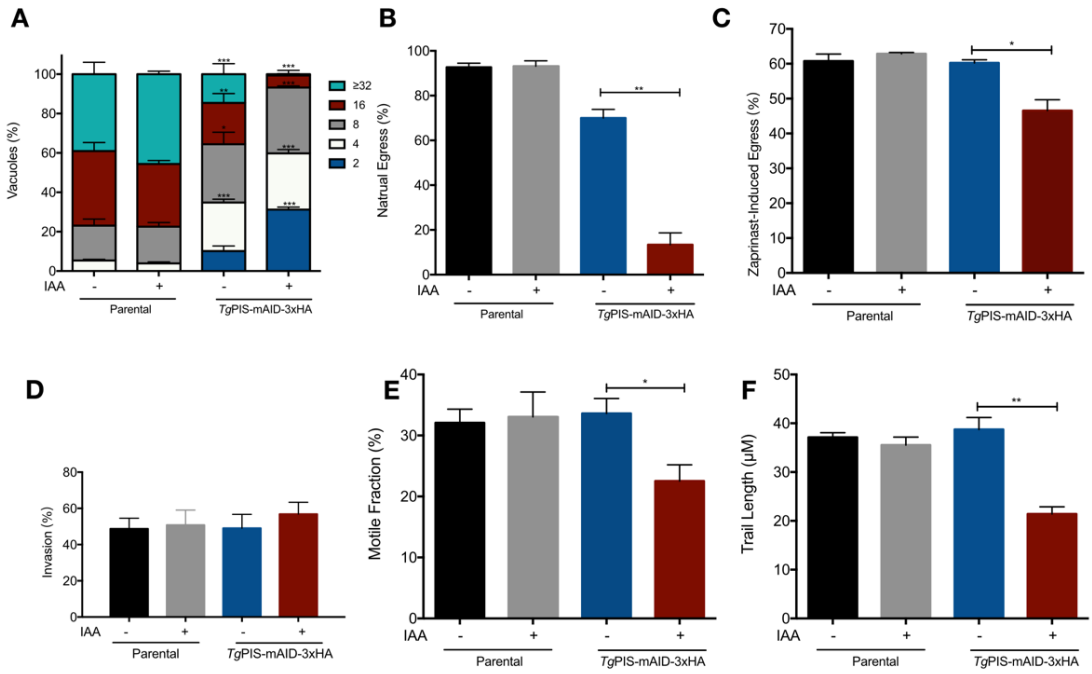

Figure.12: Depletion of *Tg*PIS impairs the replication, egress and gliding motility of tachyzoites. (A) Quantification of tachyzoites within their vacuoles to evaluate the proliferation of the *Tg*PIS-mAID-3xHA mutant with respect to its parental strain (RH*Δku80Δhxgprt*-TIR1). Tachyzoites were pretreated with 500 μM indole-3-acetic acid (+IAA) or 0.1% ethanol (-IAA) for 48 h, and then used to perform the replication assay for 40 h. Graphs show the mean percentage of vacuoles harboring specified number of parasites. A total of 400-500 vacuoles for each condition in both strains were scored (n= 3 assays). **(B-C)** Egress efficiency of the indicated parasites following treatment with IAA (500 μM) or solvent in the absence **(B)** or presence of Zaprinast **(C)**. The latter compound inhibits phosphodiesterases, and consequently induces egress, presumably by activating cGMP signaling within tachyzoites. Parasites were precultured in the presence of IAA or 0.1% ethanol for 48 h prior to setting up egress assays. Parasitized cultures were treated with 500 μM Zaprinast for 30 min to measure drug-induced egress. The natural egress **(B)** was measured 40 h and 64 h post-infection. To quantify egress, intracellular tachyzoites were stained red by α-*Tg*GAP45 antibody, while extracellular ones appeared two-colored (red and green) stained with both α-*Tg*GAP45 and α-*Tg*SAG1 antibodies. The percentage of ruptured vacuoles was determined by numerating 400-500 vacuoles for each strain (n= 3 assays). Note that a severe defect in natural egress is likely due to the delayed replication (see panel **(A)**), while a modestly impaired Zaprinast-induced egress reflects a defective gliding motility. **(C-D)** The motile fraction and trail lengths of the *Tg*PIS-mAID-3xHA and parental strains. Samples were stained with α-*Tg*SAG1 antibody. In total, 600 parasites were analyzed for the motile fraction, and 100 trail lengths were measured using ImageJ software (n= 3 assays). **(E)** Invasion rates of the specified tachyzoite strains. 1,000-1,200 parasites for each strain were scored to calculate the invasion efficiency (n= 3 assays), essentially as described for egress assays. For gliding motility and invasion, parasites were precultured with 500 μM IAA or 0.1% ethanol for 96 h. Numerical values in graphs show the means with S.E. from 3 independent experiments. Statistical significance was measured by comparing the auxin and ethanol-treated samples of each strain (*, p≤0.1, **, p≤0.05, ***, p≤0.001).

3.1.6 Conditional downregulation of PtdIns synthase disrupts homeostasis of anionic lipids

To understand the basis of observed phenotypes, auxin-regulated conditional mutant of *Tg*PIS was subjected to lipidomic analysis. In this regard, we first performed the parasite yield assay as reported earlier[115] to determine an appropriate time point for sample collection. Parasitized cultures of the mutant and parental strains infected at a defined multiplicity of infection were incubated in the absence or presence of auxin, and the yield was calculated after successive rounds of passage **(Figure.13A)**. As expected the growth rate of the parental strain remained unaltered irrespective of hormone treatment. In contrast, the yield of auxin-exposed mutant cultures declined gradually and abrogated after 2 serial passages. We therefore collected lipidomic samples at 96 h time point when the yield dropped to about 75% with respect to control untreated cultures. Lipidomic studies revealed six phospholipid classes, namely PtdCho, PtdEtn, PtdSer, PtdThr, PtdIns and PtdGro in the parental and mutant strains **(Figure.13B)** confirming our earlier reports[39,51]. Surprisingly, the amount of all major lipid species remained unaltered. Especially, given the severity of the phenotype in *Tg*PIS-mAID-3xHA mutant, the reduction in PtdIns upon auxin exposure appeared rather minor, prompting us to investigate in-depth changes in lipid species.

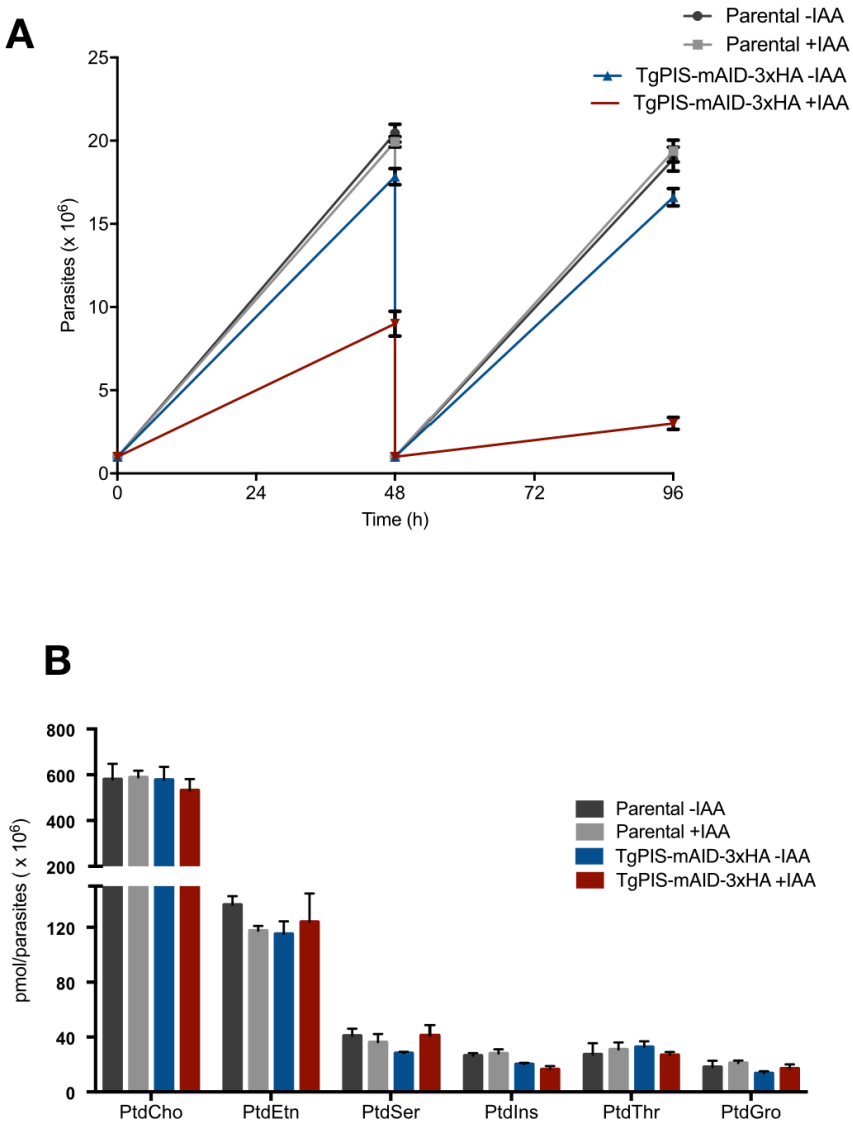

Figure.13: Auxin-mediated depletion of PIS affects phospholipid contents in *T. gondii*. (A) Yield assay of parental and *Tg*PIS-mAID-3xHA. 10^6 tachyzoites of each strain were used to infect HFF cells seeded in petri dish for two generations in presence of 500 µM IAA or 0.1% ethanol. Results of three independent assays were shown (mean ± S.E.). **(B)** Concentration of individual phospholipid species in parental or *Tg*PIS-mAID-3xHA in presence of 500 µM IAA or 0.1% ethanol treatment. Samples were harvested after two generations of culturing as optimized by yield assay. Four replicates of each strain were collected and quantified by lipidomic analysis (mean ± S.E.). (*, p≤0.1, **, p≤0.05, ***, *p*≤0.001)

We quantified the most abundant species of each lipid class in untreated and auxin-treated samples of the parental and PIS mutant strains. *Tg*PIS-mAID-3xHA strain showed a clear shift in selected species of PtdSer, PtdIns and PtdThr **(Figure.14)**. In particular, the PIS

mutant displayed a significant reduction in certain species (C28, C30, C32, C34) of PtdIns after auxin exposure. Similarly, C36 and C38 species of PtdThr were also reduced, whereas C34 and C36 species of PtdSer were increased. The content of individual lipid species was not affected in the parental strain. Species of other major phospholipid classes (PtdCho, PtdEtn, PtdGro) also did not change upon auxin treatment in any of the two strains **(Appendix.6)**. To consolidate our results, we plotted the magnitude of change in all detectable species from all shown phospholipids (irrespective of abundance) in volcano plots, which illustrated the fold-change *versus* statistical significance in response to auxin treatment **(Figure.15A-B)**. As expected, the majority of lipid species in the parental strain showed no perturbation except for some EPC and SM species that were modulated ≥1.5-fold (p value ≤0.05) **(Figure.15A)**. The *Tg*PIS-mAID-3xHA mutant by contrast exhibited significant modulation of several species of PtdIns, PtdSer and PtdThr above the threshold **(Figure.15B)**. As shown in heatmaps **(Figure.15C)**, we noted an evident decline in species of PtdIns and PtdThr, while the level of most PtdSer species was induced. These data together suggest that the knockdown of PIS exerts a selective modulation of certain phospholipids such as, PtdIns, PtdSer and PtdThr.

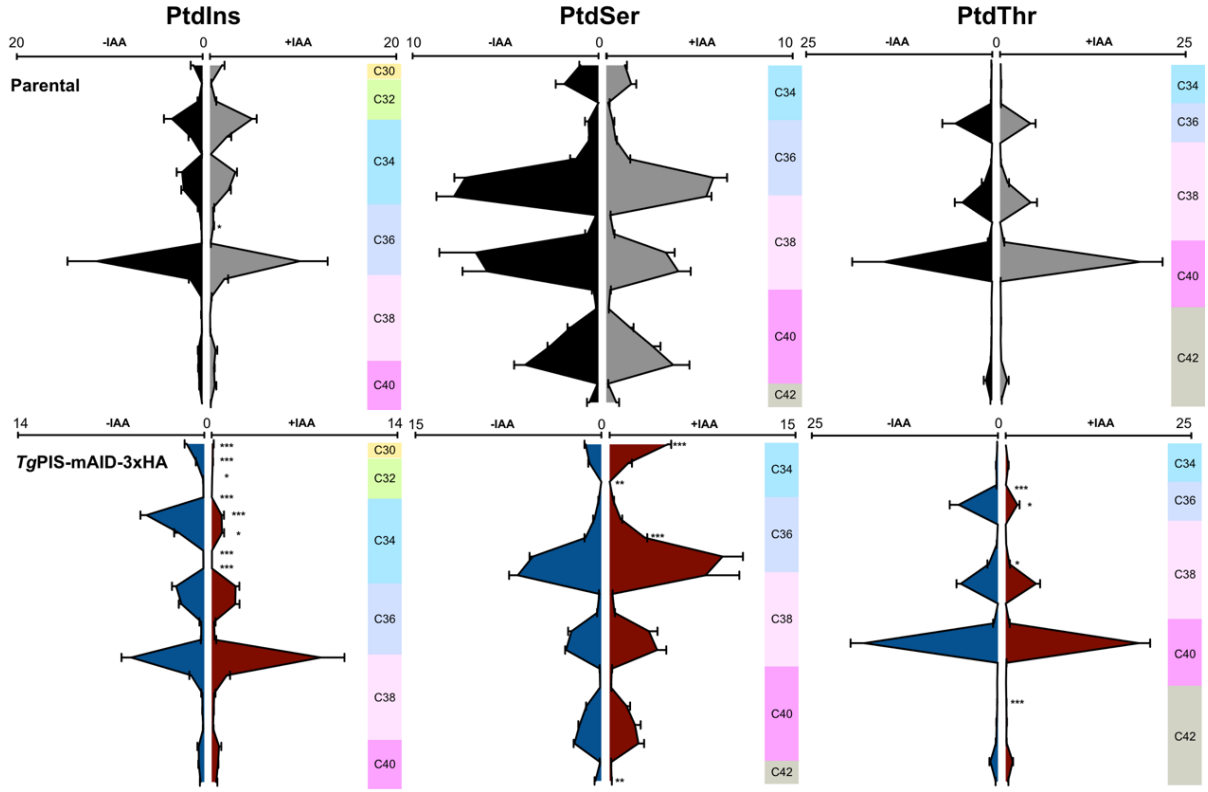

Figure.14: Auxin-mediated down-regulation of *Tg*PIS perturbs PtdIns, PtdSer and PtdThr species. Lipids isolated from the *Tg*PIS-mAID-3xHA mutant and parental strain (RH*Δku80Δhxgprt*-TIR1) were subjected to lipidomic analysis. For each phospholipid class shown, the amount of all major species (accounting for >90% of total lipid) was plotted in pmol/10^6 parasites. Numerical values showing the means with S.E. were from 4 independent experiments. Samples with (+) or without (-) IAA treatments were colored differently for the parental and mutants . Lipid species were ordered based on their acyl chain from top to bottom of the graph. Changes in the contour of violin-like graphs were meant to show the overall variation in given lipids. Statistical significance was measured for each lipid species by comparing auxin-treated and control samples (Student's t test; *, p≤0.1, **, p≤0.05, ***, p≤0.001).

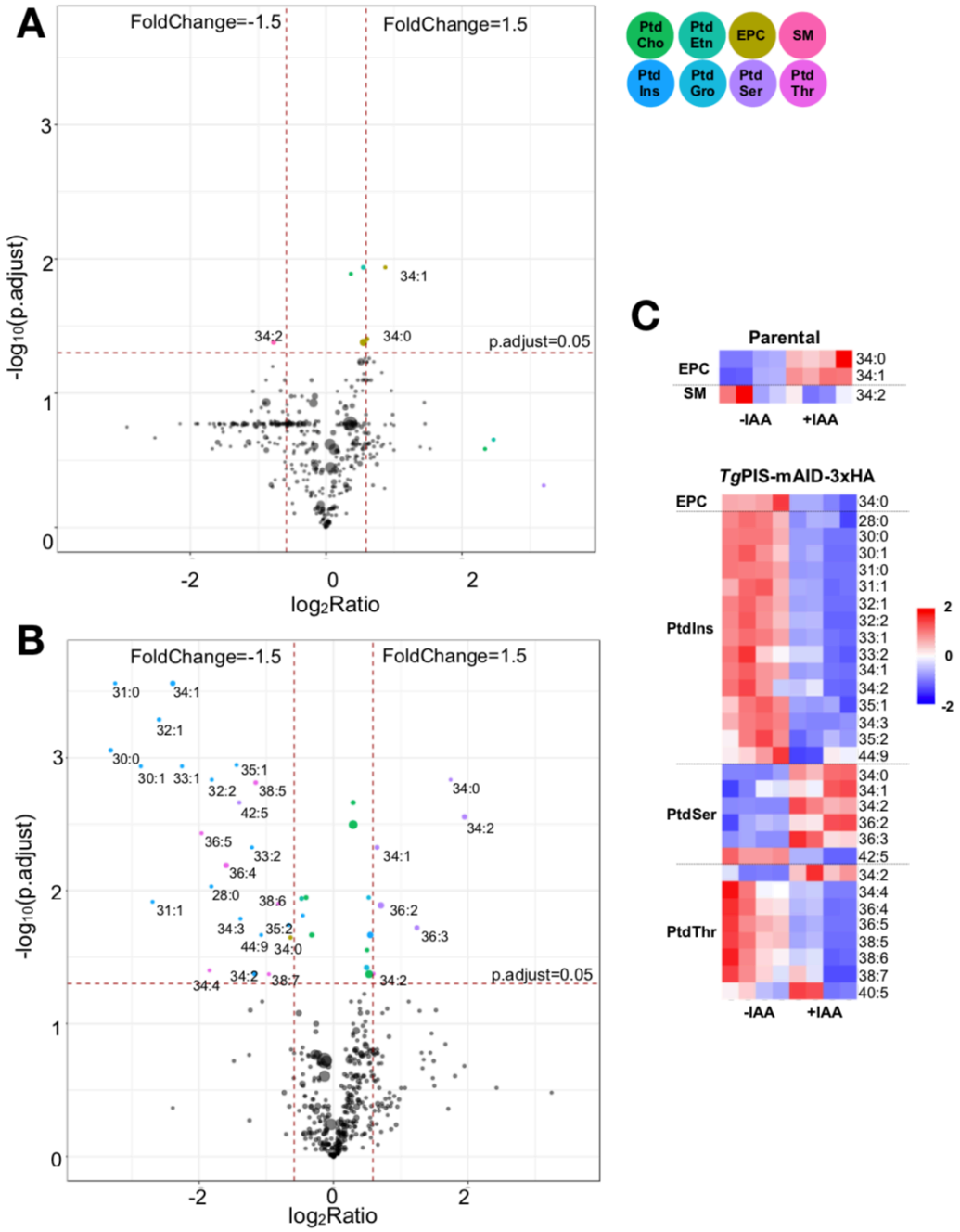

Figure.15: Conditional silencing of PtdIns synthase causes modulation of selected lipid species. (A-B) Volcano plots illustrating changes in all (detectable) lipid species upon auxin treatment of the parental and *Tg*PIS-mAID-3xHA strains. Thresholds of false-discovery rate (FDR)-corrected p-value (<0.05) and fold change (>1.5) were used to define significantly altered metabolites. Lipid species (represented as circles) were scaled to abundance. The lipid species passing the threshold were colored according to phospholipid class, whereas all others were shown in gray/black. The horizontal dashed line corresponds to statistical significance; the two vertical dashed lines to a decrease or increase by a factor 1.5 (n= 4 assays). **(C)** Heatmaps showing the induction or repression of lipid species selected from panel **(A)** and **(B)**. Images were generated by Qlucore Omics Explorer® using FPKM normalization.

3.1.7 Knockdown of PIS perturbs the anionic phospholipids and membrane stability

The above results prompted us to deduce the effect of PIS mutation on the physical-chemical related properties of membrane lipids. In this regard, we generated violin plots based on calculated equivalent carbon numbers (ECN) for all indicated lipid classes **(Figure.16)**. The ECN is commonly used in reversed phase chromatography of lipids and proportional to the strength of interaction between a lipid and the hydrocarbon tails of the stationary phase[116,117]. In biological membranes, hydrophobic interactions between lipids with higher ECN are stronger and *vice versa*.

The ECN can therefore be regarded as one of the key characteristics determining the membrane stability. When the ECN density of major lipids was plotted, we observed alterations in the contour of PtdIns, PtdThr, PtdSer and PtdGro as well as one minor lipid Bis(monoacylglycerol)phosphate (BMP) in the PIS mutant upon auxin treatment, but not in the parental strain. The ECN results resonated rather well with our analysis of individual lipid species **(Figure 14-15)**. Because the lipids showing modulation in the PIS mutant are anionic in nature, it seems as if the parasite attempts to balance the overall membrane charge by selectively regulating anionic phospholipids.

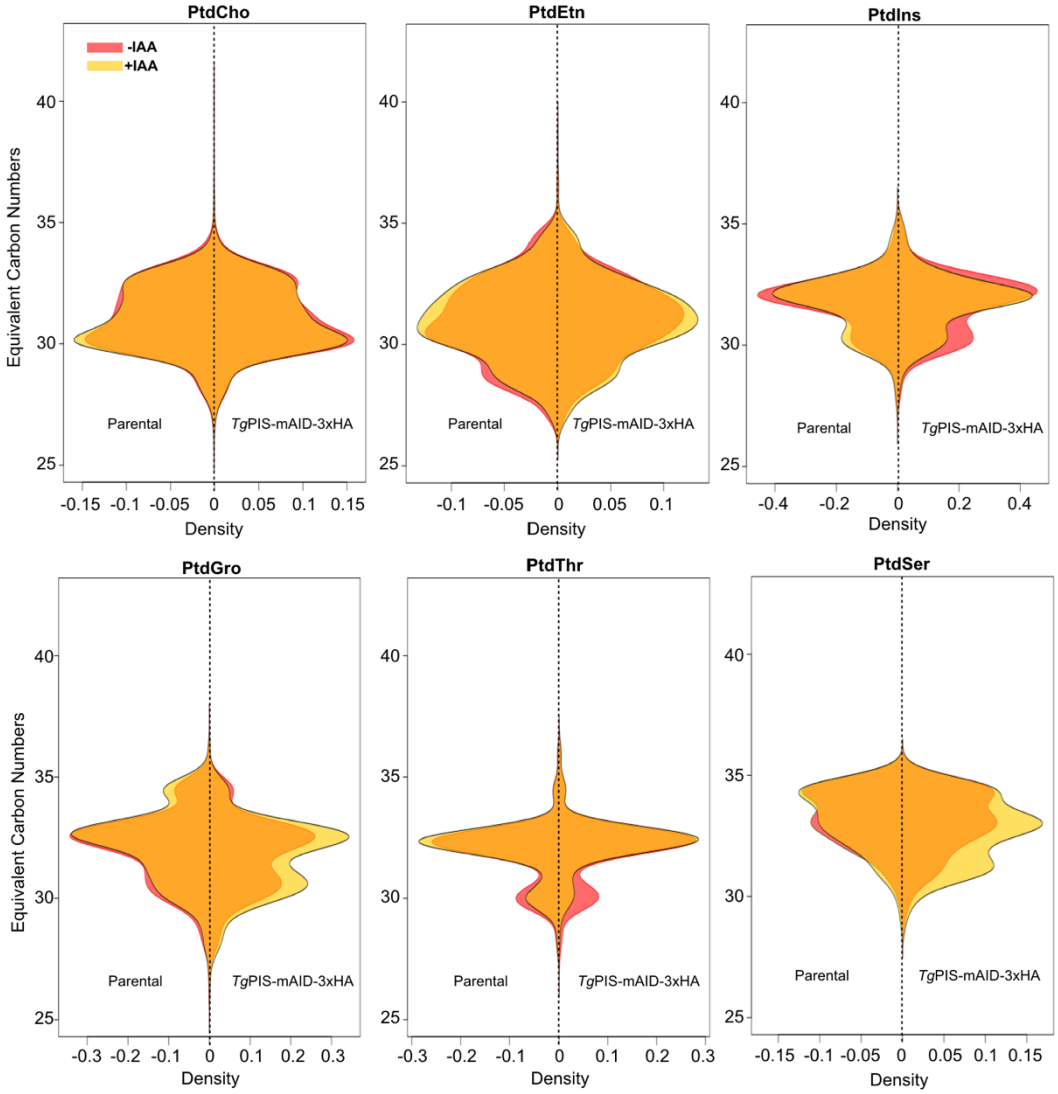

Figure.16: Knockdown of *Tg*PIS alters the ECN profile of anionic phospholipids. Violin plots of the acyl chain composition for the major phospholipid classes. Based on the acyl chain length and degree of unsaturation, equivalent carbon number (ECN) were calculated for all detectable lipid species. For each phospholipid class, the ECN density was calculated and plotted for parental strain (to the left) and *Tg*PIS-mAID-3xHA strain (to the right) as shown. In each panel, an overlay of the ECN density was shown in the presence (red) or absence (yellow) of IAA. Note that the treatment of IAA in both strains had little effect on the ECN profiles of the major glycerophospholipid classes PtdCho and PtdEtn. In contrast, repression of PtdIns synthase resulted in a notable decrease of species with a low ECN in PtdIns and PtdThr (red), while a significant increase in PtdSer, PtdGro and BMP (yellow) could be detected in the *Tg*PIS-mAID-3xHA strain.

3.2 PtdEtn biogenesis in *T. gondii*

3.2.1 *T. gondii* encodes mammalian-like *Tg*CCT and *Tg*ECT

Next, we aim to study the biogenesis of PtdEtn by focusing on the rate-limiting enzyme *Tg*ECT. Because of the high structure similarity between ECT and CCT, we first tried to distinguish the two cytidylyltransferases. Through motif analyses based on ToxoDB, we identified two hypothetical candidates termed *Tg*CCT (*Tg*GT1_216930) and *Tg*ECT (*Tg*GT1_310280). We extracted sequence information from representative species of apicomplexan, kinetoplastid and mammalian cell for comparison. We employed InterProScan, a tool that can be used for the prediction of conserved motif, for the sequence analysis, and thereby located the catalytic domain of selected genes **(Figure. 17)**.

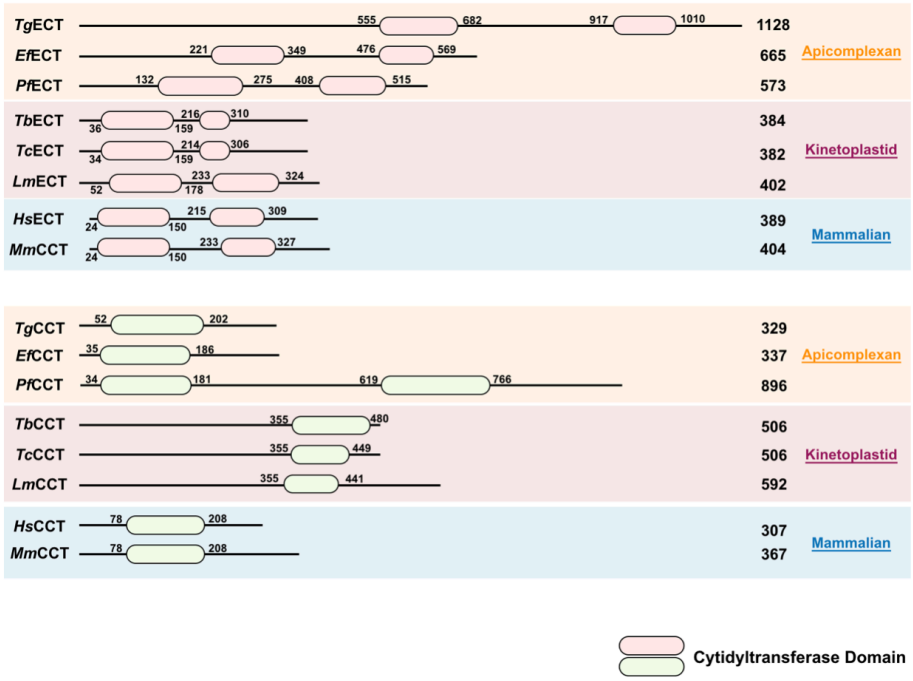

Figure.17: Sequence alignment of hypothetical *Tg*ECT/CCT and predicted or tested ECT/CCT from other organisms. The number of amino acid in each protein was shown on the right side. The predicted regions of cytidylyltransferase domain were highlighted in green (ECT) and red (CCT). Shown numbers were the starting and ending residue of each domain. *Tg, Toxoplasma gondii; Ef, Eimeria falciformis; Pf, Plasmodium falciparum; Tb, Trypanosoma brucei; Tc, Trypanosoma cruzi; Lm, Leishmania major; Hs, Homo sapiens; Mm, Mus musculus.* Detail of selected sequences was shown in Table S2.

There are two functional CCTs identified in human and mouse species[118] , while only one CCT could be annotated in apicomlexan and kinetoplastid parasites. BLAST analysis revealed that CCT from *T. gondii* are more alike to CCTα from mammalian cell, which is the main CCT accounting for the *de novo* synthesis of PtdCho[118]. All CCTs selected for sequence alignment possess one functional domain with the exceptional of *Pf*CCT, which contains an extra catalytic region near C-terminal. Higher similarities in structure were observed between *Tg*CCT and *Ef*CCT in comparison to mammalian-type CCTs, with a length of 300 residues and catalytic motif near N-terminal or in the center, while the structure of kinetoplastid CCTs shows significant differences. The length of selected kinetoplastid-type CCTs is above 500 residues, with predicted catalytic center located near C-terminal instead of being at the N-terminal or in the central region.

All ECTs selected for the alignment are around 300-600 residues in length with two cytidylyltransferase motifs. In addition, the hypothetical *Tg*ECT encodes a long N-terminal extension which does not harbor a conserved domain that can be predicted by BLAST. This extension makes the protein nearly three times longer than the mammalian-type ECT. The sequence alignment of the two functional motifs however, revealed high-conservation at the catalytic center of cytidylyltransferase motifs **(Appendix.7).** Because of the high similarities between *Tg*ECT and tested ECTs, this work focused on that protein for the functional study.

3.2.2 *Tg*ECT is crucial for the intracellular replication of *T. gondii*

Our attempt to delete *Tg*ECT in RH strain failed, suggesting that the *Tg*ECT is likely to be essential for the lytic cycle of *T. gondii*. Thus, we constructed conditional mutant with AID-system. CRISPR/Cas9 construction allowing the expression of Cas9 and guide RNA targeting at the 3'UTR region of *Tg*ECT was co-transfected with a PCR-amplicon containing AID, HA epitope tag and DHFR-TS selection marker, which was used as template for

homology-direct-repair (HDR) **(Figure.18A)**. The successful integration of AID-motif and HA-tag was confirmed by screening PCR using primers binding to the upstream of integration locus and the C-terminal of insert **(Figure.18B)**. By using *Tg*HSP90 as co-localization marker[119], we revealed the cytosolic localization of *Tg*ECT *via* immunofluorescence assay, and confirmed that the expression of *Tg*ECT can be shut down with the presence of IAA, as expected **(Figure.18C-D)**. Severe growth defect was witnessed in plaque assay in the presence of auxin. No plaques could be detected when *Tg*ECT-AID-3xHA was treated with 100 μM IAA, while the addition of IAA did not affect the growth of the parental strains **(Figure.18E-F)**.

Auxin-regulated conditional knockdown of *Tg*ECT paved the way for in-depth phenotyping to investigate the role of *Tg*ECT during events of lytic cycle. We monitored the replication and egress processes of *Tg*ECT-AID-3xHA with or without the treatment of IAA, and recorded significantly reduction **(Figure. 19A)** when treated with 100 μM IAA. After 48 h infection there was no parasite vacuole containing more than 8 tachyzoites detected. The natural egress in auxin-treated *Tg*ECT-AID-3xHA strain was also impaired, only less than 10% tachyzoites could egress from PV after 64 h infection. However, when the parasites were induced to egress by Zaprinast, the auxin-treated *Tg*ECT-AID-3xHA can egress normally, suggesting that the egress capacity of the parasites was not affected by knockdown of *Tg*ECT. Taken together, our result revealed the crucial role of *Tg*ECT in the intracellular replication of the parasite.

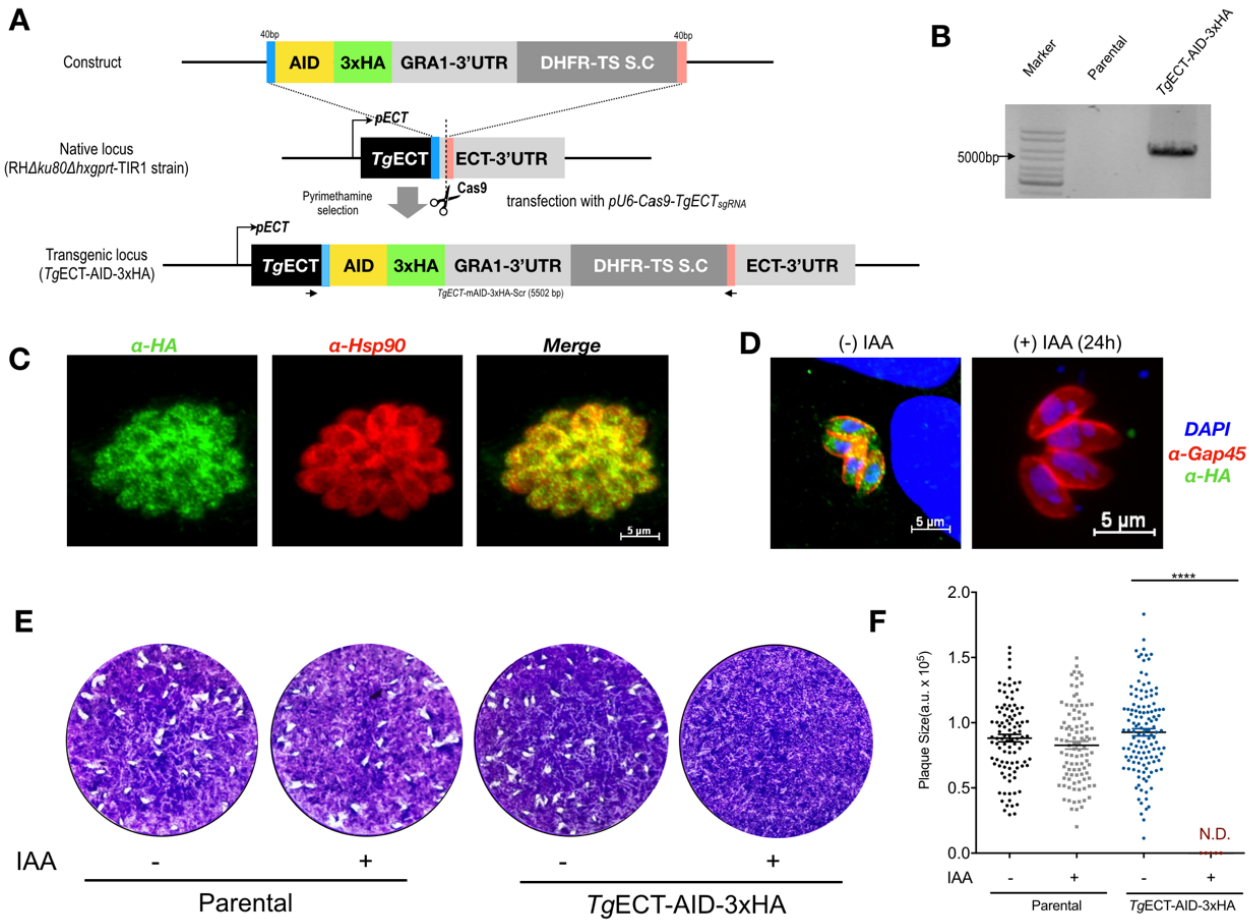

Figure.18: Auxin-induced degradation of *Tg*ECT confers a lethal phenotype to *T. gondii.* (A) Scheme showing CRISPR-assisted 3'insertional tagging of *Tg*ECT with auxin-inducible degron related components. Template used for HDR containing short (40 bp) crossover sequence (COS) was transfected to the RH*Δku80Δhxgprt*-TIR1 together with *pU6-Cas9-TgECT*$_{sgRNA.}$ **(B)** Screening PCR confirmed the integration of HDR template to the *Tg*ECT locus. Primer binding sites of the screening were marked as arrows in panel **(A)**. **(C-D)** Immunofluorescence images showing the punctum cytosolic localization and auxin-dependent regulation of *Tg*ECT. Fresh parasites were harvested and cultured for 24 h with or without 100 μM IAA (indole-3-acetic acid), fixed and stained

with α-HA and α-*Tg*GAP45/α-*Tg*HSP90 for visualization. HA-tagged *Tg*ECT was shown in green and *Tg*GAP45/*Tg*HSP90 stained inner membrane complex/cytosol was shown in red. **(E-F)** Plaque assays showing the growth fitness of *Tg*ECT-AID-3xHA and parental strains in presence of 100 µM IAA or 0.1% ethanol. Crystal violet-stained images **(E)** reveal plaques formed by successive lytic cycles of the indicated strains in the absence or presence of IAA (100 µM). The plaque area, depicted as arbitrary units (a.u.), was scored by ImageJ software. A total of 100-150 plaques for each strain were quantified from 3 assays. Size of individual plaques was presented as the confetti plot (mean ± S.E.; ***, p<0.001).

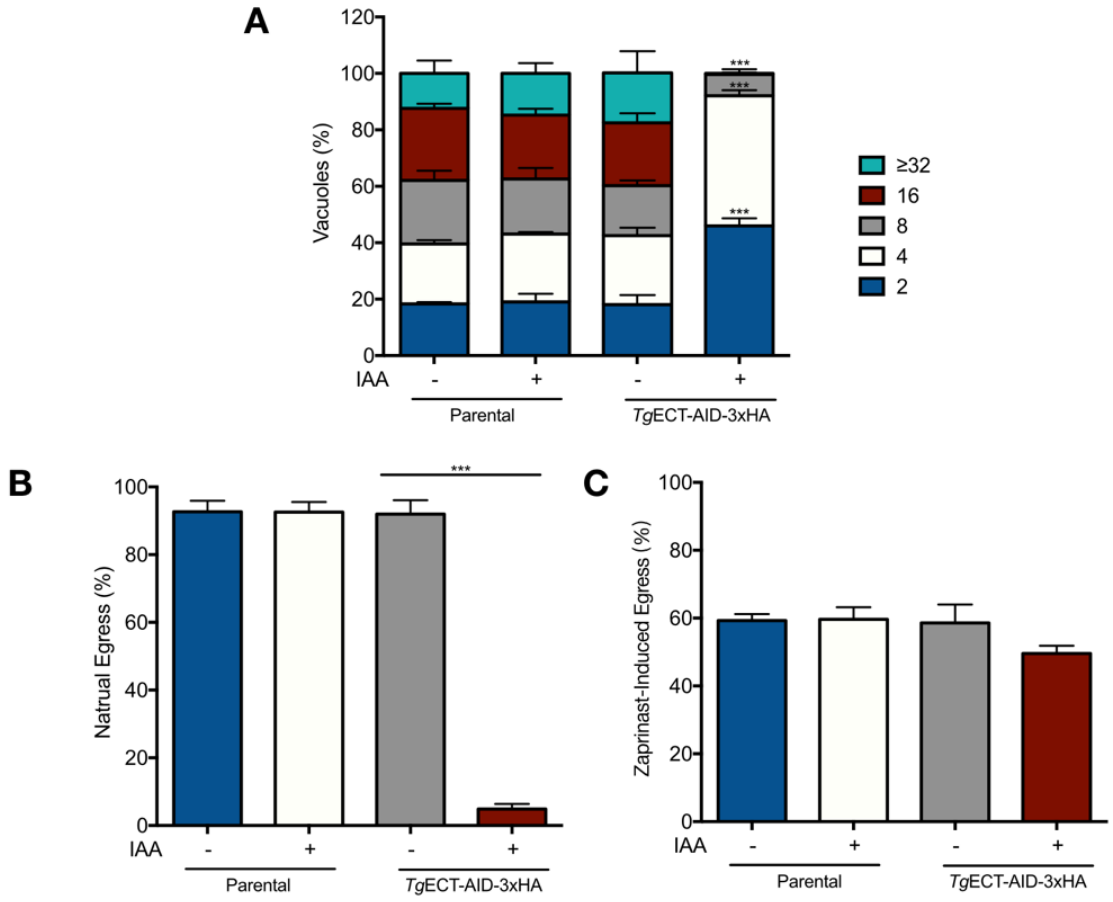

Figure.19: Depletion of *Tg*ECT delays the replication process of tachyzoites but does not affect the egress. (A) Quantification of the PVs containing different number of parasites to evaluate the replication profile of the *Tg*ECT-AID-3xHA mutant with respect to the parental (RH*Δku80Δhxgprt*-TIR1). All samples were treated with either 0.1% ethanol (-) or 100 µM IAA (+) for 40 h and fixed for further staining. Graphs indicate the fractions of PVs containing different numbers of parasites. In total >400 vacuoles for each assay were quantified. **(B-C)** Egress efficiency of selected parasites following treatment of IAA 100 µM. For natural egress **(B)**, parasite samples treated either with 0.1%

ethanol (-) or 100μM IAA (+) were harvested and fixed at 40 h/64 h post infection. The egress rate was determined by the ratio of numbers of integrated vacuole counted at both time points. For Zaprinast-induced egress **(C)**, parasites treated with either 0.1% ethanol (-) or 100 μM IAA (+) were fixed 24 h post infection, and treated with 500 μM Zaprinast. Egress rate was determined by the ratio of numbers of integrated vacuole in induced group *versus* non-induced group. Numerical values in graphs show the means with S.E. from 3 independent experiments. Statistical significance was measured by comparing the auxin and ethanol-treated samples of each strain (***, p≤0.001).

3.2.3 Conditional deletion of *Tg*ECT dysregulates phospholipid biogenesis.

To further investigate the role of *Tg*ECT in phospholipid biogenesis, we conducted lipidomic analyses using *Tg*ECT-AID-3xHA transgenic line. In prior to the analysis, we performed yield assay as reported earlier to determine the time point for sample collection **(Figure.21A)**. Proliferation of parental line was not altered when being treated with IAA, while the hormone conferred significant delay to the growth of *Tg*ECT-AID-3xHA mutant. After 48 h treatment the parasite yield dropped nearly 90%. Thus, we chose 48 h post infection as the time point for sample collection.

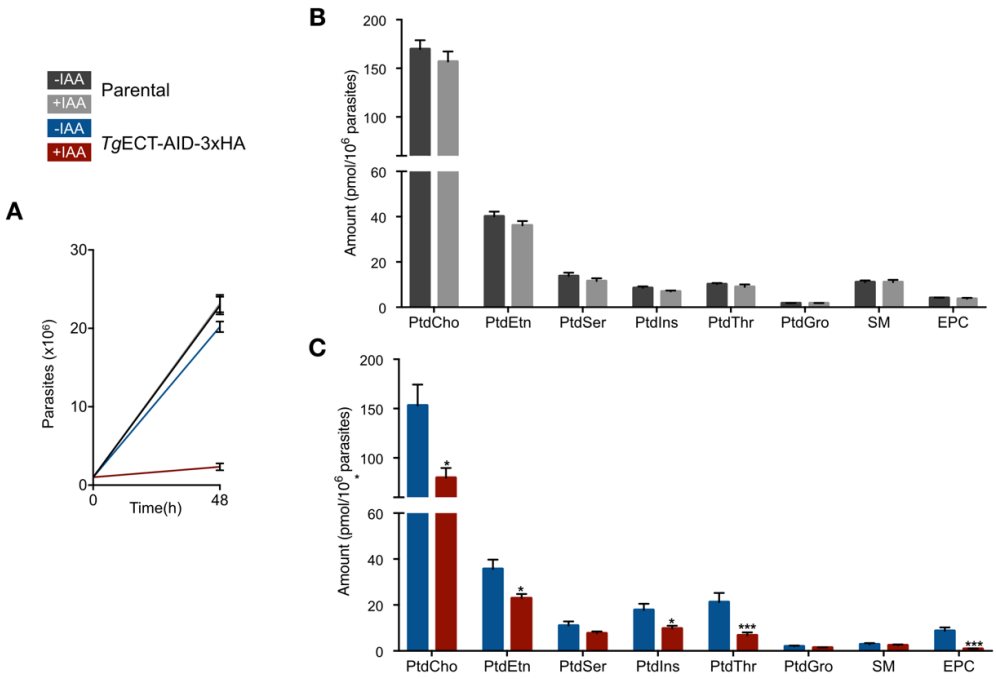

Figure.20: Auxin-mediated depletion of *Tg*ECT impairs phospholipid biogenesis in *T. gondii*. **(A)** Yield assay of parental and *Tg*ECT-AID-3xHA. 10^6 freshly harvested tachyzoites of each strain were used to infect HFF cells seeded in petri dish for 48 h in presence of 100µM IAA (+IAA) or 0.1% ethanol (-IAA). Results of three independent assays were shown (mean ± S.E.). **(B-C)** Concentration of phospholipid species in parental **(B)** or *Tg*ECT-AID-3xHA **(C)** in presence or absence of 100 µM IAA treatment. Samples were harvested after 48 h post infection, as optimized by yield assay. Five replicates of each strain were collected and quantified by lipidomic analysis (mean ± S.E.). (*, p≤0.1, **, p≤0.05, ***, *p*≤0.001)

Lipidomic analysis revealed significant reduction in all detectable phospholipid classes of auxin-mediated *Tg*ECT-AID-3xHA mutant, whereas the addition of auxin conferred very slight effect in parental strain **(Figure.20B-C)**. However, we noticed that the total phospholipid content detected by HPLC-MS in parental -IAA group was four times less comparing to same parental -IAA group that was used in *Tg*PIS lipidomic study, as well as reported in other publication[39] **(Appendix.7A)**. We calculated the percentage of major glycerophospholipid class, and found that the composition of phospholipid was not altered. Therefore, we assumed that the abnormal phospholipid content calculated from the lipidomic data was likely due to inappropriate usage of response factor for the calculation, or less efficient phospholipid extraction from the parasite. To avoid any misleading statements from the pending actual amount, we reported our data in relative abundance with a normalized dataset. The average phospholipid content of the five replicates of non-treated parental and *Tg*ECT-AID-3xHA were calculated and set to 100%. The relative abundance was therefore calculated by comparing the phospholipid content of each replicates (both -IAA and +IAA) to the average as illustrated **(Figure.21A)**.

We found that the alternation of phospholipid content in parental strain treated with +IAA was negligible, while significant decrease of PtdCho, PtdEtn, PtdIns, PtdThr and EPC was observed **(Figure.21B-C)**. The level of PtdCho and PtdEtn declined 52% and 54%, while PtdSer, PtdIns and PtdGro decreased by 31%, 46% and 29%, respectively. PtdThr was the most affected glycerolphospholipid, only 31% of PtdThr could be detected comparing to the

control group. For sphingolipids, SM was only slightly affected, while EPC decreased by 90% in *Tg*ECT-AID-3xHA mutant.

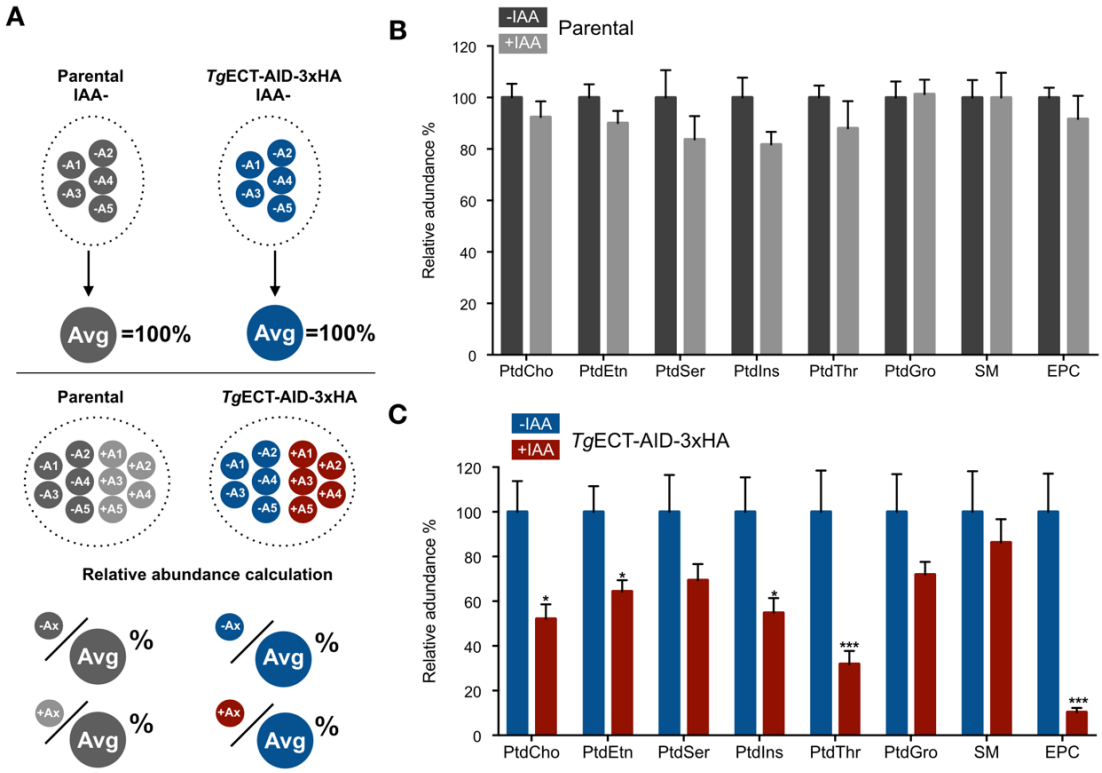

Figure.21: Auxin-induced knockdown of *Tg*ECT leads to impaired phospholipid biogenesis in *T. gondii*. (A) Schematic showing the normalization strategy for calculation of the relative abundance. **(B-C)** Relative abundance of phospholipid species in parental **(B)** or *Tg*ECT-AID-3xHA **(C)** in presence or absence of 100 µM IAA treatment. Samples were harvested after 48 h culturing as optimized by yield assay. Five replicates of each strain were collected and quantified by lipidomic analysis (mean ± S.E.). (*, p≤0.1, **, p≤0.05, ***, *p*≤0.001) *Avg: average.*

For in-depth analysis, we plotted the phospholipid species of each class of all 8 phospholipid classes. The most abundant phospholipid species (accounting for >90% of each class) were plotted for the analysis **(Figure.22)**. We observed obvious shift in species in nearly every phospholipid classes. Among those, PtdGro and SM were the unaffected classes, C32 species of PtdGro exhibited a 50% reduction, whereas none of the species of SM was altered significantly. The C36:0 and C40:3 species of SM however, exhibited an up-regulation of nearly 2-fold. Overall reduction of PtdCho, PtdIns PtdEtn, PtdSer species was detected, with exception of several species namely PtdCho C36:4 (2.7-fold

upregulation) , PtdEtn C38:4 (1.5-fold up-regulation) and C40:5 (1.5-fold up-regulation), PtdSer C42:5 (2.5-fold upregulation) and PtdIns 38:4 (1.1-fold up-regulation). All detected species of PtdThr and EPC were down-regulated in auxin-mediated *Tg*ECT knockdown strain.

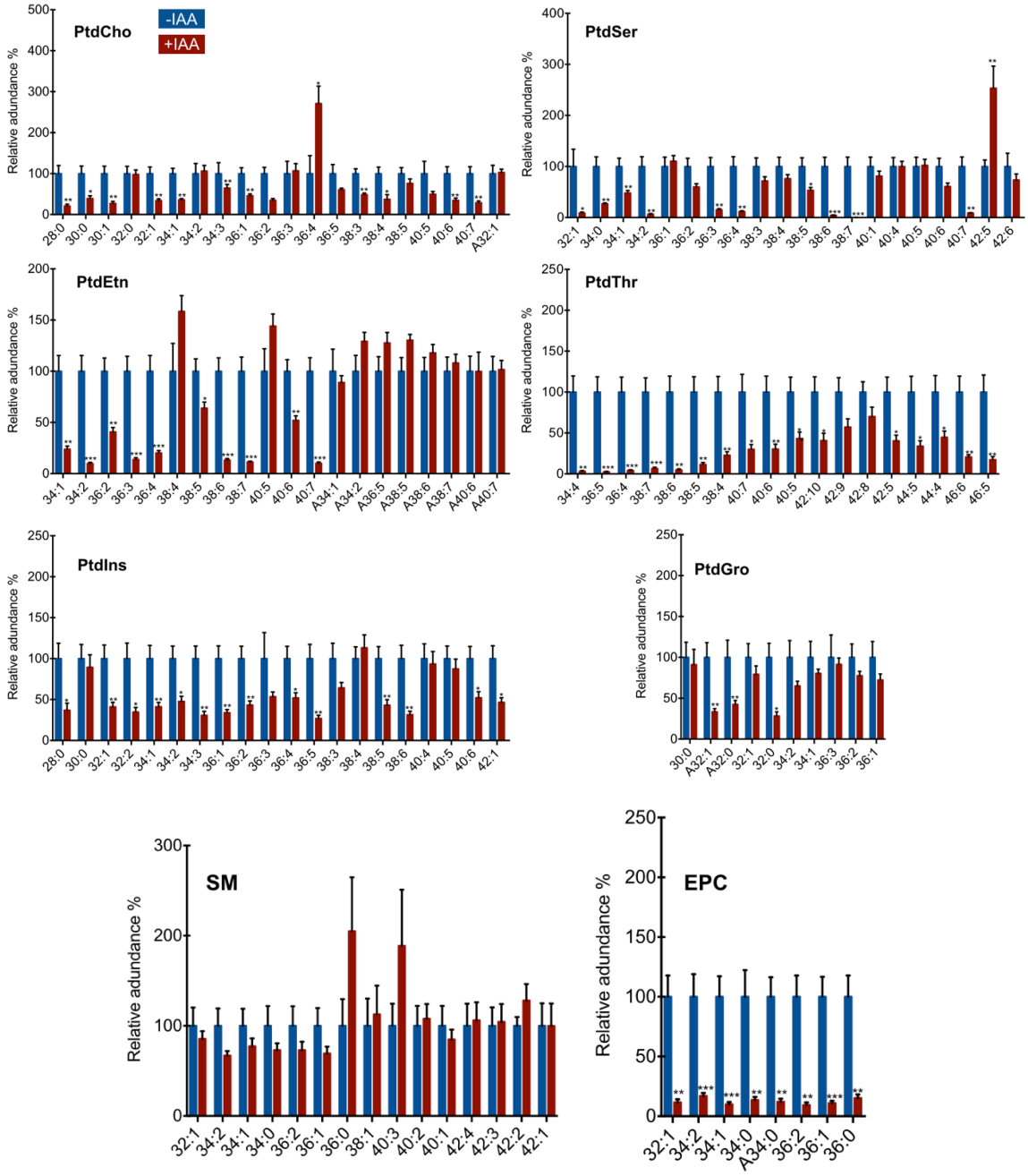

Figure.22: Deletion of *Tg*ECT disrupts the content of several phospholipid species. Lipids isolated from the *Tg*ECT-AID-3xHA mutant were subjected to lipidomic analysis. For each phospholipid class shown, the amount of all major species (accounting for >90% of total lipid) was normalized to relative abundance as described. Values comes from samples collected from 5

independent replicates. Statistical significance was measured for each lipid species by comparing -IAA and +IAA groups. (Student's t test; *, p≤0.1, **, p≤0.05, ***, p≤0.001).

Interestingly, we noticed in the species-based analysis that, the extent of phospholipid down-regulation differed. Some species exhibited an even stronger decrease than the rest, which were barely detectable. To highlight these species, we set a threshold at 85% reduction in response to auxin-treatment **(Figure.23)**. We noticed C34:2, C38:6, C38:7 and C40:7 species were all missing from PtdEtn and PtdSer. Moreover, we found C38:6 and C38:7 of PtdThr also reduced upon ECT-depletion. Not surprisingly, nearly all (6 out of 8) species of EPC exhibited a reduction of more than 85%, suggesting *Tg*ECT plays an important role in EPC biogenesis.

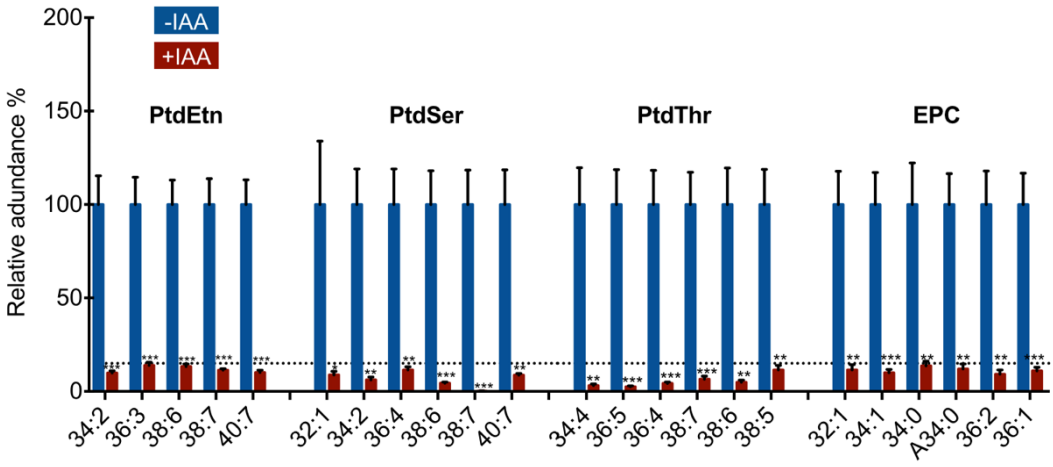

Figure.23: Auxin-mediated depletion of *Tg*ECT nearly abolishes the biogenesis of phospholipid species from PtdEtn, PtdSer, PtdThr and EPC. Lipids isolated from the *Tg*ECT-mAID-3xHA mutant were subjected to lipidomic analysis. For each phospholipid class shown, the amount of all plotted species was normalized in relative abundance as described. Values come from samples collected from 5 independent replicates. Dotted line marked 15% of relative abundance. Statistical significance was measured for each lipid species by comparing IAA+ and IAA- groups. (Student's t test; *, p≤0.1, **, p≤0.05, ***, p≤0.001).

Based on the lipidomic results, we concluded that the disruption of *Tg*ECT leads to impaired biogenesis of nearly all phospholipid classes in *T. gondii*. At the same time, a few phospholipid species of PtdEtn, PtdSer and PtdThr seem to depend strictly on the expression of *Tg*ECT. Among sphingolipids, the content of SM is not affected by the

repression of *Tg*ECT; whereas the synthesis of all EPC species in the *Tg*ECT mutant is nearly ablated.

3.2.4 Identification of an insect-type EPC-synthase (EPCS) in *T. gondii*

The *Tg*ECT-dependent biogenesis of EPC raises questions as to why *Tg*ECT is essential for the process. In mammalian cells, EPC is synthesized by sphingomyelin synthase (SMS) using ceramide and PtdEtn[120]. In addition, different types of SMSs drive the synthesis of SM and IPC in a similar manner, using ceramide and PtdCho/PtdIns as the donor phospholipid[121] **(Figure.24A)**. In *T. gondii*, one mammalian-type SMS termed *Tg*SLS has been identified[122]. However, *in vitro* enzymatic assay using ectopically expressed *Tg*SLS in yeast did not lead to the production of any sphingolipids other than IPC, indicating that the parasite is likely to use another pathway for EPC biogenesis.

Insects take a different strategy to realize EPC production which uses CDP-ethanolamine instead of PtdEtn as the doner[123]. In *T. gondii*, CDP-ethanolamine is synthesized by *Tg*ECT, hence the decrease in of *Tg*ECT enzyme is likely to block the synthesis of EPC. Thus, we hypothesize that *T. gondii* harbors a strategy similar to insects for EPC biogenesis. In *Drosophila*, the reaction is carried out by an insect-type EPCS, previously described as CerPE-synthase (CPES), which belongs to CDP-alcohol phosphotransferase superfamily. It contains highly-conserved functional motif ($DX_2DGX_2ARX_{8/9}GX_3DX_3D$). We screened ToxoDB for the presence of the proteins belonging to the CDP-alcohol phosphotransferase superfamily. *T. gondii* encodes four proteins of the CDP-alcohol phosphotransferase superfamily, including PIS reported in this work **(Figure.24B)**. Other than *Tg*PIS， the other two of them have been previously studied and annotated as *Tg*CEPT1 and *Tg*CEPT2[49]. Therefore we assumed the one which is currently annotated as a hypothetical protein to be *Tg*EPCS. *Tg*EPCS **(Figure.24C)** exhibited a CRISPR-score[124] of -3.94, suggesting it is

likely to be critical for the lytic cycle of the parasite. As it is assumed essential, we deployed AID-mediated strategy to construct a mutant allowing for conditional knockdown of the hypothetical gene.

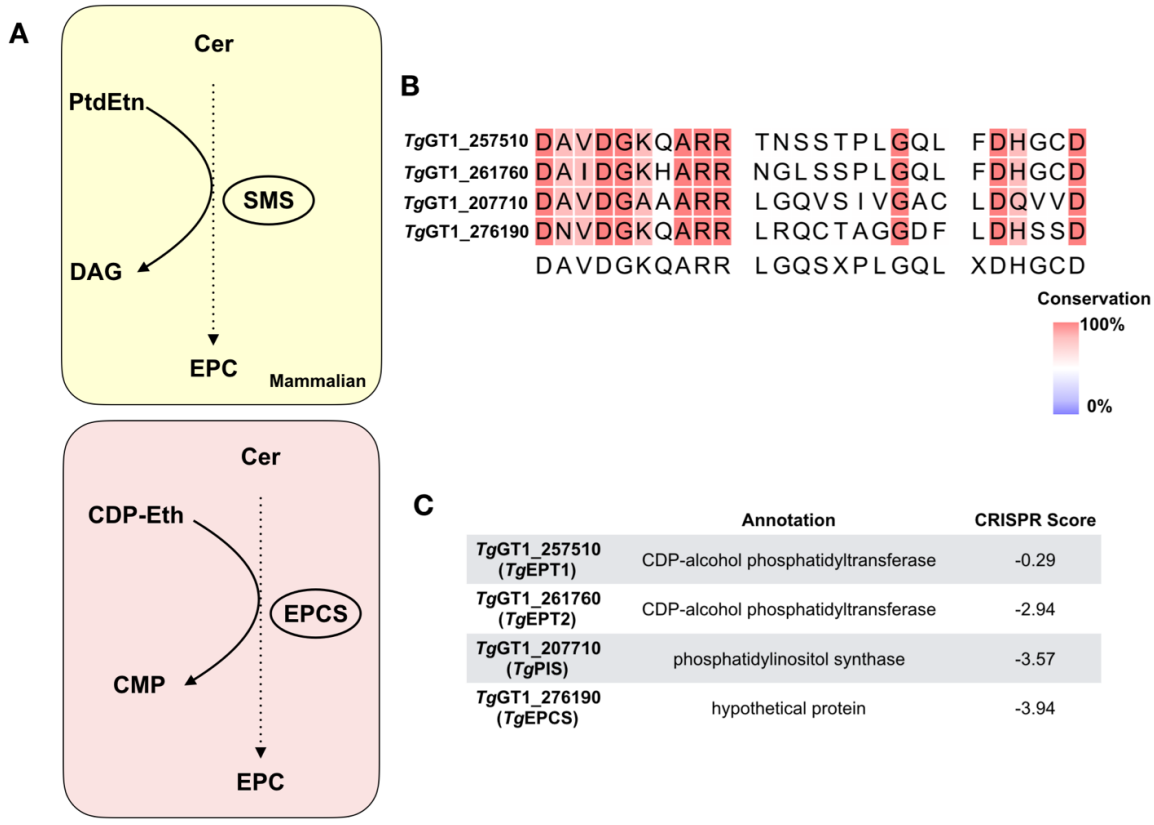

	Annotation	CRISPR Score
*Tg*GT1_257510 (*Tg*EPT1)	CDP-alcohol phosphatidyltransferase	-0.29
*Tg*GT1_261760 (*Tg*EPT2)	CDP-alcohol phosphatidyltransferase	-2.94
*Tg*GT1_207710 (*Tg*PIS)	phosphatidylinositol synthase	-3.57
*Tg*GT1_276190 (*Tg*EPCS)	hypothetical protein	-3.94

Figure.24: Identification of an insect-type EPCS in *T. gondii*. (A) Scheme showing biogenesis of EPC in mammalian cell (yellow) and in insects (red). **(B)** Sequence alignment of the catalytic motif of four CDP-alcohol phosphatidyltransferases in *T. gondii.* Color coding of the sequences indicates the conservation. **(C)** Annotation and CRISPR-score of four selected proteins obtained from ToxoDB. As reported by *Sidik SM .et.al*[124] , proteins with CRISPR-score <- 3 is likely to be important for the lytic cycle. *Cer: ceramide, SMS: sphingomyelin synthase, CDP-Etn: CDP-ethanolamine, CMP: Cytidine monophosphate.*

We co-transfected CRISPR/Cas9 system containing guide-RNA targeting at 3'UTR region of *Tg*EPCS with PCR amplicon containing auxin-regulated degron together with DHFR-TS cassette that allows for drug selection **(Figure.25A)**. To verify the successful integration, screening PCR was performed which revealed a 5 kb band only in transgenic line **(Figure. 25B)**. Using antibody against *Tg*SERCA (an ER marker), we revealed that *Tg*EPCS located at ER in tachyzoites **(Figure.25C)**. IFA showed that exposure to 500 µM auxin for 24 h

triggered the degradation of AID-tagged *Tg*EPCS **(Figure.25D)**. The crucial role of *Tg*EPCS was further determined by plaque assay **(Figure.25E-F)**. No plaques were detected in auxin-treated *Tg*EPCS-AID-3xHA strain, while the parental strain was not affected.

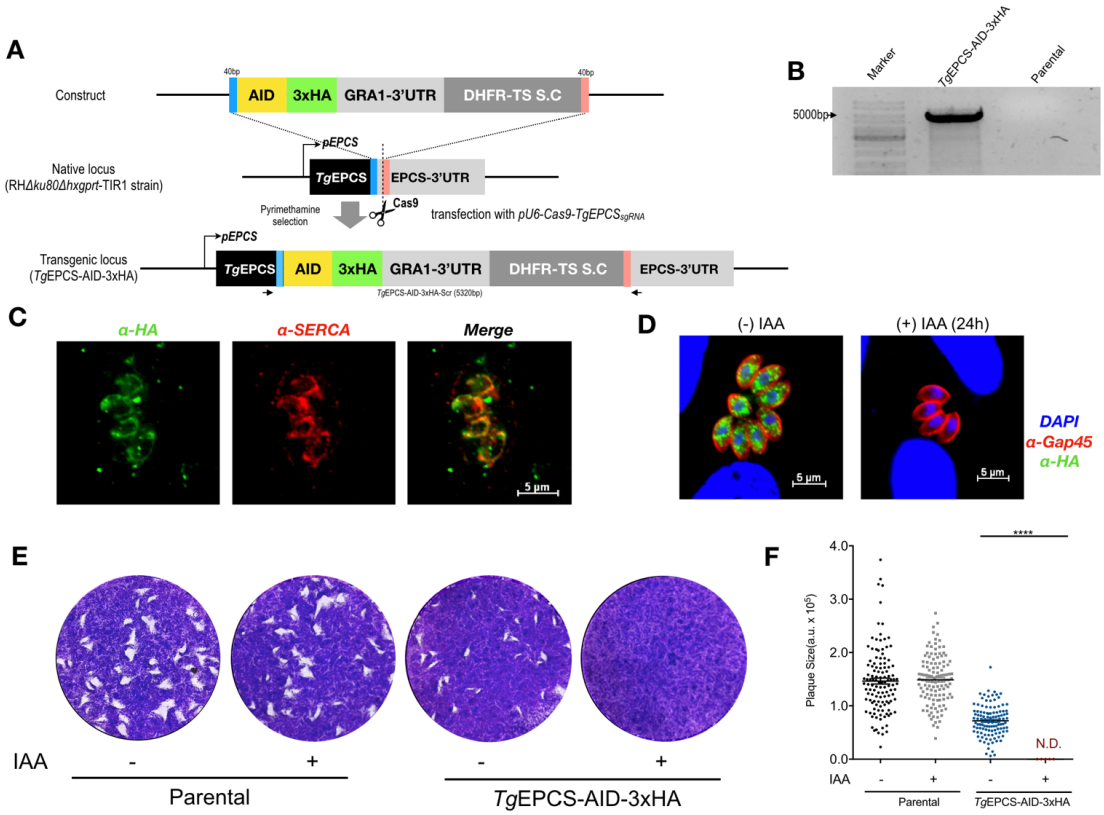

Figure.25: Conditional deletion of *Tg*EPCS leads to lethal phenotype of *T. gondii*. (A) Scheme showing CRISPR-assisted 3'insertional tagging of *Tg*EPCS with auxin-inducible degron. Template used for HDR containing short (40 bp) crossover sequence (COS) was transfected to the tachyzoites together with *pU6-Cas9-TgEPCS*$_{sgRNA}$. **(B)** Screening PCR confirming the integration of HDR template to *Tg*EPCS locus. Primer binding site to initiate the screening were marked as arrows in panel **(A)**. **(C)** Immunofluorescence images showing the endoplasmic reticulum localization and **(D)** auxin-dependent regulation of *Tg*EPCS. Fresh parasites were harvested and cultured for 24 h with or without 500 μM IAA (indole-3-acetic acid), fixed and stained with α-HA and α-*Tg*SERCA/*Tg*GAP45 for visualization. HA-tagged *Tg*EPCS was shown in green and *Tg*SERCA/TgGAP45 stained endoplasmic reticulum/inner membrane complex was shown in red. **(E-F)** Plaque assays showing growth fitness of the *Tg*EPCS-AID-3xHA and parental strains. Crystal violet-stained images **(E)** revealed plaques formed by successive lytic cycles of the indicated strains in absence or presence of IAA (500 μM). The plaque area, depicted as arbitrary units (a.u.), was measured by ImageJ software. A total of 100-150 plaques for each strain were scored from 3 assays. The size of individual plaques was presented as the dot graph. (mean ± S.E.; ***, p<0.001)

4. Discussion

4.1 Biogenesis of PtdIns in *T. gondii*

4.1.1 *De novo* synthesis of PtdIns in *T. gondii*

This work characterized PtdIns synthesis (PIS) during asexual reproduction of *T. gondii*. The enzyme PIS is conserved in all eukaryotic organisms but absent in prokaryotes. It utilizes CDP-DAG and *myo*-inositol to generate PtdIns **(Figure.26)**. In mammalian cells, *myo*-inositol can be produced, as well as imported from the milieu. Autonomous synthesis involves conversion of glucose to glucose-6-phosphate (G6P) by hexokinase, followed by the catalytic action of inositol-3P synthase to produce inositol-3-phosphate (Ins3P). Subsequently, Ins3P is dephosphorylated to make inositol by inositol-3P monophosphatase. Most protozoan parasites possess all 3 enzymes for *myo*-inositol synthesis[125] in addition to the sugar transporter(s), which have been characterized in *Trypanosoma* and *Leishmania*[126-128].

In *T. brucei*, the *de novo* synthesis and import of *myo*-inositol are both essential for the parasite survival but for distinct reasons. Endogenously synthesized *myo*-inositol is used for PtdIns and GPI synthesis in the ER[103,129], while *myo*-inositol acquired from the milieu drives the bulk production of PtdIns in the Golgi complex[104,105]. Similarly, *Plasmodium falciparum* also relies on the *de novo myo*-inositol synthesis for GPI assembly[130]. In contrast, one of the genes encoding Ins3P synthase could not be identified in the genome database of *T. gondii*, and tachyzoites cultivated with exogenous [^{13}C]-glucose showed the labeling of G6P but not of Ins3P and *myo*-inositol[131].

Conversely, this work revealed that tachyzoites can import *myo*-inositol for PtdIns biogenesis. In previous work, four sugar transporters were identified in *T. gondii*, of which

only two are located in the plasmalemma[41]. One of them, *Tg*GT1, transports glucose (besides mannose, fructose and galactose), while the other yet-to-be-characterized permease (*Tg*ST2) remains a strong candidate for *myo*-inositol import. Surprisingly though, *Tg*ST2 is dispensable for the lytic cycle; hence it remains equivocal whether the parasite is indeed strictly dependent (auxotrophic) for host-derived inositol.

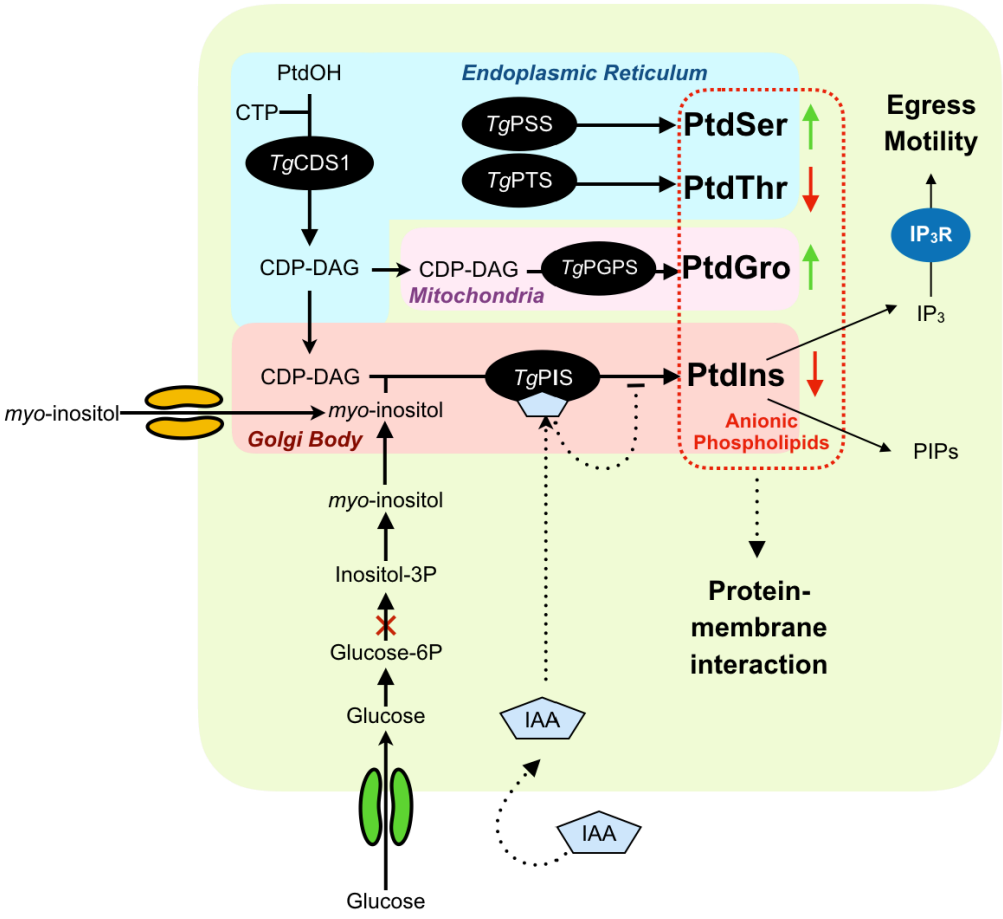

Figure.26: Model of PtdIns biogenesis and possible roles in tachyzoites of *T. gondii*. The model is based on this work, as well as previous results and literature cited herein. PtdIns is synthesized by *Tg*PIS in the Golgi bodies using CDP-DAG and *myo*-inositol. CDP-DAG is generated primarily by *Tg*CDS1 in the ER, whereas *myo*-inositol needs to be imported from the host cell. Membrane transporters, membrane contact sites or other lipid trafficking mechanisms, as indicated, mediate transport of *myo*-inositol and CDP-DAG between the membranes of parasites and organelles. An auxin-mediated knockdown of PtdIns synthase (shown by dotted line) reduces the level of major PtdIns species along with modulation of other anionic phospholipids, as shown. As reported in mammalian cells, negatively-charged lipids can regulate a range of functions by interacting with membrane proteins. Likewise, PtdIns-derived phosphoinositides (*e.g.* IP_3) govern calcium-mediated processes among many others.

Another precursor for PtdIns biogenesis is CDP-DAG, which is synthesized by the enzyme CDS using phosphatidic acid and CTP. The genes encoding for eukaryotic-type CDS have been identified in the genomes of all protozoan parasites, and proved to be essential for the synthesis of PtdIns in *T. gondii*, *P. falciparum* and *T. brucei*[78,132-135]. Additionally, previous members of our lab reported prokaryotic-type CDS proteins in selected parasites including in *T. gondii* that drives the synthesis of phosphatidylglycerol[135]. This study shows that a knockdown of *Tg*CDS1 in the ER of *T. gondii* impaired the incorporation of [^{3}H]-*myo*-inositol into PtdIns. It can thus be concluded that the pool of CDP-DAG generated in the parasite ER is the primary source for PtdIns biogenesis. Expression of *Tg*PIS primarily in the Golgi-complex necessitates transportation of CDP-DAG from ER to Golgi. Similarly, PtdIns should be transferred back to the ER for GPI production. The mechanism of such inter-organelle exchange of CDP-DAG and PtdIns warrant further investigation. Our data also signify that tachyzoites are capable of utilizing exogenous CDP-DAG into PtdIns, albeit modestly. Surprisingly, there has been no report thus far on the transport of CDP-DAG from the milieu, nonetheless, given the intracellular lifestyle of *T. gondii*, it is plausible that the parasite can scavenge host-derived precursor from its surrounding environment.

4.1.2 Physiological role of *Tg*PIS in phospholipid homeostasis of *T. gondii*

This study deployed several strategies to eventually reveal the indispensable nature of PtdIns biosynthesis. Our initial attempts to construct a workable conditional mutant of *Tg*PIS based on tetracycline and Cre-loxP systems implies a marked catalytic and transcriptional resilience of PtdIns synthase, which impeded a comprehensive characterization. Nevertheless, using a post-translational control of protein stability by auxin-inducible degradation, not only were we able to confirm a vital function of PtdIns synthesis, but also perform in-depth phenotyping and lipid analyses. We observed a role of *Tg*PIS in the

parasite replication, motility and egress. PtdIns is expected to drive the synthesis of IP_3, which is deemed critical for the activation of motility and ensuing egress[85]. Nonetheless, knockdown of PIS leading to a lethal phenotype may be due to several reasons, and may have multiple consequences. As stated in the introduction, PtdIns and its downstream metabolites are known to be involved in numerous other aspects of apicomplexan biology. In this regard, our lipidomic analysis provided additional insights, primarily inter-regulation and homeostasis of anionic phospholipids.

Anionic phospholipids account for less than 30% of total membrane phospholipids in eukaryotic cells[136]. A balanced composition of anionic phospholipids is required for an optimal functioning of many enzymes including protein kinase C, phospholipase A2 and CTP-phosphocholine cytidylyltransferase in mammalian cells[137]. It is proposed that the negatively charged region of the membrane interacts with the cationic motif of proteins[138,139]. The size of the head-groups and acyl chains are considered as determinant factors for that processes[137]. In addition, anionic phospholipids are reported to be critical for the functioning of membrane transporters, such as glucose transporters[140] and ATP-sensitive potassium channel[141] in mammalian cells. In our study, we observed a somewhat selective alternation in PtdIns, PtdThr, PtdSer and PtdGro in the PIS mutant. The data showed a reduction in several species of PtdIns and PtdThr, whereas many species of PtdSer and PtdGro were induced. It therefore seems as though the parasite strives to maintain a net negative charge on organelle membranes, further supported by the fact that overall amount of all major lipid classes were unaltered. While the increase in species of PtdSer and PtdGro can be partly explained by rerouting of excess CDP-DAG when synthesis of PtdIns is inhibited, it is surprising to see a concurrent decline in PtdThr. Notably however the inter-regulation of PtdThr, PtdSer and PtdIns was also observed in other mutants, where PtdThr and PtdSer synthesis were impaired[51].

Notably, the level of an exclusive lipid termed BMP was significantly increased in the *Tg*PIS-mAID-3xHA mutant. BMP is a negatively charged glycerophospholipid with an unusual sn-1;sn-1′ structural configuration. Generated using PtdGro as a precursor, it is a marker of

late endosome and lysosome in mammalian cells. The rise in BMP levels may result from the alternation in PtdGro species[142]. The perturbation of BMP can disrupt the endomembrane system, which in turn impair the subcellular trafficking process[143]. Likewise, it will be interesting to examine the function of BMP during autophagy events in *T. gondii*[144]. Not least, it will indeed be worth probing the mechanisms of CDP-DAG homeostasis and inter-regulation of anionic lipids in *T. gondii.*

4.2 *Tg*ECT and the biogenesis of PtdEtn and EPC in *T. gondii*

4.2.1 Physiological role of *Tg*ECT in PtdEtn biogenesis of *T. gondii*

PtdEtn serves as one of the crucial membrane phospholipid in both eukaryotic and prokaryotic cell as for its contribution to the construction of organelles and plasma membrane. In this study, we characterized the key enzyme controlling the CDP-ethanolamine branch of Kennedy pathway, *Tg*ECT, and dissect its crucial role in phospholipid synthesis and lytic cycle of *T. gondii*. The essentiality of CDP-choline branch of Kennedy pathway has been partially investigated by conditional knockdown of *Tg*CK and inhibition of its activity *via* a choline analog, DME[47]. However, the role of *Tg*EK and the CDP-ethanolamine in facilitating the synthesis of PtdEtn has not been proven yet. *Tg*CK was reported to harbor dual-specificity for catalyzing both choline and ethanolamine to phosphor-choline and phosphor-ethanolamine, so it is likely that the parasite can keep the activity of CDP-ethanolamine branch of Kennedy pathway in the absence of *Tg*EK.

*Tg*ECT, in contrast, seems to be crucial needed for the Kennedy pathway. The essentiality of ECT in driving CDP-ethanolamine branch of Kennedy pathway has been intensively investigated in mammalian cell as well as in some protozoan parasites, such as in *T. brucei*[145] and *P. bergei*[71]. In both cases, the ECTs have been proved to be essential for the blood stages of *T. brucei* and *P. bergei*. Other than significantly delayed reproduction, the conditional knockdown of *Tb*ECT in *T. brucei* led to several detectable defects, such as

altered morphology of mitochondrion, abnormal cellular dimension, and delayed cell cycle[66]. These effects led by ablation of ECT remain to be studied in *T. gondii.*

One major outcome of knockdown of *Tg*ECT is the impaired phospholipid biogenesis **(Figure.27)**, which was not presented in other parasite such as *T. brucei.* While the conditional knockdown of *Tb*ECT impaired the synthesis of only PtdEtn, the auxin-mediated deletion of *Tg*ECT led to reduction of all detectable classes of glycerophospholipid in *T. gondii*, especially for PtdEtn, PtdSer and PtdThr. Interestingly, this work identified that *Tg*ECT seems to be particularly crucial the synthesis of several species of PtdEtn, PtdSer and PtdThr. The acyl chain assembly of some species is in consistence across different classes, namely C34:2, C40:7 (PtdEtn, PtdSer), C36:4 (PtdThr, PtdSer), C38:6 and C38:7 (PtdEtn, PtdSer and PtdThr). *T. gondii* encodes two base-exchange type of enzymes (*Tg*PSS and *Tg*PTS) that account for PtdSer and PtdThr synthesis[50,51]. *Tg*PSS-mediated synthesis of PtdSer likely uses PtdEtn as precursor, whereas the precursor for PtdThr biogenesis remains unclear. Our data indicates that *Tg*ECT is required for the biogenesis of at least several species of PtdThr. It can also be hypothesized that some species of PtdEtn or PtdSer are used as the precursors for PtdThr synthesis, perhaps *via* the base-exchange type *Tg*PTS.

In addition to the CDP-ethanolamine branch of Kennedy pathway, *T. gondii* adapts an alternative pathway for PtdEtn biogenesis *via* decarboxylation of PtdSer. However, it seems that the additional pathway for PtdEtn biogenesis cannot compensate the loss of the *de novo* synthesis of PtdEtn through impaired CDP-ethanolamine branch of Kennedy pathway. Two PSDs localized at mitochondrion (*Tg*PSDmt) and PV (*Tg*PSDpv) were reported[48,49] to catalyze the reaction. The ablation of *Tg*PSDmt caused approximately 50% growth defect in plaque assays[49], while the deletion of *Tg*PSDpv exhibited no growth defect, suggesting neither of them is critical for the parasite survival. It is noted that the consumption of ethanolamine increased in the *Δtgpsdmt* mutant, suggesting that parasite can spontaneously induced the activity of CDP-ethanolamine branch of Kennedy pathway to compensate the loss of PSDs. These data implied that up-regulation of CDP-ethanolamine

branch of Kennedy pathway may occur when the biogenesis of PtdEtn *via* PSD-driven route is impaired, while the role of *Tg*ECT involving in the regulatory of CDP-ethanolamine branch of Kennedy pathway remains to be further examined.

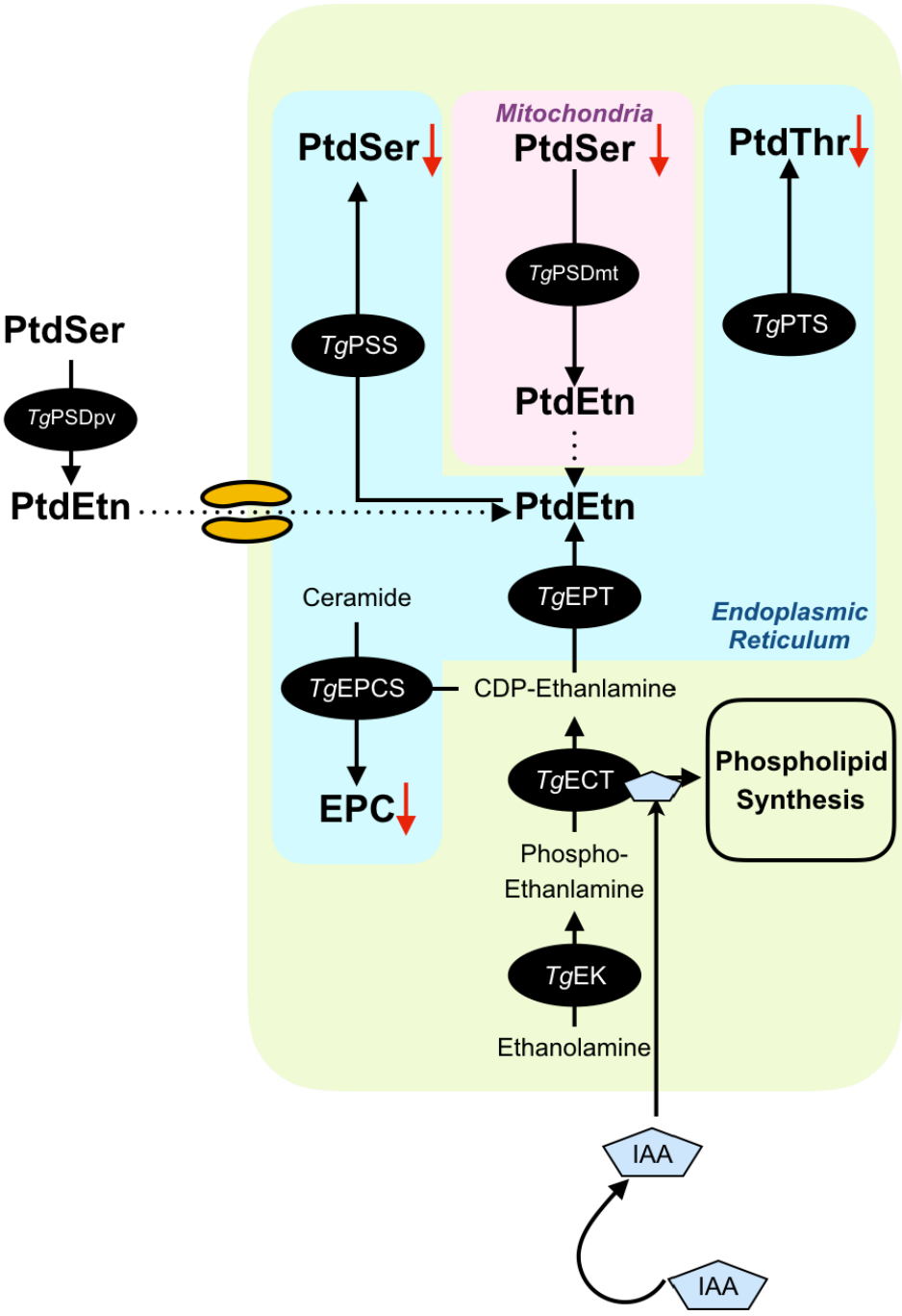

Figure.27: Model of PtdEtn biogenesis and possible roles of *Tg*ECT in tachyzoites of *T. gondii*. The model is based on this work, as well as our previous results and literature cited herein. Biogenesis of PtdEtn involves multiple routes as indicated, driven by PSDs or CDP-ethanolamine branch of Kennedy pathway. Transporters for PtdEtn uptake are hypothetical. Auxin-mediated disruption of *Tg*ECT leads to impaired phospholipid synthesis, and conferred strongest effect on some species of PtdEtn, PtdSer, PtdThr. Ablation of *Tg*ECT should inhibit the production of CDP-ethanolamine, precursor required for EPC synthesis. Thus resulted in the down-regulation of EPC level in the parasites.

4.2.2 Sphingolipid metabolism of *T. gondii*

In addition to glycerophospholipids, our research revealed an unexpected role of *Tg*ECT possibly contributing to the synthesis of EPC, one rarely studied sphingolipid. Compared to glycerophospholipids, the distribution of sphingolipid differs significantly among various organisms. For example, inositol-phosphorylceramide (IPC) is the major sphingolipid class synthesized by fungi and plants, while in mammalian the majority of sphingolipids are sphingomyelin and EPC. The difference in sphingolipid profiles also occurs in the protozoan parasites. In *Eimeria*, SM and IPC are the major sphingolipid synthesized during its sporozoite stage, while *T. gondii* tachyzoite possesses SM and EPC as the main sphingolipids [39]. In *Trypanosoma*, synthesis of IPC and SM is required for the procyclic stage, whereas EPC and SM are important for the blood stage[146]. It is reported that cell division of *T.gondii* tachyzoites can be blocked by aureobasidin A[147], an IPC-synthase inhibitor, indicating that the trace amount of IPC is likely to be synthesized by the parasites. Alternatively, the compound may also inhibit the EPC and SM production of *T. gondii*.

Biosynthesis of SM and EPC was expected to be driven by the mammalian-type *Tg*SLS, however, we revealed the occurrence of an insect-type pathway for EPC synthesis carried out by a hypothetical *Tg*EPCS. Although further study has to be done to confirm its catalytic role involving in EPC synthesis of tachyzoites, it has already been proved that *in vitro* expressed *Tg*EPCS can produce EPC by using CDP-ethanolamine and ceramide as precursors (*Mina J, et. al,* unpublished data).

The physiological importance of EPC in *T. gondii* is not yet clear. In arthropods[148-150], EPC seems to substitute the role of SM in supporting the mechanical stability of biological membrane. It is also particularly important for the neuronal development in *Drosophila*[151-153], suggesting its potential role in signal transduction. Interestingly, mosquitos (*Aedes*

aegypti) that are infected by arboviruses causing dengue fever show a reduction of EPC content in the mid-gut cells[154]. In mammalian intestine, EPC is important for the growth fitness of bacteria, such as *Bacteroides fragilis*[155] and *Porphyromonas gingivalis*[156]*.* It is noted that mammalian-derived EPC is required only by *P. gingivalis* that survive in station phase or those who suffer from oxidative stress[157], but dispensable during normal growth period. These information suggest that host-derived EPC may be utilized by the intracellular pathogen for the survival under environmental stress.

The conditional knock-down of *Tg*EPCS by AID system confirmed its essential role during the lytic cycle of the tachyzoites. It needs be tested further whether EPC-synthesis in the auxin-induced *Tg*EPCS knockdown strain is ablated. Investigation should be done to dissect the role of EPC in membrane integrity, signaling and host-microbe interaction of *T. gondii.*

5. Conclusion and Perspectives

This work investigated the biogenesis of two important phospholipids, PtdEtn and PtdIns, by targeting at two key enzymes: *Tg*ECT and *Tg*PIS. We demonstrated the essential role of the two studied gene, with function of *Tg*PIS characterized by *in vitro* biochemical assay. Our work of *Tg*PIS shed light on its role in the CDP-DAG and anionic lipid homeostasis maintenance, while the mechanism should be further investigated. We dissected the role of *Tg*ECT relating to phospholipid biogenesis of *T. gondii*, suggesting the parasite may regulate its phospholipid synthesis through *Tg*ECT or CDP-ethanolamine branch of Kennedy pathway. Last but not least, our work identified an insect-type EPC biogenesis pathway, while its physiological importance remains to be revealed.

There are still further questions that can be addressed in the future:

- Functional characterization of *Tg*ECT and *Tg*EPCS to confirm the catalytic activity;
- Dissecting the role of EPC in regulating *T. gondii* survival and development;
- Identification of the transporters accounting for phospholipid uptake;
- Characterization of the pathway for SM and IPC production;
- Mechanism of anionic phospholipid homeostasis;
- Trafficking of PtdEtn, PtdIns and EPC in the parasite.

6. References

1 Aldridge, J. R. & Vogel, I. A. Macrophage biology and their activation by protozoan-derived glycosylphosphatidylinositol anchors and hemozoin. *J Parasitol* **100**, 737-742, doi:10.1645/14-646.1 (2014).

2 Levine, N. D. *Protozoan Parasites of Domestic Animals and Man*. (Minnneapolis, 1961).

3 Cable, J. *et al.* Global change, parasite transmission and disease control: lessons from ecology. *Philos Trans R Soc Lond B Biol Sci* **372**, doi:10.1098/rstb.2016.0088 (2017).

4 Torgerson, P. R. *et al.* World Health Organization Estimates of the Global and Regional Disease Burden of 11 Foodborne Parasitic Diseases, 2010: A Data Synthesis. *PLoS Med* **12**, e1001920, doi:10.1371/journal.pmed.1001920 (2015).

5 de Koning-Ward, T. F., Gilson, P. R. & Crabb, B. S. Advances in molecular genetic systems in malaria. *Nat Rev Microbiol* **13**, 373-387, doi:10.1038/nrmicro3450 (2015).

6 Reinke, A. W. & Troemel, E. R. The Development of Genetic Modification Techniques in Intracellular Parasites and Potential Applications to Microsporidia. *PLoS Pathog* **11**, e1005283, doi:10.1371/journal.ppat.1005283 (2015).

7 Teixeira, S. M. & daRocha, W. D. Control of gene expression and genetic manipulation in the Trypanosomatidae. *Genet Mol Res* **2**, 148-158 (2003).

8 Wang, J. L. *et al.* The Past, Present, and Future of Genetic Manipulation in Toxoplasma gondii. *Trends Parasitol* **32**, 542-553, doi:10.1016/j.pt.2016.04.013 (2016).

9 Lendner, M. & Daugschies, A. Cryptosporidium infections: molecular advances. *Parasitology* **141**, 1511-1532, doi:10.1017/S0031182014000237 (2014).

10 Walker, R. A., Ferguson, D. J., Miller, C. M. & Smith, N. C. Sex and Eimeria: a molecular perspective. *Parasitology* **140**, 1701-1717, doi:10.1017/S0031182013000838 (2013).

11 Smith, T. G., Walliker, D. & Ranford-Cartwright, L. C. Sexual differentiation and sex determination in the Apicomplexa. *Trends Parasitol* **18**, 315-323 (2002).

12 Fayer, R. Sarcocystis spp. in human infections. *Clin Microbiol Rev* **17**, 894-902, table of contents, doi:10.1128/CMR.17.4.894-902.2004 (2004).

13 Krause, P. J. *et al.* Shared features in the pathobiology of babesiosis and malaria. *Trends Parasitol* **23**, 605-610, doi:10.1016/j.pt.2007.09.005 (2007).

14 Tretina, K., Gotia, H. T., Mann, D. J. & Silva, J. C. Theileria-transformed bovine leukocytes have cancer hallmarks. *Trends Parasitol* **31**, 306-314, doi:10.1016/j.pt.2015.04.001 (2015).

15 Plattner, F. & Soldati-Favre, D. Hijacking of host cellular functions by the Apicomplexa. *Annu Rev Microbiol* **62**, 471-487, doi:10.1146/annurev.micro.62.081307.162802 (2008).

16 Striepen, B., Jordan, C. N., Reiff, S. & van Dooren, G. G. Building the perfect parasite: cell division in apicomplexa. *PLoS Pathog* **3**, e78, doi:10.1371/journal.ppat.0030078 (2007).

17 Black, M. W. & Boothroyd, J. C. Lytic cycle of Toxoplasma gondii. *Microbiol Mol Biol Rev* **64**, 607-623, doi:10.1128/mmbr.64.3.607-623.2000 (2000).

18 Blader, I. J., Coleman, B. I., Chen, C. T. & Gubbels, M. J. Lytic Cycle of Toxoplasma gondii: 15 Years Later. *Annu Rev Microbiol* **69**, 463-485, doi:10.1146/annurev-micro-091014-104100 (2015).

19 Weiss, L. M. & Dubey, J. P. Toxoplasmosis: A history of clinical observations. *Int J Parasitol* **39**, 895-901, doi:10.1016/j.ijpara.2009.02.004 (2009).

20 Flegr, J., Prandota, J., Sovickova, M. & Israili, Z. H. Toxoplasmosis--a global threat. Correlation of latent toxoplasmosis with specific disease burden in a set of 88 countries. *PLoS One* **9**, e90203, doi:10.1371/journal.pone.0090203 (2014).

21 Zhang, M., Joyce, B. R., Sullivan, W. J., Jr. & Nussenzweig, V. Translational control in Plasmodium and toxoplasma parasites. *Eukaryot Cell* **12**, 161-167, doi:10.1128/EC.00296-12 (2013).

22 Blader, I. J., Manger, I. D. & Boothroyd, J. C. Microarray analysis reveals previously unknown changes in Toxoplasma gondii-infected human cells. *J Biol Chem* **276**, 24223-24231, doi:10.1074/jbc.M100951200 (2001).

23 Molestina, R. E., Payne, T. M., Coppens, I. & Sinai, A. P. Activation of NF-kappaB by Toxoplasma gondii correlates with increased expression of antiapoptotic genes and localization of phosphorylated IkappaB to the parasitophorous vacuole membrane. *J Cell Sci* **116**, 4359-4371, doi:10.1242/jcs.00683 (2003).

24 Payne, T. M., Molestina, R. E. & Sinai, A. P. Inhibition of caspase activation and a requirement for NF-kappaB function in the Toxoplasma gondii-mediated blockade of host apoptosis. *J Cell Sci* **116**, 4345-4358, doi:10.1242/jcs.00756 (2003).

25 Mun, H. S. *et al.* Toll-like receptor 4 mediates tolerance in macrophages stimulated with Toxoplasma gondii-derived heat shock protein 70. *Infect Immun* **73**, 4634-4642, doi:10.1128/IAI.73.8.4634-4642.2005 (2005).

26 Debierre-Grockiego, F. *et al.* Activation of TLR2 and TLR4 by glycosylphosphatidylinositols derived from Toxoplasma gondii. *J Immunol* **179**, 1129-1137, doi:10.4049/jimmunol.179.2.1129 (2007).

27 Sinai, A. P. & Joiner, K. A. The Toxoplasma gondii protein ROP2 mediates host organelle association with the parasitophorous vacuole membrane. *J Cell Biol* **154**, 95-108, doi:10.1083/jcb.200101073 (2001).

28 Sheetz, M. P., Sable, J. E. & Dobereiner, H. G. Continuous membrane-cytoskeleton adhesion requires continuous accommodation to lipid and cytoskeleton dynamics. *Annu Rev Biophys Biomol Struct* **35**, 417-434, doi:10.1146/annurev.biophys.35.040405.102017 (2006).

29 Pernas, L., Bean, C., Boothroyd, J. C. & Scorrano, L. Mitochondria Restrict Growth of the Intracellular Parasite Toxoplasma gondii by Limiting Its Uptake of Fatty Acids. *Cell Metab* **27**, 886-897 e884, doi:10.1016/j.cmet.2018.02.018 (2018).

30 Meissner, M., Breinich, M. S., Gilson, P. R. & Crabb, B. S. Molecular genetic tools in Toxoplasma and Plasmodium: achievements and future needs. *Curr Opin Microbiol* **10**, 349-356, doi:10.1016/j.mib.2007.07.006 (2007).

31 Fox, B. A., Ristuccia, J. G., Gigley, J. P. & Bzik, D. J. Efficient gene replacements in Toxoplasma gondii strains deficient for nonhomologous end joining. *Eukaryot Cell* **8**, 520-529, doi:10.1128/EC.00357-08 (2009).

32 Shen, B., Brown, K. M., Lee, T. D. & Sibley, L. D. Efficient gene disruption in diverse strains of Toxoplasma gondii using CRISPR/CAS9. *MBio* **5**, e01114-01114, doi:10.1128/mBio.01114-14 (2014).

33 Sidik, S. M., Hackett, C. G., Tran, F., Westwood, N. J. & Lourido, S. Efficient genome engineering of Toxoplasma gondii using CRISPR/Cas9. *PLoS One* **9**, e100450, doi:10.1371/journal.pone.0100450 (2014).

34 Andenmatten, N. *et al.* Conditional genome engineering in Toxoplasma gondii uncovers alternative invasion mechanisms. *Nat Methods* **10**, 125-127, doi:10.1038/nmeth.2301 (2013).

35 Jullien, N., Sampieri, F., Enjalbert, A. & Herman, J. P. Regulation of Cre recombinase by ligand-induced complementation of inactive fragments. *Nucleic Acids Res* **31**, e131, doi:10.1093/nar/gng131 (2003).

36 Meissner, M., Brecht, S., Bujard, H. & Soldati, D. Modulation of myosin A expression by a newly established tetracycline repressor-based inducible system in Toxoplasma gondii. *Nucleic Acids Res* **29**, E115, doi:10.1093/nar/29.22.e115 (2001).

37 Herm-Gotz, A. *et al.* Rapid control of protein level in the apicomplexan Toxoplasma gondii. *Nat Methods* **4**, 1003-1005, doi:10.1038/nmeth1134 (2007).

38 Brown, K. M., Long, S. & Sibley, L. D. Plasma Membrane Association by N-Acylation Governs PKG Function in Toxoplasma gondii. *MBio* **8**, doi:10.1128/mBio.00375-17 (2017).

39 Kong, P., Lehmann, M. J., Helms, J. B., Brouwers, J. F. & Gupta, N. Lipid analysis of Eimeria sporozoites reveals exclusive phospholipids, a phylogenetic mosaic of endogenous synthesis, and a host-independent lifestyle. *Cell Discov* **4**, 24, doi:10.1038/s41421-018-0023-4 (2018).

40 Nitzsche, R., Zagoriy, V., Lucius, R. & Gupta, N. Metabolic Cooperation of Glucose and Glutamine Is Essential for the Lytic Cycle of Obligate Intracellular Parasite Toxoplasma gondii. *J Biol Chem* **291**, 126-141, doi:10.1074/jbc.M114.624619 (2016).

41 Blume, M. *et al.* Host-derived glucose and its transporter in the obligate intracellular pathogen Toxoplasma gondii are dispensable by glutaminolysis. *Proc Natl Acad Sci U S A* **106**, 12998-13003, doi:10.1073/pnas.0903831106 (2009).

42 Mazumdar, J., E, H. W., Masek, K., C, A. H. & Striepen, B. Apicoplast fatty acid synthesis is essential for organelle biogenesis and parasite survival in Toxoplasma gondii. *Proc Natl Acad Sci U S A* **103**, 13192-13197, doi:10.1073/pnas.0603391103 (2006).

43 Ramakrishnan, S. *et al.* Apicoplast and endoplasmic reticulum cooperate in fatty acid biosynthesis in apicomplexan parasite Toxoplasma gondii. *J Biol Chem* **287**, 4957-4971, doi:10.1074/jbc.M111.310144 (2012).

44 Ramakrishnan, S. *et al.* The intracellular parasite Toxoplasma gondii depends on the synthesis of long-chain and very long-chain unsaturated fatty acids not supplied by the host cell. *Mol Microbiol* **97**, 64-76, doi:10.1111/mmi.13010 (2015).

45 Amiar, S. *et al.* Apicoplast-Localized Lysophosphatidic Acid Precursor Assembly Is Required for Bulk Phospholipid Synthesis in Toxoplasma gondii and Relies on an Algal/Plant-Like Glycerol 3-Phosphate Acyltransferase. *PLoS Pathog* **12**, e1005765, doi:10.1371/journal.ppat.1005765 (2016).

46 Gupta, N., Zahn, M. M., Coppens, I., Joiner, K. A. & Voelker, D. R. Selective disruption of phosphatidylcholine metabolism of the intracellular parasite Toxoplasma gondii arrests its growth. *J Biol Chem* **280**, 16345-16353, doi:10.1074/jbc.M501523200 (2005).

47 Sampels, V. *et al.* Conditional mutagenesis of a novel choline kinase demonstrates plasticity of phosphatidylcholine biogenesis and gene expression in Toxoplasma gondii. *J Biol Chem* **287**, 16289-16299, doi:10.1074/jbc.M112.347138 (2012).

48 Gupta, N., Hartmann, A., Lucius, R. & Voelker, D. R. The obligate intracellular parasite Toxoplasma gondii secretes a soluble phosphatidylserine decarboxylase. *J Biol Chem* **287**, 22938-22947, doi:10.1074/jbc.M112.373639 (2012).

49 Hartmann, A., Hellmund, M., Lucius, R., Voelker, D. R. & Gupta, N. Phosphatidylethanolamine synthesis in the parasite mitochondrion is required for efficient growth but dispensable for survival of Toxoplasma

gondii. *J Biol Chem* **289**, 6809-6824, doi:10.1074/jbc.M113.509406 (2014).

50 Arroyo-Olarte, R. D. Biogenesis and functions of phosphatidylserine and phosphatidylthreonine in Toxoplasma gondii *PhD Thesis* (2014).

51 Arroyo-Olarte, R. D. *et al.* Phosphatidylthreonine and Lipid-Mediated Control of Parasite Virulence. *PLoS Biol* **13**, e1002288, doi:10.1371/journal.pbio.1002288 (2015).

52 Kuchipudi, A., Arroyo-Olarte, R. D., Hoffmann, F., Brinkmann, V. & Gupta, N. Optogenetic monitoring identifies phosphatidylthreonine-regulated calcium homeostasis in Toxoplasma gondii. *Microb Cell* **3**, 215-223, doi:10.15698/mic2016.05.500 (2016).

53 Dixon, H. & Williamson, J. The lipid composition of blood and culture forms of Trypanosoma lewisi and Trypanosoma rhodesiense compared with that of their environment. *Comp Biochem Physiol* **33**, 111-128 (1970).

54 Wassef, M. K., Fioretti, T. B. & Dwyer, D. M. Lipid analyses of isolated surface membranes of Leishmania donovani promastigotes. *Lipids* **20**, 108-115 (1985).

55 Foussard, F., Gallois, Y., Girault, A. & Menez, J. F. Lipids and fatty acids of tachyzoites and purified pellicles of Toxoplasma gondii. *Parasitol Res* **77**, 475-477 (1991).

56 Vial, H. J. & Ancelin, M. L. Malarial lipids. An overview. *Subcell Biochem* **18**, 259-306 (1992).

57 Emoto, K. & Umeda, M. An essential role for a membrane lipid in cytokinesis. Regulation of contractile ring disassembly by redistribution of phosphatidylethanolamine. *J Cell Biol* **149**, 1215-1224, doi:10.1083/jcb.149.6.1215 (2000).

58 McMahon, H. T. & Boucrot, E. Membrane curvature at a glance. *J Cell Sci* **128**, 1065-1070, doi:10.1242/jcs.114454 (2015).

59 Giorgione, J., Epand, R. M., Buda, C. & Farkas, T. Role of phospholipids containing docosahexaenoyl chains in modulating the activity of protein kinase C. *Proc Natl Acad Sci U S A* **92**, 9767-9770, doi:10.1073/pnas.92.21.9767 (1995).

60 Emoto, K. *et al.* Redistribution of phosphatidylethanolamine at the cleavage furrow of dividing cells during cytokinesis. *Proc Natl Acad Sci U S A* **93**, 12867-12872, doi:10.1073/pnas.93.23.12867 (1996).

61 Escriba, P. V. *et al.* Role of lipid polymorphism in G protein-membrane interactions: nonlamellar-prone phospholipids and peripheral protein binding to membranes. *Proc Natl Acad Sci U S A* **94**, 11375-11380, doi:10.1073/pnas.94.21.11375 (1997).

62 Xie, Z. & Klionsky, D. J. Autophagosome formation: core machinery and adaptations. *Nat Cell Biol* **9**, 1102-1109, doi:10.1038/ncb1007-1102 (2007).

63 Kennedy, E. P. & Weiss, S. B. The function of cytidine coenzymes in the biosynthesis of phospholipides. *J Biol Chem* **222**, 193-214 (1956).

64 Schuiki, I. & Daum, G. Phosphatidylserine decarboxylases, key enzymes of lipid metabolism. *IUBMB Life* **61**, 151-162, doi:10.1002/iub.159 (2009).

65 Farine, L. & Butikofer, P. The ins and outs of phosphatidylethanolamine synthesis in Trypanosoma brucei. *Biochim Biophys Acta* **1831**, 533-542, doi:10.1016/j.bbalip.2012.09.008 (2013).

66 Signorell, A. *et al.* Perturbation of phosphatidylethanolamine synthesis affects mitochondrial morphology and cell-cycle progression in procyclic-form Trypanosoma brucei. *Mol Microbiol* **72**, 1068-1079, doi:10.1111/j.1365-2958.2009.06713.x (2009).

67 Lykidis, A. Comparative genomics and evolution of eukaryotic phospholipid biosynthesis. *Prog Lipid Res* **46**, 171-199, doi:10.1016/j.plipres.2007.03.003 (2007).

68 Zhang, K. & Beverley, S. M. Phospholipid and sphingolipid metabolism in Leishmania. *Mol Biochem Parasitol* **170**, 55-64, doi:10.1016/j.molbiopara.2009.12.004 (2010).

69 Signorell, A., Rauch, M., Jelk, J., Ferguson, M. A. & Butikofer, P. Phosphatidylethanolamine in Trypanosoma brucei is organized in two separate pools and is synthesized exclusively by the Kennedy pathway. *J Biol Chem* **283**, 23636-23644, doi:10.1074/jbc.M803600200 (2008).

70 Choi, J. Y. *et al.* Characterization of Plasmodium phosphatidylserine decarboxylase expressed in yeast and application for inhibitor screening. *Mol Microbiol* **99**, 999-1014, doi:10.1111/mmi.13280 (2016).

71 Dechamps, S. *et al.* The Kennedy phospholipid biosynthesis pathways are refractory to genetic disruption in Plasmodium berghei and therefore appear essential in blood stages. *Mol Biochem Parasitol* **173**, 69-80, doi:10.1016/j.molbiopara.2010.05.006 (2010).

72 Bakovic, M., Fullerton, M. D. & Michel, V. Metabolic and molecular aspects of ethanolamine phospholipid biosynthesis: the role of CTP:phosphoethanolamine cytidylyltransferase (Pcyt2). *Biochem Cell Biol* **85**, 283-300, doi:10.1139/o07-006 (2007).

73 Johnson, C. M., Yuan, Z. & Bakovic, M. Characterization of transcription factors and cis-acting elements that regulate human CTP: phosphoethanolamine cytidylyltransferase (Pcyt2). *Biochim Biophys Acta* **1735**, 230-235, doi:10.1016/j.bbalip.2005.06.002 (2005).

74 Mukherjee, J. J., Chung, T., Ways, D. K. & Kiss, Z. Protein kinase Calpha is a major mediator of the stimulatory effect of phorbol ester on phospholipase D-mediated hydrolysis of phosphatidylethanolamine. *J Biol Chem* **271**, 28912-28917, doi:10.1074/jbc.271.46.28912 (1996).

75 Patnaik, P. K. *et al.* Molecular species analysis of phospholipids from Trypanosoma brucei bloodstream and procyclic forms. *Mol Biochem Parasitol* **58**, 97-105 (1993).

76 Welti, R. *et al.* Lipidomic analysis of Toxoplasma gondii reveals unusual polar lipids. *Biochemistry* **46**, 13882-13890, doi:10.1021/bi7011993 (2007).

77 Dechamps, S., Shastri, S., Wengelnik, K. & Vial, H. J. Glycerophospholipid acquisition in Plasmodium - a puzzling assembly of biosynthetic pathways. *Int J Parasitol* **40**, 1347-1365, doi:10.1016/j.ijpara.2010.05.008 (2010).

78 Bligh, E. G. & Dyer, W. J. A rapid method of total lipid extraction and purification. *Can J Biochem Physiol* **37**, 911-917 (1959).

79 Schofield, L., Hewitt, M. C., Evans, K., Siomos, M. A. & Seeberger, P. H. Synthetic GPI as a candidate anti-toxic vaccine in a model of malaria. *Nature* **418**, 785-789, doi:10.1038/nature00937 (2002).

80 McNamara, C. W. *et al.* Targeting Plasmodium PI(4)K to eliminate malaria. *Nature* **504**, 248-253, doi:10.1038/nature12782 (2013).

81 Gotze, S. *et al.* Diagnosis of toxoplasmosis using a synthetic glycosylphosphatidylinositol glycan. *Angew Chem Int Ed Engl* **53**, 13701-13705, doi:10.1002/anie.201406706 (2014).

82 Gotze, S. *et al.* Investigation of the protective properties of glycosylphosphatidylinositol-based vaccine candidates in a Toxoplasma gondii mouse challenge model. *Glycobiology* **25**, 984-991, doi:10.1093/glycob/cwv040 (2015).

83 Mbengue, A. *et al.* A molecular mechanism of artemisinin resistance in Plasmodium falciparum malaria. *Nature* **520**, 683-687, doi:10.1038/nature14412 (2015).

84 Gurale, B. P. *et al.* Toward the Development of the Next Generation of a Rapid Diagnostic Test: Synthesis of Glycophosphatidylinositol (GPI) Analogues of Plasmodium falciparum and Immunological Characterization. *Bioconjug Chem* **27**, 2886-2899, doi:10.1021/acs.bioconjchem.6b00542 (2016).

85 Garcia, C. R. S. *et al.* InsP3 Signaling in Apicomplexan Parasites. *Curr Top Med Chem* **17**, 2158-2165, doi:10.2174/1568026617666170130121042 (2017).

86 Manjunatha, U. H. *et al.* A Cryptosporidium PI(4)K inhibitor is a drug candidate for cryptosporidiosis. *Nature* **546**, 376-380, doi:10.1038/nature22337 (2017).

87 Tawk, L. *et al.* Phosphatidylinositol 3-monophosphate is involved in toxoplasma apicoplast biogenesis. *PLoS Pathog* **7**, e1001286, doi:10.1371/journal.ppat.1001286 (2011).

88 Daher, W. *et al.* Lipid kinases are essential for apicoplast homeostasis in Toxoplasma gondii. *Cell Microbiol* **17**, 559-578, doi:10.1111/cmi.12383 (2015).

89 Bhattacharjee, S., Speicher, K. D., Stahelin, R. V., Speicher, D. W. & Haldar, K. PI(3)P-independent and -dependent pathways function together in a vacuolar translocation sequence to target malarial proteins

to the host erythrocyte. *Mol Biochem Parasitol* **185**, 106-113, doi:10.1016/j.molbiopara.2012.07.004 (2012).

90 Bhattacharjee, S., Stahelin, R. V., Speicher, K. D., Speicher, D. W. & Haldar, K. Endoplasmic reticulum PI(3)P lipid binding targets malaria proteins to the host cell. *Cell* **148**, 201-212, doi:10.1016/j.cell.2011.10.051 (2012).

91 Brochet, M. *et al.* Phosphoinositide metabolism links cGMP-dependent protein kinase G to essential Ca(2)(+) signals at key decision points in the life cycle of malaria parasites. *PLoS Biol* **12**, e1001806, doi:10.1371/journal.pbio.1001806 (2014).

92 Burda, P. C., Caldelari, R. & Heussler, V. T. Manipulation of the Host Cell Membrane during Plasmodium Liver Stage Egress. *MBio* **8**, doi:10.1128/mBio.00139-17 (2017).

93 Demmel, L. *et al.* The endocytic activity of the flagellar pocket in Trypanosoma brucei is regulated by an adjacent phosphatidylinositol phosphate kinase. *J Cell Sci* **127**, 2351-2364, doi:10.1242/jcs.146894 (2014).

94 Manna, P. T. & Field, M. C. Phosphoinositides, kinases and adaptors coordinating endocytosis in Trypanosoma brucei. *Commun Integr Biol* **8**, e1082691, doi:10.1080/19420889.2015.1082691 (2015).

95 Wang, Z. *et al.* Genome-wide association analysis identifies genetic loci associated with resistance to multiple antimalarials in Plasmodium falciparum from China-Myanmar border. *Sci Rep* **6**, 33891, doi:10.1038/srep33891 (2016).

96 Schoijet, A. C., Sternlieb, T. & Alonso, G. D. The Phosphatidylinositol 3-kinase Class III Complex Containing TcVps15 and TcVps34 Participates in Autophagy in Trypanosoma cruzi. *J Eukaryot Microbiol* **64**, 308-321, doi:10.1111/jeu.12367 (2017).

97 Nebl, T., De Veer, M. J. & Schofield, L. Stimulation of innate immune responses by malarial glycosylphosphatidylinositol via pattern recognition receptors. *Parasitology* **130 Suppl**, S45-62, doi:10.1017/S0031182005008152 (2005).

98 Debierre-Grockiego, F. & Schwarz, R. T. Immunological reactions in response to apicomplexan glycosylphosphatidylinositols. *Glycobiology* **20**, 801-811, doi:10.1093/glycob/cwq038 (2010).

99 Passero, L. F. *et al.* Differential modulation of macrophage response elicited by glycoinositolphospholipids and lipophosphoglycan from Leishmania (Viannia) shawi. *Parasitol Int* **64**, 32-35, doi:10.1016/j.parint.2015.01.006 (2015).

100 Dobson, D. E. *et al.* Leishmania major survival in selective Phlebotomus papatasi sand fly vector requires a specific SCG-encoded lipophosphoglycan galactosylation pattern. *PLoS Pathog* **6**, e1001185, doi:10.1371/journal.ppat.1001185 (2010).

101 Wichroski, M. J. & Ward, G. E. Biosynthesis of glycosylphosphatidylinositol is essential to the survival of the protozoan parasite Toxoplasma gondii. *Eukaryot Cell* **2**, 1132-1136 (2003).

102 Gardocki, M. E., Jani, N. & Lopes, J. M. Phosphatidylinositol biosynthesis: biochemistry and regulation. *Biochim Biophys Acta* **1735**, 89-100, doi:10.1016/j.bbalip.2005.05.006 (2005).

103 Martin, K. L. & Smith, T. K. The glycosylphosphatidylinositol (GPI) biosynthetic pathway of bloodstream-form Trypanosoma brucei is dependent on the de novo synthesis of inositol. *Mol Microbiol* **61**, 89-105, doi:10.1111/j.1365-2958.2006.05216.x (2006).

104 Gonzalez-Salgado, A. *et al.* Trypanosoma brucei Bloodstream Forms Depend upon Uptake of myo-Inositol for Golgi Complex Phosphatidylinositol Synthesis and Normal Cell Growth. *Eukaryot Cell* **14**, 616-624, doi:10.1128/EC.00038-15 (2015).

105 Gonzalez-Salgado, A. *et al.* myo-Inositol uptake is essential for bulk inositol phospholipid but not glycosylphosphatidylinositol synthesis in Trypanosoma brucei. *J Biol Chem* **287**, 13313-13323, doi:10.1074/jbc.M112.344812 (2012).

106 Elabbadi, N., Ancelin, M. L. & Vial, H. J. Characterization of phosphatidylinositol synthase and evidence of a polyphosphoinositide cycle in Plasmodium-infected erythrocytes. *Mol Biochem Parasitol* **63**, 179-192 (1994).

107 Seron, K., Dzierszinski, F. & Tomavo, S. Molecular cloning, functional complementation in Saccharomyces cerevisiae and enzymatic properties of phosphatidylinositol synthase from the protozoan parasite Toxoplasma gondii. *Eur J Biochem* **267**, 6571-6579 (2000).

108 Wengelnik, K. & Vial, H. J. Characterisation of the phosphatidylinositol synthase gene of Plasmodium species. *Res Microbiol* **158**, 51-59, doi:10.1016/j.resmic.2006.11.005 (2007).

109 Meissner, M., Schluter, D. & Soldati, D. Role of Toxoplasma gondii myosin A in powering parasite gliding and host cell invasion. *Science* **298**, 837-840, doi:10.1126/science.1074553 (2002).

110 Pieperhoff, M. S. *et al.* Conditional U1 Gene Silencing in Toxoplasma gondii. *PLoS One* **10**, e0130356, doi:10.1371/journal.pone.0130356 (2015).

111 Olshina, M. A. *et al.* Plasmodium falciparum coronin organizes arrays of parallel actin filaments potentially guiding directional motility in invasive malaria parasites. *Malar J* **14**, 280, doi:10.1186/s12936-015-0801-5 (2015).

112 Brown, K. M., Long, S. & Sibley, L. D. Conditional Knockdown of Proteins Using Auxin-inducible Degron (AID) Fusions in Toxoplasma gondii. *Bio Protoc* **8**, doi:10.21769/BioProtoc.2728 (2018).

113 Howard, B. L. *et al.* Identification of potent phosphodiesterase inhibitors that demonstrate cyclic nucleotide-dependent functions in apicomplexan

parasites. *ACS Chem Biol* **10**, 1145-1154, doi:10.1021/cb501004q (2015).

114 Frenal, K., Dubremetz, J. F., Lebrun, M. & Soldati-Favre, D. Gliding motility powers invasion and egress in Apicomplexa. *Nat Rev Microbiol* **15**, 645-660, doi:10.1038/nrmicro.2017.86 (2017).

115 Nitzsche, R., Gunay-Esiyok, O., Tischer, M., Zagoriy, V. & Gupta, N. A plant/fungal-type phosphoenolpyruvate carboxykinase located in the parasite mitochondrion ensures glucose-independent survival of Toxoplasma gondii. *J Biol Chem* **292**, 15225-15239, doi:10.1074/jbc.M117.802702 (2017).

116 Podlaha, O., & Töregård, B. Some new observations on the equivalent carbon numbers of triglycerides and relationship between changes in equivalent carbon number and molecular structure. *Journal of Chromatography A* **482**, 215-226 (1989).

117 Brouwers, J. F., Vernooij, E. A., Tielens, A. G. & van Golde, L. M. Rapid separation and identification of phosphatidylethanolamine molecular species. *J Lipid Res* **40**, 164-169 (1999).

118 Cornell, R. B. & Ridgway, N. D. CTP:phosphocholine cytidylyltransferase: Function, regulation, and structure of an amphitropic enzyme required for membrane biogenesis. *Prog Lipid Res* **59**, 147-171, doi:10.1016/j.plipres.2015.07.001 (2015).

119 Rojas, P. A. *et al.* Expression of a cDNA encoding a Toxoplasma gondii protein belonging to the heat-shock 90 family and analysis of its antigenicity. *FEMS Microbiol Lett* **190**, 209-213, doi:10.1111/j.1574-6968.2000.tb09288.x (2000).

120 Ternes, P., Brouwers, J. F., van den Dikkenberg, J. & Holthuis, J. C. Sphingomyelin synthase SMS2 displays dual activity as ceramide phosphoethanolamine synthase. *J Lipid Res* **50**, 2270-2277, doi:10.1194/jlr.M900230-JLR200 (2009).

121 Chen, Y. & Cao, Y. The sphingomyelin synthase family: proteins, diseases, and inhibitors. *Biol Chem* **398**, 1319-1325, doi:10.1515/hsz-2017-0148 (2017).

122 Pratt, S. *et al.* Sphingolipid synthesis and scavenging in the intracellular apicomplexan parasite, Toxoplasma gondii. *Mol Biochem Parasitol* **187**, 43-51, doi:10.1016/j.molbiopara.2012.11.007 (2013).

123 Vacaru, A. M., van den Dikkenberg, J., Ternes, P. & Holthuis, J. C. Ceramide phosphoethanolamine biosynthesis in Drosophila is mediated by a unique ethanolamine phosphotransferase in the Golgi lumen. *J Biol Chem* **288**, 11520-11530, doi:10.1074/jbc.M113.460972 (2013).

124 Sidik, S. M. *et al.* A Genome-wide CRISPR Screen in Toxoplasma Identifies Essential Apicomplexan Genes. *Cell* **166**, 1423-1435 e1412, doi:10.1016/j.cell.2016.08.019 (2016).

125 Ramakrishnan, S., Serricchio, M., Striepen, B. & Butikofer, P. Lipid synthesis in protozoan parasites: a comparison between kinetoplastids

and apicomplexans. *Prog Lipid Res* **52**, 488-512, doi:10.1016/j.plipres.2013.06.003 (2013).

126 Drew, M. E. *et al.* Functional expression of a myo-inositol/H+ symporter from Leishmania donovani. *Mol Cell Biol* **15**, 5508-5515 (1995).

127 Einicker-Lamas, M. *et al.* Characterization of the myo-inositol transport system in Trypanosoma cruzi. *Eur J Biochem* **267**, 2533-2537 (2000).

128 Seyfang, A. & Landfear, S. M. Four conserved cytoplasmic sequence motifs are important for transport function of the Leishmania inositol/H(+) symporter. *J Biol Chem* **275**, 5687-5693 (2000).

129 Martin, K. L. & Smith, T. K. The myo-inositol-1-phosphate synthase gene is essential in Trypanosoma brucei. *Biochem Soc Trans* **33**, 983-985, doi:10.1042/BST20050983 (2005).

130 Macrae, J. I. *et al.* Plasmodium falciparum is dependent on de novo myo-inositol biosynthesis for assembly of GPI glycolipids and infectivity. *Mol Microbiol* **91**, 762-776, doi:10.1111/mmi.12496 (2014).

131 MacRae, J. I. *et al.* Mitochondrial metabolism of glucose and glutamine is required for intracellular growth of Toxoplasma gondii. *Cell Host Microbe* **12**, 682-692, doi:10.1016/j.chom.2012.09.013 (2012).

132 Martin, D. *et al.* Characterization of Plasmodium falciparum CDP-diacylglycerol synthase, a proteolytically cleaved enzyme. *Mol Biochem Parasitol* **110**, 93-105 (2000).

133 Shastri, S. *et al.* Plasmodium CDP-DAG synthase: an atypical gene with an essential N-terminal extension. *Int J Parasitol* **40**, 1257-1268, doi:10.1016/j.ijpara.2010.03.006 (2010).

134 Lilley, A. C., Major, L., Young, S., Stark, M. J. & Smith, T. K. The essential roles of cytidine diphosphate-diacylglycerol synthase in bloodstream form Trypanosoma brucei. *Mol Microbiol* **92**, 453-470, doi:10.1111/mmi.12553 (2014).

135 Kong, P. *et al.* Two phylogenetically and compartmentally distinct CDP-diacylglycerol synthases cooperate for lipid biogenesis in Toxoplasma gondii. *J Biol Chem* **292**, 7145-7159, doi:10.1074/jbc.M116.765487 (2017).

136 Dowhan, W. Molecular basis for membrane phospholipid diversity: why are there so many lipids? *Annu Rev Biochem* **66**, 199-232, doi:10.1146/annurev.biochem.66.1.199 (1997).

137 Buckland, A. G. & Wilton, D. C. Anionic phospholipids, interfacial binding and the regulation of cell functions. *Biochim Biophys Acta* **1483**, 199-216 (2000).

138 Ben-Tal, N., Honig, B., Miller, C. & McLaughlin, S. Electrostatic binding of proteins to membranes. Theoretical predictions and experimental results with charybdotoxin and phospholipid vesicles. *Biophys J* **73**, 1717-1727, doi:10.1016/S0006-3495(97)78203-1 (1997).

139 Mulgrew-Nesbitt, A. *et al.* The role of electrostatics in protein-membrane interactions. *Biochim Biophys Acta* **1761**, 812-826, doi:10.1016/j.bbalip.2006.07.002 (2006).

140 Hresko, R. C., Kraft, T. E., Quigley, A., Carpenter, E. P. & Hruz, P. W. Mammalian Glucose Transporter Activity Is Dependent upon Anionic and Conical Phospholipids. *J Biol Chem* **291**, 17271-17282, doi:10.1074/jbc.M116.730168 (2016).

141 Fan, Z. & Makielski, J. C. Anionic phospholipids activate ATP-sensitive potassium channels. *J Biol Chem* **272**, 5388-5395 (1997).

142 Hullin-Matsuda, F. *et al.* De novo biosynthesis of the late endosome lipid, bis(monoacylglycero)phosphate. *J Lipid Res* **48**, 1997-2008, doi:10.1194/jlr.M700154-JLR200 (2007).

143 Lecommandeur, E., Baker, D., Cox, T. M., Nicholls, A. W. & Griffin, J. L. Alterations in endo-lysosomal function induce similar hepatic lipid profiles in rodent models of drug-induced phospholipidosis and Sandhoff disease. *J Lipid Res* **58**, 1306-1314, doi:10.1194/jlr.M073395 (2017).

144 Eskelinen, E. L. & Saftig, P. Autophagy: a lysosomal degradation pathway with a central role in health and disease. *Biochim Biophys Acta* **1793**, 664-673, doi:10.1016/j.bbamcr.2008.07.014 (2009).

145 Gibellini, F., Hunter, W. N. & Smith, T. K. The ethanolamine branch of the Kennedy pathway is essential in the bloodstream form of Trypanosoma brucei. *Mol Microbiol* **73**, 826-843, doi:10.1111/j.1365-2958.2009.06764.x (2009).

146 Sutterwala, S. S. *et al.* Developmentally regulated sphingolipid synthesis in African trypanosomes. *Mol Microbiol* **70**, 281-296, doi:10.1111/j.1365-2958.2008.06393.x (2008).

147 Sonda, S., Sala, G., Ghidoni, R., Hemphill, A. & Pieters, J. Inhibitory effect of aureobasidin A on Toxoplasma gondii. *Antimicrob Agents Chemother* **49**, 1794-1801, doi:10.1128/AAC.49.5.1794-1801.2005 (2005).

148 O'Connor, J. D., Polito, A. J., Monroe, R. E., Sweeley, C. C. & Bieber, L. L. Characterization of invertebrate sphingolipid bases: occurrence of eicosasphinga-4, 11-dienine and eicosasphing-11-enine in scorpion. *Biochim Biophys Acta* **202**, 195-197, doi:10.1016/0005-2760(70)90234-1 (1970).

149 Yang, T. K., Means, E., Anderson, L. E. & Jenkin, H. M. Sphingophospholipids of species of Aedes and Culex mosquito cells cultivated in suspension culture from logarithmic and stationary phases of growth. *Lipids* **9**, 1009-1013 (1974).

150 Abeytunga, D. T. *et al.* Presence of unsaturated sphingomyelins and changes in their composition during the life cycle of the moth Manduca sexta. *J Lipid Res* **45**, 1221-1231, doi:10.1194/jlr.M300392-JLR200 (2004).

151 Ghosh, A. *et al.* A global in vivo Drosophila RNAi screen identifies a key role of ceramide phosphoethanolamine for glial ensheathment of axons. *PLoS Genet* **9**, e1003980, doi:10.1371/journal.pgen.1003980 (2013).

152 Kunduri, G. *et al.* Defective cortex glia plasma membrane structure underlies light-induced epilepsy in cpes mutants. *Proc Natl Acad Sci U S A* **115**, E8919-E8928, doi:10.1073/pnas.1808463115 (2018).

153 Inaba, T. *et al.* Formation of tubules and helical ribbons by ceramide phosphoethanolamine-containing membranes. *Sci Rep* **9**, 5812, doi:10.1038/s41598-019-42247-1 (2019).

154 Chotiwan, N. *et al.* Dynamic remodeling of lipids coincides with dengue virus replication in the midgut of Aedes aegypti mosquitoes. *PLoS Pathog* **14**, e1006853, doi:10.1371/journal.ppat.1006853 (2018).

155 An, D., Na, C., Bielawski, J., Hannun, Y. A. & Kasper, D. L. Membrane sphingolipids as essential molecular signals for Bacteroides survival in the intestine. *Proc Natl Acad Sci U S A* **108 Suppl 1**, 4666-4671, doi:10.1073/pnas.1001501107 (2011).

156 Moye, Z. D., Valiuskyte, K., Dewhirst, F. E., Nichols, F. C. & Davey, M. E. Synthesis of Sphingolipids Impacts Survival of Porphyromonas gingivalis and the Presentation of Surface Polysaccharides. *Front Microbiol* **7**, 1919, doi:10.3389/fmicb.2016.01919 (2016).

157 O. Geiger, J. P.-G., I. López-Lara. in *Biogenesis of Fatty Acids, Lipids and Membranes* 1-15 (Springer Nature, 2018).

7. Appendices

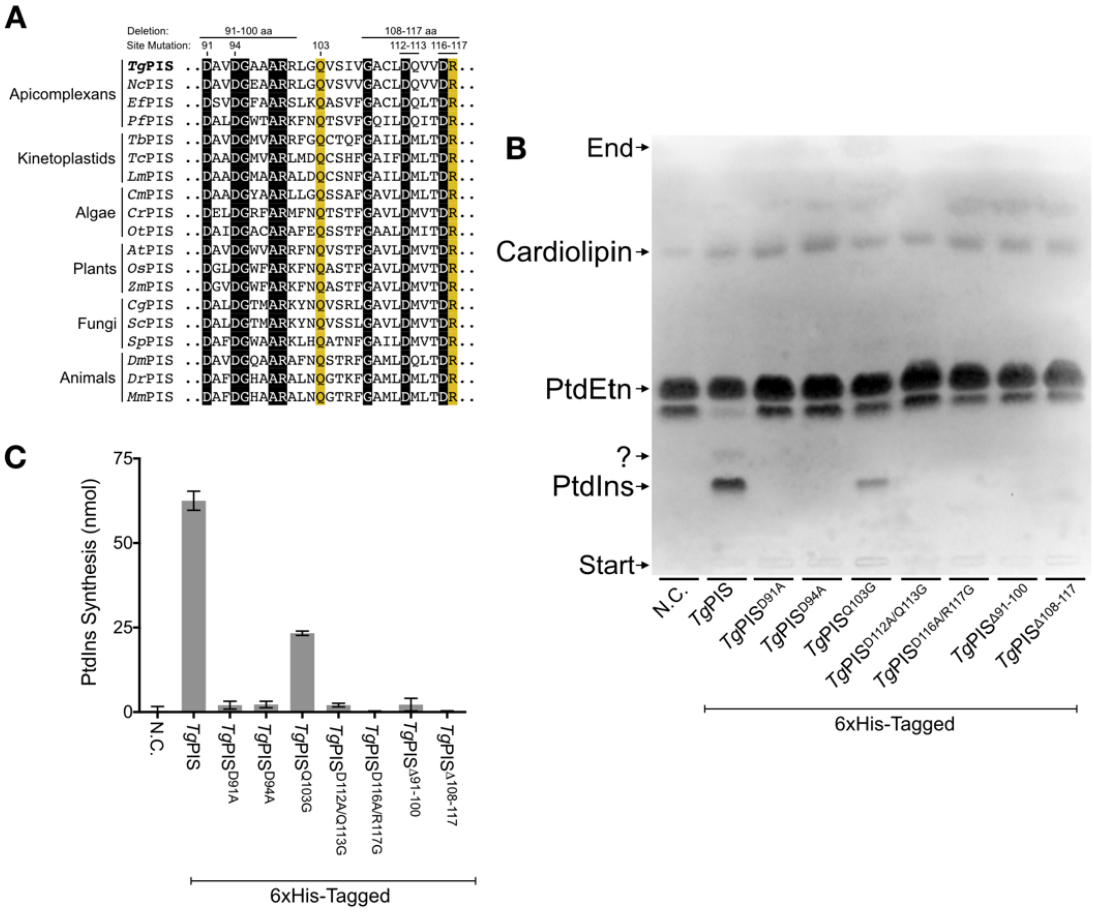

Appendix.1: CDP-alcohol phosphotransferase motif is essential for the catalytic activity of *Tg*PIS. (A) Alignment of the CDP-alcohol phosphotransferase motifs present in PIS sequences. The residues conserved only in PIS sequences were highlighted in yellow, whereas those that are identical across all CDP-alcohol phosphotransferase domain-containing proteins were shaded in black (also see Table S1). The amino acids chosen for site-directed mutagenesis or deletion were marked for their position on top. Organism abbreviations: *Nc*, *Neospora caninum*; *Ef*, *Eimeria falciformis*; *Pb*, *Plasmodium berghei*; *Pf*, *Plasmodium falciparum*; *Tb*, *Trypanosoma brucei*; *Tc*, *Trypanosoma cruzi*; *Lm*, *Leishmania major*; *Cm*, *Cyanidioschyzon merolae*; *Cr*, *Chlamydomonas reinhardtii*; *Ot*, *Ostreococcus tauri*; *At*, *Arabidopsis thaliana*; *Os*, *Oryza sativa*; *Zm*, *Zea mays*; *Cg*, *Candida glabrata*; *Sc*, *Saccharomyces cerevisiae*; *Sp*, *Schizosaccharomyces pombe*; *Dm*, *Drosophila melanogaster*; *Dr*, *Danio rerio*; *Hs*, *Homo sapiens*. **(B)** TLC-resolved lipid profile of *E. coli* (M15/pREP4) strains harboring *pQE60* (N.C., negative control), or *pQE60* constructs expressing the 6xHis-tagged *Tg*PIS and its mutated variants, as indicated. Bacterial cultures were cultivated with 1 mM *myo*-inositol, as described in Material and Methods. **(C)** Phosphorus analysis of PtdIns-containing TLC band from panel **(B)** (n= 3 assays, mean ± S.E.). These data were generated by Fatima Heider and Pengfei Kong.

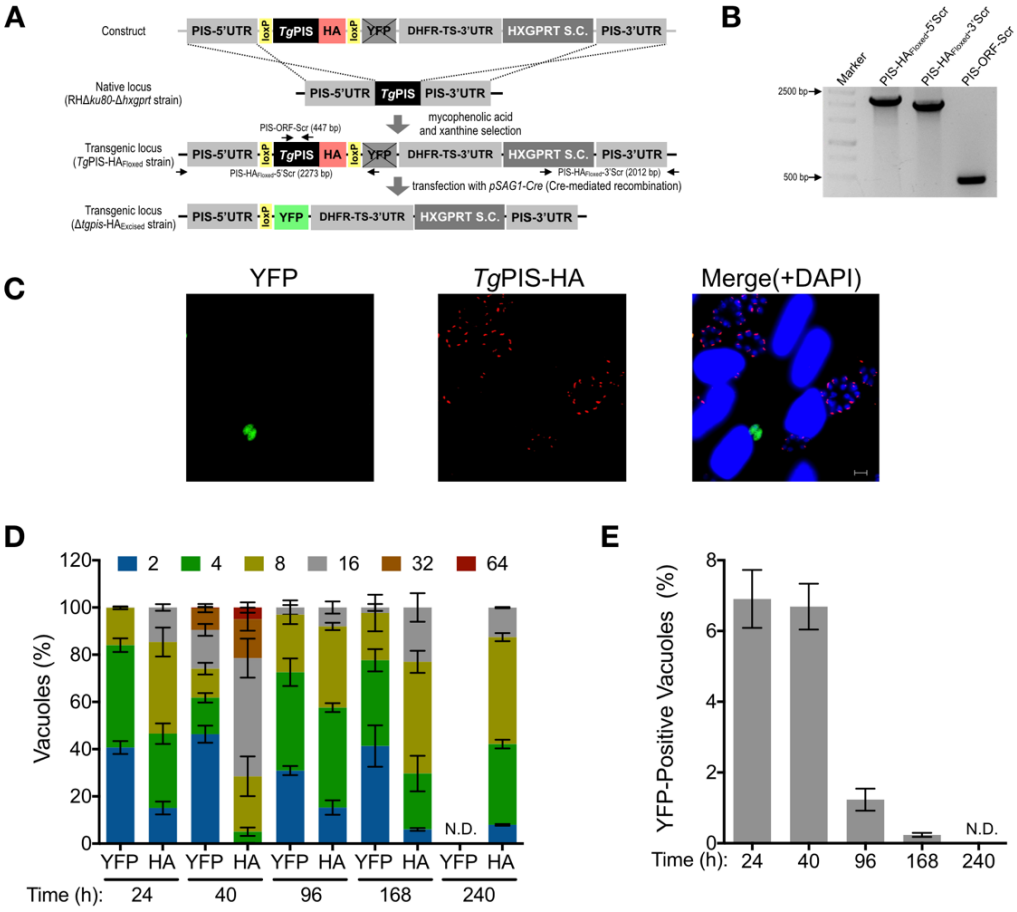

Appendix.2: Cre-mediated excision of *Tg*PIS abrogates the parasite growth. (A) Scheme illustrating the gene deletion strategy for *Tg*PIS. In the first step, the *Tg*PIS gene in the RH*Δku80Δhxgprt* strain was replaced by a cassette comprising loxP-flanked (floxed) HA-tagged open reading frame of *Tg*PIS (*Tg*PIS-HA), YFP sequence and HXGPRT selection cassette (S.C.) to generate the stably transgenic *Tg*PIS-HA$_{Floxed}$ strain. The second step involved transient transfection of the *Tg*PIS-HA$_{Floxed}$ strain with pSAG1-Cre vector to induce Cre-mediated recombination, which excised *Tg*PIS-HA and repositioned YFP sequence in the eventual *Δtgpis*-HA$_{Excised}$ mutant. Note that YFP in not expressed in the *Tg*PIS-HA$_{Floxed}$ strain, but Cre-mediated excision of *Tg*PIS-HA brings it in the proximity of the PIS promoter, which enabled YFP expression in the *Δtgpis*-HA$_{Excised}$ mutant. **(B)** Genomic PCR of the *Tg*PIS-HA$_{Floxed}$ strain confirming the events of 5'- and 3'-crossovers and insertion of TgPIS-HA. Primers used for the PCR-screening of 5'- and 3'-recombination events at the *Tg*PIS locus were marked as arrows in panel **(A)**. **(C)** Immunofluorescence detection of *Tg*PIS-HA (red) and YFP expression (green) in the *Δtgpis*-HA$_{Excised}$ strain 24 h after transfection with pSAG1-Cre construct. Nuclei were stained with DAPI (blue). Scale bars: 5 µm. **(D)** Quantification of tachyzoites in the parasite vacuoles showing YFP or HA signal at different times after transfection with the *pSAG1-Cre* vector. Colors represented the variable number of parasites developing in the vacuoles. The number of tachyzoites/vacuole was counted from 400-500 vacuoles for each strain.

(E) The proportion of parasitophorous vacuoles with YFP signal in the *Δtgpis*-HA$_{Excised}$ mutant. Data in panel **(D-E)** showed mean values with S.E. from three independent assays (N.D., not detectable). These data were generated by Fatima Heider and Pengfei Kong.

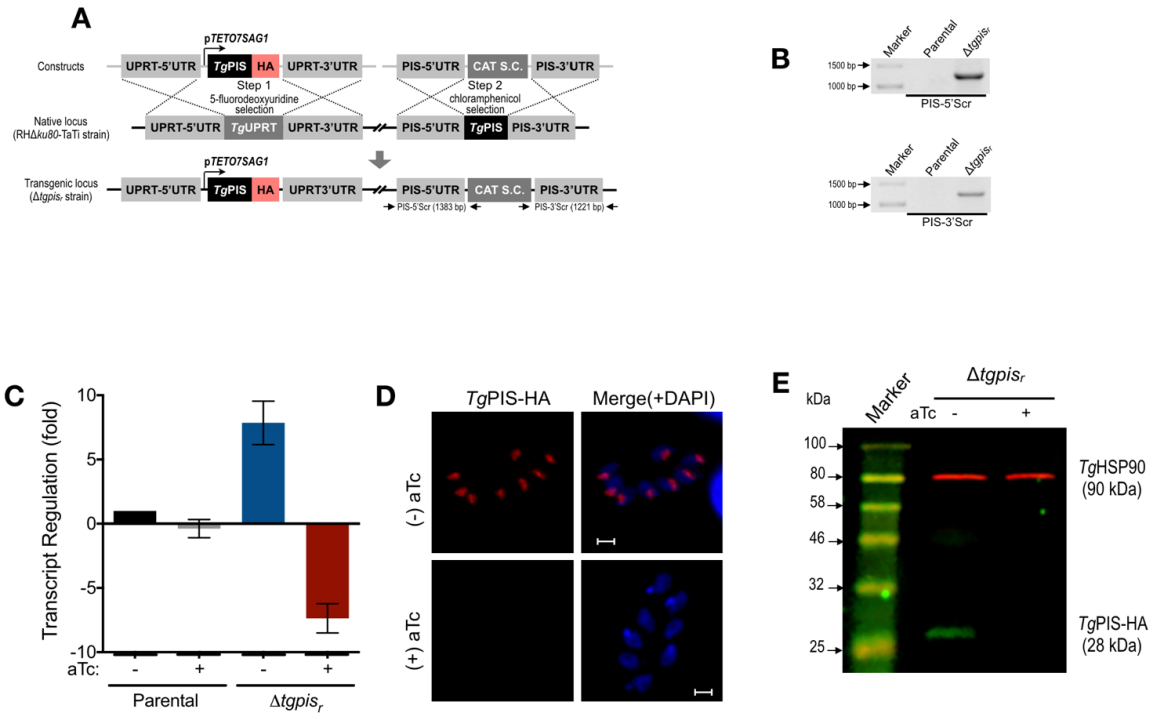

Appendix.3: Transcriptional repression of *Tg*PIS by tetracycline in tachyzoites of *T. gondii*. **(A)** Construction of the Δ*tgpis*$_r$ mutant. A tetracycline-regulatable open reading frame of *Tg*PIS (*Tg*PIS-HA) was first integrated at the *Tg*UPRT locus in the RHΔ*ku80*-TaTi strain (*Step 1*), followed by deletion of the *TgPIS* gene by CAT selection cassette (S.C.) *via* homologous recombination (*Step 2*). Primers used to screen for the 5'- and 3'-crossover events at the *TgPIS* locus are marked as *arrows*. **(B)** PCR screening of the Δ*tgpis*$_r$ strain confirming the mutagenesis. Genomic DNA of the RHΔ*ku80*-TaTi strain was included as a negative control. **(C)** Quantitative PCR of *Tg*PIS transcript in the Δ*tgpis*$_r$ mutant. The relative levels of transcript were measured in the *on* (-aTc) and *off* (+aTc) states using the $\Delta\Delta^{CT}$ method. **(D-E)** Immunofluorescence and immunoblot images of the Δ*tgpis*$_r$ mutant illustrating a conditional repression of *Tg*PIS-HA after aTc treatment for 4 days. Staining was performed using α-HA and α-*Tg*HSP90 antibodies (loading control in *panel **(E)***), as indicated. Nuclei were stained with DAPI (blue). *Scale bar*, 2 μm. Note that the colors of *Tg*PIS-HA staining differ in *panel D* and *E* due to different secondary antibodies. These data were generated by Pengfei Kong.

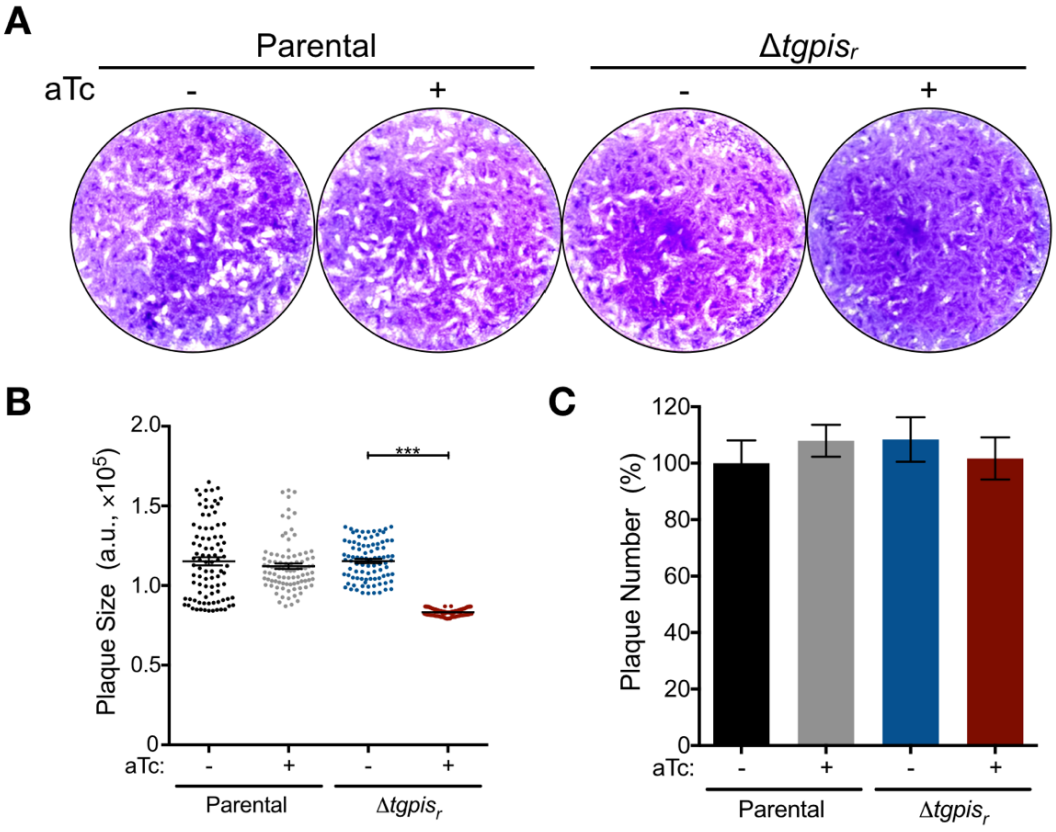

Appendix.4: Tetracycline-regulated downregulation of *Tg*PIS causes only modest growth defect. (A) Plaque assays displaying the growth fitness of the RHΔ*ku80*-TaTi and Δ*tgpis*$_r$ strains, cultured in the presence or absence of aTc. HFF monolayers were infected with 250 tachyzoites (pre-cultured without or with 1 µM aTc for 4 days) and incubated for 1 week without any perturbation to allow plaque formation. **(B)** Plaque numbers of the parasite strains from panel *F*. **(C)** Size of individual plaques formed by the strains specified in panel **(C)**. 90 plaques of each strain were measured for area using ImageJ software (*a.u.*, arbitrary units). Graphs in panel **(B)** and **(C)** showed the mean values with S.E. from three independent assays (***, $p \leq 0.001$). These data were generated by Pengfei Kong.

\

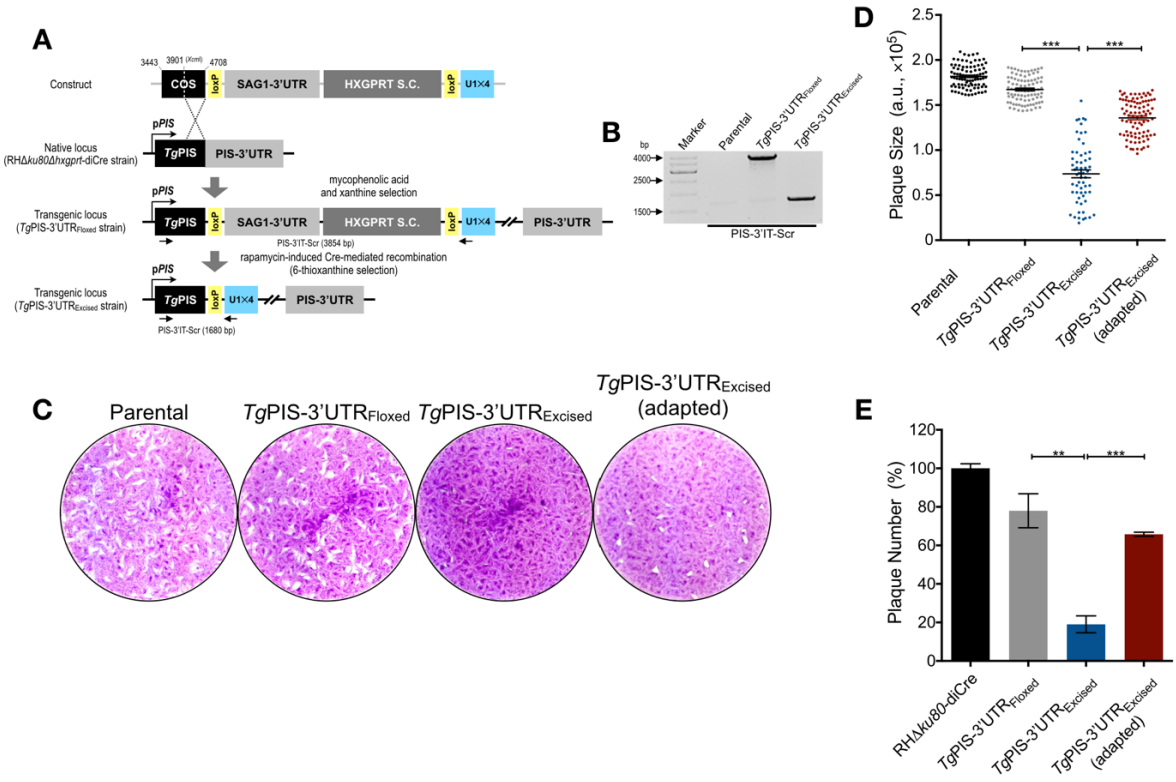

Appendix.5: Cre-recombinase mediated excision of *Tg*PIS-3'UTR imposes an acute but adaptable impairment in the lytic cycle. (A) Schematic illustration of *Tg*PIS-3'UTR deletion. Plasmid harboring the crossover sequence (COS) of *Tg*PIS was linearized with *Xcm*I and transfected into tachyzoites of the RHΔ*ku80*Δ*hxgprt*-diCre strain that resulted in 3'-insertional tagging (3'-IT) of the *TgPIS* gene with a loxP-flanked *Tg*SAG1-3'UTR (*Tg*PIS-3'UTR$_{Floxed}$ strain). Subsequent diCre-mediated recombination induced by rapamycin (50 nM) excised the *Tg*SAG1-3'UTR and yielded the *Tg*PIS-3'UTR$_{Excised}$ mutant. Primers for the PCR screening of floxed and excised 3'UTR are shown as *arrows*. **(B)** Genomic PCR screening endorsing the floxed or excised *Tg*SAG1-3'UTR. DNA of the RHΔ*ku80*Δ*hxgprt*-diCre strain served as a negative control. **(C-E)** Plaque assays depicting the phenotypic impairment in the *Tg*PIS-3'UTR$_{Excised}$ mutant. Note that the rapamycin-induced Cre-mediated deletion of *Tg*SAG1-3'UTR severely impaired the plaque sizes **(D)** and numbers **(E)**, both of which were however notably convalesced within 2-3 weeks (adapted). For panel **D-E**, the mean values with S.E. from three independent assays are shown (**, $p \leq 0.01$; ***, $p \leq 0.001$). These data were generated by Pengfei Kong.

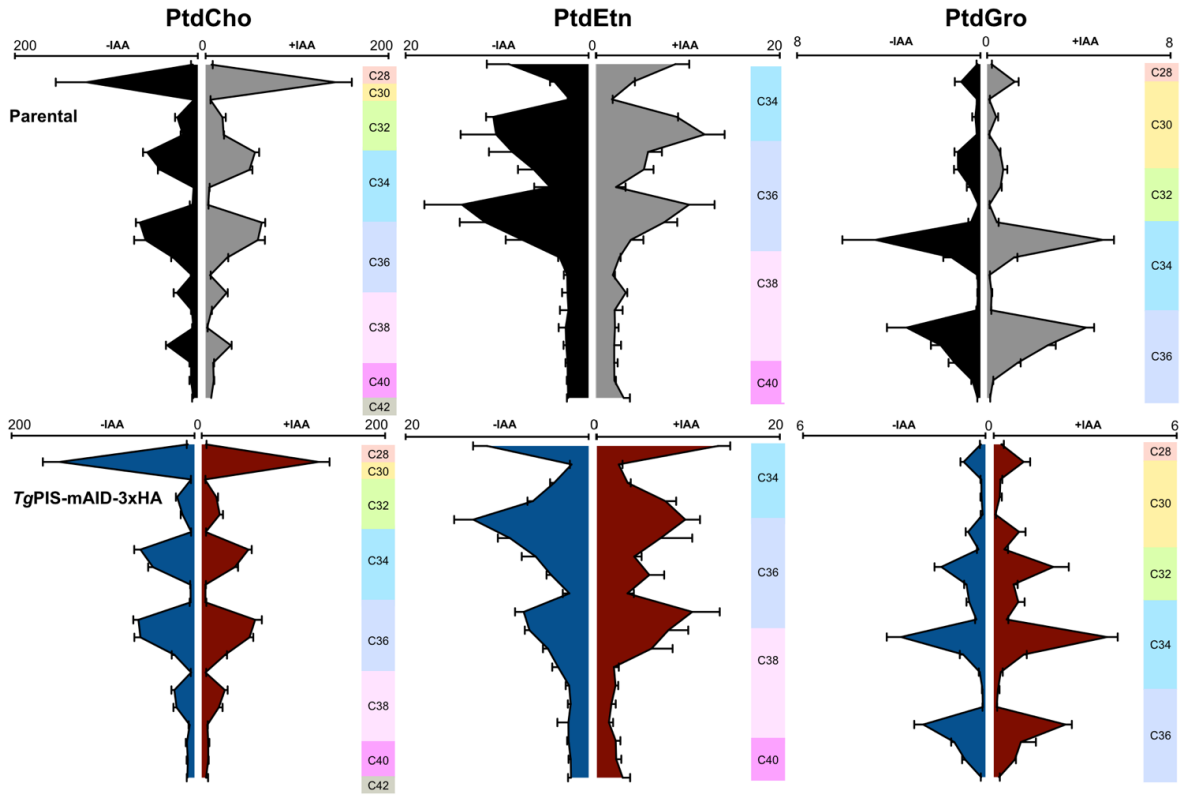

Appendix.6: Downregulation of *Tg*PIS does not affect PtdCho, PtdEtn and PtdGro species. Lipids from the *Tg*PIS-mAID-3xHA (mutant) and RH*Δku80Δhxgprt*-TIR1 (parental) strains were analyzed by lipidomic analysis. For each lipid class, the amount of all major species (amounting to >90% of lipid) was plotted (pmol/10^6 parasites) as violin-like plots. Changes in the contour of graphs reflected the overall alteration in given lipids (n= 4 assays with S.E.). Samples with (+) or without (-) IAA treatments were colored differently. Species were ordered with increasing acyl chain lengths from the top to bottom. Statistical significance was measured for each lipid species by comparing auxin-treated and control samples. None of the species qualified the significance test.

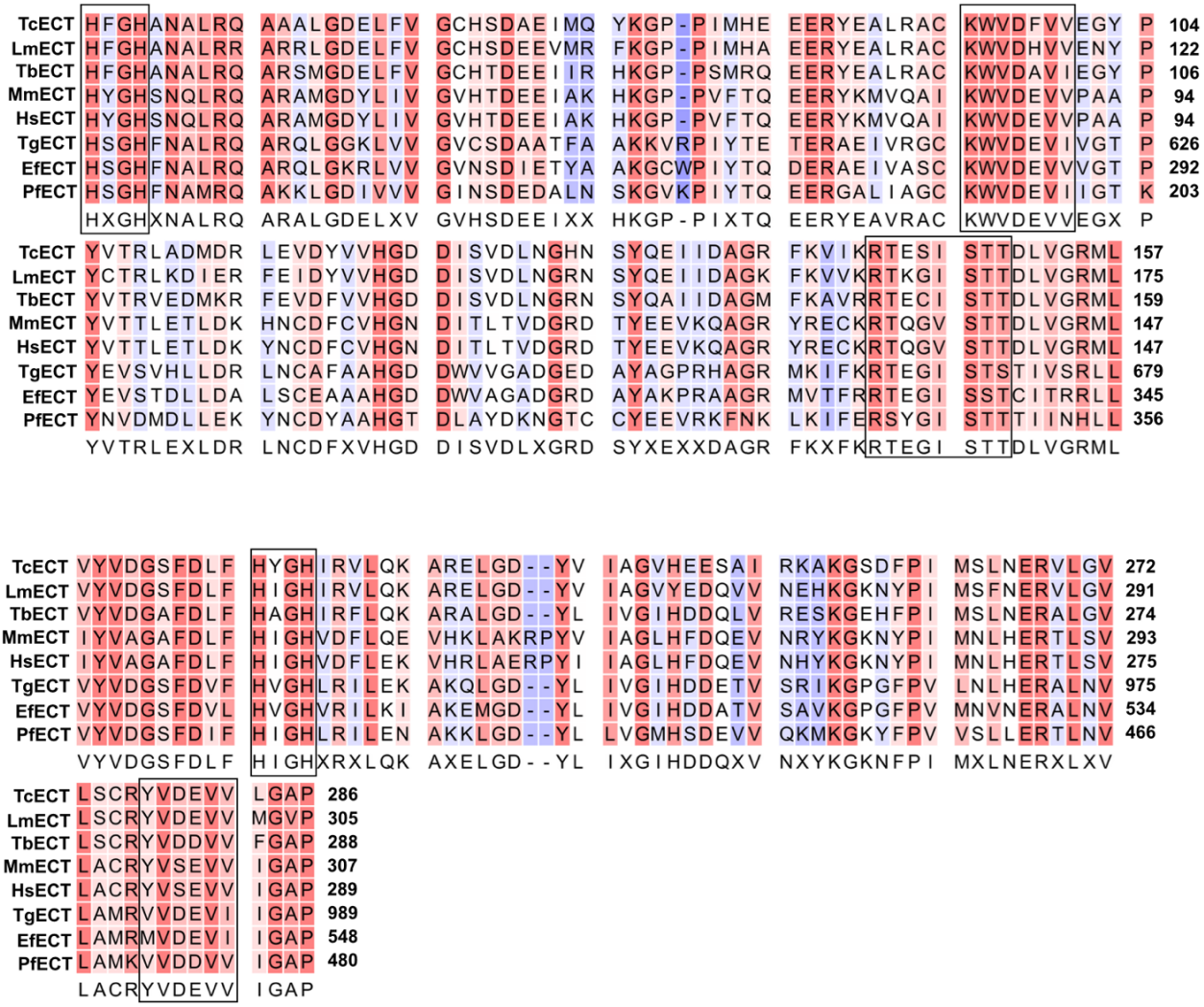

Appendix.7: High conservation can be identified at two catalytic centers of ECTs. Aligned amino acid residues were colored based on its conservation from 0-100%. Structures predicted to be essential for catalytic activity were framed. **(A)**, alignment of N-terminal cytidylyltransferase domains of all ECTs. **(B)**, alignment of C-terminal cytidylyltransferase domains of all ECTs. *Tg, Toxoplasma gondii; Ef, Eimeria falciformis; Pf, Plasmodium falciparum; Tb, Trypanosoma brucei; Tc, Trypanosoma cruzi; Lm, Leishmania major; Hs, Homo sapiens; Mm, Mus musculus.* Details of selected sequences was shown in Table S2.

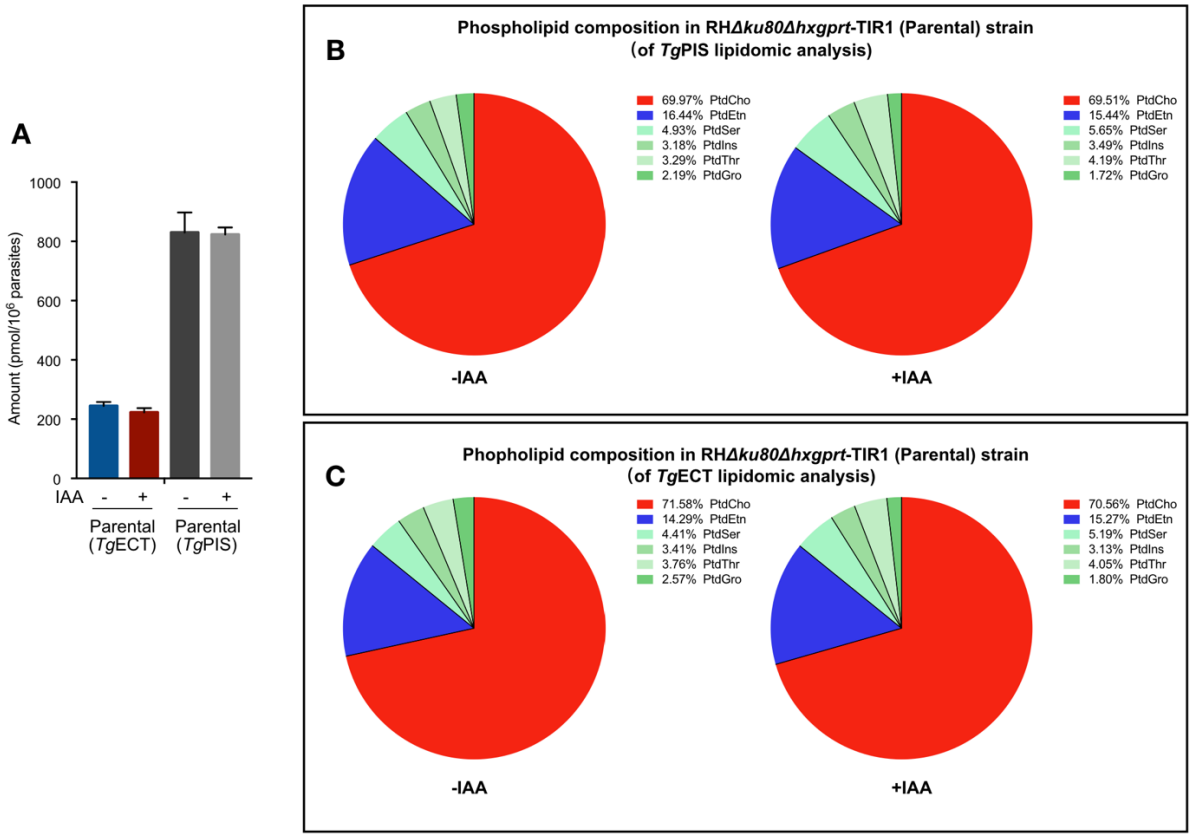

Appendix.8: Comparison of phospholipid content between parental strain in the lipidomic analysis of *Tg*PIS and *Tg*ECT. (A) Actual detected phospholipid amount from parental RH strain used in *Tg*PIS and *Tg*ECT lipidomic analysis. Average phospholipid content of four replicates in *Tg*PIS lipidomic analysis and five replicates in *Tg*ECT lipidomic analysis were selected for the plotting. **(B-C)** Phospholipid composition of individual lipid class were plotted. The percentage was calculated by using the average content of four replicates (in *Tg*PIS lipidomic analysis, panel **(B)**) or five replicates (in *Tg*ECT lipidomic analysis, panel **(C)**)

Appendix. 9: Gene and vector sequences

*Tg*PIS (*Tg*GT1_207710)

gDNA (intron in lower cases)

ATGGCGGGGACTTCTGCAAGCCGCGAGGACAGCCAGTCTCCCGCTGTTCGACAG
AGAGTGGGCAGCGCTTCTGGAGGCAAAAGTGTCCAAGCGGCGTCAGATTCTGAC
CTTTCTCATGAACAAAAATGGGCGCGGGAGTTGAAAGTTTTCCTCTACGTGCCAA
ACATCATTGgtaagaagggtccgtcccaccagacttggagttccccagaaacagtgggggttggggatggtagtc
gcggctcttgtatggggtttaggggacaatagctgcggatcttctgcaattgaaccgttactgctgtacgcatcttatctcgcc
ttttatgcggtgtactacaatagttctacacttcttctactgacatttaactggtcctactaaccctgcaggtgactctgttcgtag
ccttggggatccagagggttgctaggttgtatttgcttcttccaatccgttacacctctcagacagggatgaaaaacgaatg
cctgtgctcttcgtttcttttccgcggtgtaacgcccgtgcaagctgcatgcggacaggcgcaaagcgaaactcgggtcca
caccgcgtgtacgatccttcttcattgtctttaagcttcattcttgcgcgcgtaccactcaaacgaaatccttaaagctcaggt
gctctgtcctgactttgatctgttggaagcctttcctcgcagtgctccagcgaactgaaaacctactgaaggtgctcagtctg
cgagatctgccgacttgtcgtgttctcagGATACGTTCGTATCGCGCTGCTGTTGGCCGCTGCAT
TTGCGTGGCGAGAAGCGTACACTTCTCTTTTCTTTGTTTCTTATGTTACATCGCAAT
GCCTGGACGCAGTCGATGGCGCTGCCGCACGCCGTCTGGGCCAAGgtgagtttcacag
gagtcttcagacaatctggactttcaatttacactgagacccccgccaacaccgctcgcgcgcttcagatccgtcggaac
ggcagaccgaatccacatcgactgcaggatacattagtctaacaccaataaagtgaaaaacatccaatgtcgcacga
atgaactgttgcatatcaaactcaacatgaaagaaccccgcagggtagcgaacctgagacaacaaaggaaggaaac
tgaagagtacggggccgagatgaagaagtagaagatttgtgctggagaccaggagtgacgtgcgcgtactgttcccac
gatccttctacagcttacacgggaacctgtgacttgcatgcagtgcgaaacatgaaaatagcgaagcagaaaagggca
ctcttgtcagtgtcgagtttcctggttctcgttcattcttgtcaatagtcgagacgaatcgacgacaattgctgtagtgctccgc
gattcgagttccgttcactcatctgcctgcacagtgcaacaccgcgctgagcaaccgagagacggaccgagggctctg
aatgtgactccagttatgagatagagagagaatcaagagctttatcatagctgtacaccacaacgcccgcaaaatgctg
ggcgagtcagaccaagatcgtgacgaaggtgtcgatacatcagaaacgataaagcgctgcttcccattttctgtcgtggtt
ctcagTTTCCATTGTCGGCGCCTGTCTCGACCAAGTTGTCGACCGGCTTTCAACATG
TCTACTGTATGTTCTGAACGCCTCGGTCTACCCTGACTTTGCTTTCGgtgagattcagtg
aatcgcagctttctgcagaagtggataaacacgcgaggtctttgtcaaatggctctcctttacatgcctgtgtatgccgccc
gctggcctttggtttccctctgagaattgggagtttctgtaaccgtgggcagtttcgcaatatacgtttgaatacgaactcgtgt
attttcacaaaaaacattcatagatatttgtgtgtatttatatttctgcattatatatatatatatgtatatgtatatgtacactctc
gcaagtagtggtttattctccgtatgtgtatagatatatctgcgcgtatgtgcggatctcagtgcggcgtgttcatatgaatgcg
ttcggtatgtataagcatgcgcgcagaactacagacgagcatgaaaatatgtttgattacctacatacaagcatgtttcgtt
accggtttctgccgagcggttcatccagacgctgcagcaagaaaaccttcgacaaatctggagtatccctctcaggattc
ctgaagtttctggcttctgtgtctttctgcgctgttgagtggctgcctttgctccgtggtggcgtatgtacagtggccctttgtctct
gtttcctctcgctttcagCGTTTTTCATCGCGCTTTTTCTGGACATGGGTGGCCACTGGGTC
CACTTCTTCGCCGCGGCCGTCGTTGGCGCAAAGTCTCACAAAACGATGGATCCG
GAAGTGAATGCCATTCTCTCCGTCTACTACCGTTCTCGCCgtaggtcgctattctgcttaaaag
gaccagctgctgttggcccttccaaatcttgttttctctccacatggaaccgtgtgcccattctggtttcctgacgaaaagaat
aattcgtttctactttcctcgaacttctgctctgctggaaagctcttcctgatatctatgtgaatttgtctctcgtccgatgcatgtat
atgaatatcactttacgttcggacaaacatgtaatataaatatatatatatatatttatatatagtatattgccttaccatgtgca

gcctactcacttcacccgttttcaactacttgtcttccttccgtttgaacaagcgcctttcaatgatgactttggagctgtcccttgt
cgctgtgggtgtgtctaaggaataaaagtgtatttgtctgtgcgttatcgagcttctgtggactcggtcgaaattcacaaggg
ccgatgtacgtgcgggtggcaaagaacgggggcactttgacggggagtttatccccgctcttaaagtcggctgcaagca
tgttgtttttcctccattctccgttgtagacgtagcagctccgccagcgtttttctctccccgcgttttatccctcaacactctgtga
aaagacaaatgcgcactgatatgcctgtgcgtgcatgtgtgcactttgggttgtgtgtctgttgtcgggtgctgatgctttccttc
tgggcctactgttttgcgcggagttttgtgttttgtgtttccgcagCGGTCATGTTTTCGGCGATCGTGGGCT
TCGAGGGGTTCTTCATGTGCCTTCTTCTTTTGGCATCGCCGGTCGTCCAGGCTTC
AGCTGCCTCGCTGTCCTCGGCACgtaggtgaatctgctgttgctaaccgtgaaacgcagaaggcagttc
agtcttctttgctgcgtcttctttgcttccctttctacgtagcttctcttccgtactcgatgggtagtctggtcaacgctaaccccag
cgcgtcagatgacgacgcaagaacggcaggaactgttctcacatatccctagagcgaagtcatgcgcgctgcagtcct
cttcacaccgcggcaatgtactggccggtgcatgcgcttttcacggttctgcaaatggctgtgttctgggggccagacagc
acggggtcatgctgcagatctgcgcatgcagacggagagagaggtatggactcatcgagcggctttcttccgacatgtct
tgtccttggaagaggatagaagcgtccgtggtaaacaccgctcctgcctatttactttgcatgcattcagTCCTCGTC
ATTGTCTACGTCACTTCTCCCCTGATGATCTTCAAGACGgtgagacgggagtttctggggtcct
acggtcgtgccgacctttccttccaatacgccgttggtaccttggcgatgtggaggatccgtcacctctgatgtagcagtcg
aacgcggttttggaggctgcttcatttgtttactggggttccgcgcctgcaaaggccaaatggaggggagcgcagctcaa
ggtgctacaaaggagaggacagacctcgatggaaaatgcaacaccgcaggaatttcataggaagtaaacaggcagt
cacatgcattttagtgccgggagggccgcagcagagggacgatggagttgaggttgaatccttctctcttctgtggaaaa
acatgggtgtgtctgtcccctcaaaagccagaaaggggtctgagaatgtgcagaaacctctccacaagtaaacaaccg
aaacggggctcgtgcacgcgaaggaggttcagtgccaagagataaagaaacaaatcaatgctgcagacgcacagt
gcgtgctgtgtcagtgctttttcacaggtctgcttcagatctcttgttgttcaagctcacacgaaatggaagctggtgaggggg
aggcaccaggatggcaaacgacgtgtacgaaatggctagtgtgtctctttgtttcctcattcggtgcctttctttctgtgtctctg
ttttcactgtctctttttttcctccattttctgcctctcgatcgttccccggccgccgcggtgcttctcccgccgtcaccttccgactctt
gggatccccggtctgcctttgctcgcaacagCTGACGAATCTCCTCCAAGGACTGTACGGAGCCA
GGCGCTTGGTTGCGTGCGACATTTTTGGTGCGCCCTCGTCGTAA

*Tg*ECT (*Tg*GT1_207710)

gDNA (intron in lower cases)

ATGACGGCGGTAGCGTCGTCGGAGGTGCTCGGCCCCGCCCGGTCGGGAGCCTT
GCCTTCCTCTCCATCCAAAAGCTGGTCTTCTCCGTTTATTTCTTCTTCCTACCTCCA
CAAACTCATTTTCCTCTACCTCCGCATCAATGCTGACGAAACGCTCTCGGCGAAA
CTCAGGCACTGGCCTTCGGTGTGCTGTCACTGCTCTTCCCGCGTTCGAGTTTCCC
TTCCACATGCGGCGGTCCGCTCCTCTTCTCACGCGTCTTCCGTCTCTTCGTTGAC
AACGTGTGCGACTGGGAACAAGAGCGCATGCAGCTACTGCGGAGCCGGAGCCG
GAGGGGCGACAGAGCCGATGGAGGAGACTGAGGACGCAGATTCAGCCGCCTCC
CGGCACCCTTGCTGCTTCTGCTGCTGTGTGAAGGACCCCAAATGGACAGCCGAG
GCAGACGCAGAGTTCTCAGCTCTGCGGGCGCATCTCCTTCAGTTTGTGGCGCGT
AGCGAAGCTTCTCCAAACCCAGGGGAGACGTCGCCTGCCGGTGAGACGGCGGA
GACAGAAACTCCAGGCTTCTCTCCATTGTCCAGTCAATCTACGGGGGAAAATCGA
ATGCACGCGAGTTCCAGAGACTGCTCTGCCTTATCGGCGCCTCTTTCTGGAGACC
GAGCTAAGACCGACAAAAAAGGCGAGGAGACGGACGCCGGTGCCGGGGCAGGG
ACGGAGACGAGTGAGCAGACCAGAGAACGCTTGGGCAGACTGCATGCGTATGCG

GCGTCTGGACTACGCAGCGAGACGGAGACGCAAGGAAGCACTCTCGGCTCCGG
ACGGATCGAGGAAGAGCAGAAGATCACAGAGGACGAAACGAAGGGCCATCGAG
GCGTCTCTCCACTGGAACAAGAGACCCTGTGCAGCGAGGTAGTTTCGCCCTGTG
ACTGCGAAGAGGAGGCAACGCCCGTCGCGCAGGTGGAAAGCGACCAAGTGACG
CCTGCAAAACCTGCCTGCGTCCGGGACGCCAGTGTCTGTACACATGAGCAGACC
AGGAACGACGACGGCGGCGTTCCAGACACGGAGGAAAACCGCGTTCAAGAAGAA
GCGTCTGCTTTTTTCTCTGGAGAAGCGCGGAAGGCGGAGAGTCACAAACATTTTT
CTGCTTGTCGAGGACCGCAGAGTCGCGCAACAGATGCTGAACTCGGAAGAACAA
ATGTCTCTCCTGCAGGCCGCTCAGAGACAGGACGAGGGGCGTTGCCTTCTGAGC
AGGCAGACGCGCCGCCTTGTCCCCCCTCTTCCCCCGCGAGTTCGTTTCTTGCGG
ACTGTGTCTCTGGACGCCAACATGTCTCTCTGTCTCCTCTCGGCGTCTCTTCCTC
GAGCGCGTGTCTAGACAGCGTCCCGGCGTATCACTGGAACGCGCTTCCTCTGGT
CTTGCCCGTTCCATCTGCCTTTTCGTCTTTCCAGCATCTGGCAAGTCCCTGTGCGT
CTCCGTCCTCTCCCTTGGCTTCGCCGTCCTCTCCCGTGGGTTCGCCGTCTGCGAA
GTCACTCGTTTTTCGACCGTCTCCGTCTTCAGGTCCGGCCGAGGAGACTCCCCC
GCATGCGTCCTTCGCTCTCGCGCCAGTGGCTCCGTCGCCGCAGCTGTCTCCGTT
CCCCGCGCGATCCGCATGCGCTCCGGGAGCTCCTGTGCGGATCTACGTGGACG
GCGTATTCGACCTCCTGCACTCGGGGCACTTCAACGCGCTTCGCCAGGCTCGAC
AGCTGGGCGGGAAGTTGGTGGTGGGCGTCTGCAGCGACGCGGCGACTTTCGCG
GCAAAGAAAGTCCGGCCTATCTACACGGAGACGGAGCGAGCGGAAATCGTTCGC
GGGTGCAAGTGGGTCGACGAAGTGATCGTCGGGACGCCGTACGAGGTGTCTGTC
CACCTGCTCGATCGACTGAACTGCGCCTTCGCGGCTCACGGCGACGATTGGGTG
GTTGGTGCCGACGGAGAGGACGCGTACGCGGGACCTCGGCATGCGGGGCGCAT
GAAGATTTTTAAGCGCACCGAGGGGATCAGTACTTCGACGATTGTCTCGCGTCTC
CTGCAGGCCACAGCTCACGTGGAGCAGCGCCACTCACTCCCGCCTCTCCAGGCT
GAAGGCCAGCTGCTGGACGCTGGCGAAGTGCAGAGCAAAAAGCCGTTGAGGAG
CCAGGCGGTAATGCAGCCGACCCGCGTGCAACGCTTCGCGAGAGACTCTCTGAG
AGAACAGAAGGAGAACTTGCTGGCGTGTTCCTGCAAGAAGAAACGCGATAAGGA
CGAGGACGAGCGACGCCGAGGGCGAGCAGAGAGACTCGGAAAGAGGCGCGAC
GTCCACGCGGCGGACGCTCGCTCGCGGGACTGTTTAGACGCCCGAGGAGGCGA
AGAAGAAGAGCGGGGAGGCAGCGACGCGGCGTCTTCAGCGAATTTGTCGAGTTT
CTTCTGCTCGTCGAGCGACGAGGGCGGCCGCAGCAACGGCGATAACTCGGCGC
ACAGAAGGAGACAGGAGTGGCGAGCGAGCTCAAGGGGGAGCGACGCGCGAGG
CGTCAGCGTCGGAGACGGTGACGCGAGCCGGGAGACAGAAAGGAGAAGGGGAA
ACGTGGAGGAGCCGAGACAAAAGAAGTCCTGCTGCGCCGTTGGTGGCCGGCAC
CATCGACCGCGGAAGCCTCAAGACCCTGAAGAACGCAGAATGCTCATGTCAACG
AAGCGCCTCCTGCAGTTCATTGGTCAACCGAAGCGTCCGAAAGCCGGCGGCAAA
ATCGTCTATGTCGATGGTTCTTTTGATGTCTTTCATGgtgagacgaactatagggcaagtgctg
gcgatacaacgcatgtggggagaagaatagcgaatggtacgctttttcgtcgacgtacgctggaggactagttctttttag
gaacgaaaagaaagaaggaacatgctgtccaaagccatgtctgtccatggatgatggtggagagatagacagacgg
gggagaggcggaggccagcgtgcagagtcggaaaactcttcagagagaatgtgtgagagcgaagaagggagacg
attcatcaggcgagttggagaatgcgccacagcgtattcctcttttgccttttctgtctttgcgtttttctcagTGGGTCACC
TGCGCATTTTGGAGAAGGCGAAGCAGCTGGGAGATTACCTGATTGTCGGCATCCA
CGgtaagacacggcgagaagacctggacaaagaggtgacgcagctcaacgaccggggcagacaaaaagtctgc

gaggaggcggcagccgaaagaaacgtacagaagaaaagagagaggagggaaaccgaagaggcagaagaag
ggaaggaggtcgaagagatcggagaacatgagggtcacccagtgcagcaacagacagagaaatgagattcgacc
cagaaaaaaatacatgcgcgagtgatggacactgcagagaagcgaatcgagaacagatatcacagagatacatctt
ctttttccttcatttccttcgtttttctgttccttgacatttttttgcagACGATGAGACGGTCTCGAGAATCAAAGG
TCCCGGGTTCCCTGTCTTGAATCTACACGAGCGAGCGCTCAACGTCCTCGgtcagtc
gttctgtcttcttcgctgcttgcgcttggaagccaccgtactcgttctgcgtgcgtccgcagtgtctgttgtgtcgaccgtgtgca
ggtgtaaacaggaggtcattctttttcgcgtcacaaaggttcctctacgttacggtgtagaaccgagactacagcatattgtc
gctccagccaaacgctccttcgtcgtcctatgtgtacattgctgctttgtaccggaggatgcgttcttctttctgtctctgcagC
CATGAGAGTCGTGGACGAAGTCATCATTGGAGCCCCGTGGGTGATTCCACACTAC
ATGCTGAAGCAGTTTCAGATCGATGTGGTGGTGCGCGGGAGTCGCATCGATTCG
ATCGCGTATCCGTTTTCTGGAGACGCGAGTGGAGAGGGGGCAGGAGAGCCTGAG
GCGCAGGCGGGCAGAAGAAAGGAGACGGAGGGTCGAGACAGCTCCTGCTCCCT
CGCAGTTCTCTCCTCTGGCGAGGAAGACGAGGACGCGGTCGATCCTTACCGCGT
ACCGAAGGAACTCGGCGTCTATAGAGAAGTGGAGAGCTCCTCCTCCTGGACAAC
CAGAGCGCTCGTGGAGCGCATTCTTGCCAACAGGGAGGCTCTGATGGCAACCAT
CGAAACCCGgtgcgtcaggtcacaaacagacgcaaacgagaacaacagcatacacagaatatatatatatatat
atatatatatgtatatatgattatatatacatgtttacacatgtatatgctttgagagaggaaagtgtggcggcactatctgtgg
gggaaacctttggtcctggaggttgtgtagagcgtttcggcgagcgcctgtgcggctttttttctcagaaggcgctccgtgtgt
gttgctgtctttgcatgcagATGCTCCAAGGAAGCAAAGTTCTGGCGCGAACAAGAGCAGGG
ACAGATGGTGTCTCTGACAGAACTCTGA

*Tg*EPCS (*Tg*GT1_276190)

gDNA (intron in lower cases)

ATGAGTCCTGCAGACCCTGAGGCAGGGTCTCTGCAAAGCAGCGCCCCGCCACTT
GCCTCGGCAGGGAAGTCTGCGGGTGCAGGCGCGCCGCGCGCTTCCCGTCGATC
CTCGTCGGCTTCTCCGTCCTCGGACTCCGCCACCGGCCCAGCCGTCTCTGCATG
CGCGACGCCCGCATGCACTCCCCCGGGGGGGTTCTCCCTTCTACCGCGCCTTTCT
GTCTCCGCTGTGCGACCAGATTTGTCTGCGGCTGGTCCCCCCCTCCGTGAGCCC
AGACGCCATTTCCTTCCTCGCGCTCTGCTGCGCCGCCCTCGCTACCTTCTTCTGC
TGGCAGGCGGACCGACGCAGCTTCACCGCTGCTGTGAAGACAGAGGCGGAGAC
GAAGGCTCTGGCCACCGACGCGGCCTTCGGCAACTCATTGACCCTCTCGCCTGT
CGTGACCTTCCTGAACTTCTGTGGGATCGACGCGCAGCCAGATACGCCGTTCTG
GGCCGTCGCCGGCCTCCTCTGGATGCTCTACTCGGTCCTCGACAACGTCGACGG
AAAGCAGgtgcgacatttgctcgagtgcatgcagtccacgctggggcgtcaggcgcaaacgcgctccggcctcgg
cctctttccttgccgagttcagcatctggagggaaggttcgcggctgtggcgagtctgctccgcgacgcagtgggagctca
ggagacaaaacggctgaacatggagagaaccgcgaaagcagtcggtgtgtgaagcgtcgtagacgaagtgaccca
ctcacggagaaagagagaaaaatgtgaactggtgacgcataactcttcaggacgttcaggtctgactgcagaccctgg
accgtttttgcggcgtcaggccgccctaatgggtgtacagacaccggaagaagtccgcatgctcgtggcaacgcatgca
ctttgtccgtctctccccgttttccccggctttttgaagagacgccccacacactcgtttttctaccgggaagtctgttccacggt
tcctgccaaagttcaaaaaatcagatcgactccggggagagactctctgccgcggttccaatccctcgacgcgactctcg
gtttacctccacccacagttcgattcgcgtttctgtttcgtttctcagGCCCGGCGTCTGCGGCAGTGCACG
GCAGGCGGCGACTTTTTGGATCACTCGAGCGACAGCATCGTGACTTCTCTGAGC

GGCTTGGTGGTTATGTGGGCGCTGCTTCTCCAGCCTGCGTCGGCGCCTCAGCGT
TCTGCGTCTTCGCGTCTCTTCTCCATTTCTTCCTCGCCCTCTGTCGCGCTCAACGA
CCGCACACACACCATCTCGCTGGGGTCGCTGGACTGTCTGGCGTTCATTTTGATT
ACGCAGCTTCCGTTCTTCATCGCAACATGGGCTCACCCGATTGTCGGCAGAACGA
TTCTCTCTTCTTCTCTGGAGGGGTGTCACTGGTTCTCGgtgagtttcggagaacggaggattc
cactcaaaggctttctctggacagcgcagacgacgaggtggacttttttgtataagttgttttttaaacagacgctgttctggc
ggcggttggacgaaggttacccttcttttcagaggcagaagatgccgctcttgtaaagctgcttttgctgtcgcgttctgtcttt
ctcctaatcgttcatgatgcatctgcagtcatgggtgtggcggtttttgtgttttcgtggatttcctcccaaattctggcgctggcc
tttaacgctgaaggagtgaaatcacatttttgaaaacgacaggcgcattgaacgctgctctgcttctcaccggcagttcttc
ctggtgagtgctctttctgaattctcctccttttagGTTGACGAAGTGAACTTCATTGTCATTCCTTCTG
TTCTCTTCGTTCGCGCTCTGACCCCCACCTTCTGGTCTACAACGCTCGTGTCTCTC
CTTCCTCACTGTCCCCCGTTCGTACACTCCGTCGTCACCGTCCTCTCAGCCGCCA
TTGGCTTCGTCTTTCAACTCGCCTCCGAAGAAGTTACTCTCGGCGTCCTCGTCGT
CTTCGCCAGCTGCATGCTCTCTTTCTTCGAGTCGACCAGgtccgtcgacaacaccgctccat
acatctaaacttcattgttccacccacaccaggtcgctgcacaaaaaaacaaacgtacgtatatatatatatatatatatgc
atgtgtgtgtgtaattccatgtgtctctacacatctctgtcagaaaacgcatgcatctatatattatatatatatatattgtgatc
aataaatagatgtaggtaatatggatagacacagagagagaagataatagagagatggagagctatagggaactagt
agatggagagaaatagagatatacaagtaataaatcgacgtatatatatatatatatatatatatataattgcagacaggt
atccttgtagataaacgatcctggacagcacatgtgtgagtggagtattctgtaggttgtttcaggccattcagctgtctgtcg
ccggaacatttcgttcggtgatcgctgtctcgactctctcctttccttttttctgacagaaaggtttttttcagaggattccttgcgat
gccgcggcgactccgaggccctagttttcttgtctgcatgttttctccggtctcttcatgtgctccgcttttcttctctccagGCT
CCTCTTGCAGCTCGTCAAGTATGAGCATCTGCCGCGCCTTTTGCCGGGCGTCGTT
CTCTTCGCAGGCgtgagtgataactggaaaaagaactgtctgcatgcagacgctctctgtcgcaaagcaggcct
caactccttggagttgcttcaggagaaatcgttttcactttcgtctgcattttcgtctctgtccgtctcgtcgtctcacgccatcca
cctcgctcttttcatctatatttttatctacatcgttgttcaagtatacctatatatatatatacatacatgtatgtactagttcacatct
gtgtgcatatttgtatatatttgtagtgcatatttgtatatatttgtatatctttatgcacctgcatattagcatatgtatgtatatgtcg
atatatctgttcctctgccacgggccgtgcttttaggaagaaggcgtgcctcggactcggcgcatgaatgtgcatggggac
ctcgcatgatttaagaccggaaagcggactgttgactcacctgcttgtttctttgaccgtgcggctacacctggaacggtga
ctcagcgacctccatgcgttttcttgctgctgcgcagTCGTTAACCTTCAAGCCGCCCATTCTGCTAC
AGCTCGGCGTCTTTTCGCTCCTCTGTTTGGAGCTCATCGCTGCTCGTCTCAAGCT
GCATGTGCGGACGCAACTGgtaaggcgagagagtgcatgtttttcgcgagagaacaaggttcgaagaaa
gaggtttctgtcgtgctttgcaggcccatgttccaggccaggggcctgcgttttctttgttttccttgcggacttctgcggatctttc
tgggtgctccttggcagggagcctcgtggcgaggctctcttcgctttccttcatggttctcgcgttcgtccatgtcttccttttggt
cctgtccatactgttttttcgatgcattcttccaccgcctctccgtcggtctctgtgttttgtctctgcgtgtgctccttcgtgctcctct
ccacgccgttcccagcggatctctctgtctgtctctcctctgtatctctgttcatctgtctcctttgtctctctcctgctctgtctcccc
atgtcgctctcgcgctggatttcgtcttctgcctgcctatgcgcatctcttgttttcttttgttttctttgtttttctcttgtttttctgtgtctg
cagTACATGTGGTGGCCTGTGACTCTCTACTACTTCTTTCTCTTAACGCTTCACGGA
GGCTCGAGCGCGGATCCTGCGCCGGGACTGCCAGCGTCTCTTGCGCGGGTGCT
GGGGAAAAACTACAACTACCACAGCGCAGCTTTCATGACGCTAGTGCTGCTCGGC
ATCTGCCTCCTCTCTTACAAGCATATCATCAACCGAAGAAACGGCACCTGCCGGG
CGCAGCGGAAAACCGAGTGA

Plasmid used in the study

pU6-Universal-ECT/PIS/EPCS (Partially)

For creating niches using CRISPR/Cas9 on genome to assist integration

*Tg*PIS

ATGTTGGAGACACTGAGGGCACACGGGAAACGCGAAAGATTTCAAATTAACGTAC
CCAAACGCGAAAGCTTGCGCAGCATACACTCGAAGCGAACATCCCGAACCATCG
AGAGGCGGAGAGCGATAAGTCTTTCACGCTGCGAAGTGTTGCGACGGCTGCGCC
GCTGCACTGTGAATTGGGCGCCAATATTGCATCCTAGGCCTGACGCGCCTCCTG
CAGAACGCGAGACACTGGGATATGTAGAGCCAAGGGGGAAACCTTCGAACTCTC
GAATGTCTTCTCTGACAAGAATCATATTTCCATCAGTTCTGTCAGATTTTCAAATGG
CGACCTGCAGAGGCCTGCTTCCTCCCTGTGCGCTCTTCGAAGGGGCTTTCTGTC
GCGCAGGGTCACCTCGTCCCCGAAGGGGGTGTTTGCCTTCTGGTAAATGGGGAT
GTCAAGTTGAGGCAAGACTGTTTTTCAGGTTTTAGAGCTAGAAATAGCAAGTTAAA
ATAAGGCTAGTCCGTTATCAACTTGAAAAAGTGGCACCGAGTCGGTGCTTTTTTTT
TCTTTT

*Tg*ECT

ATGTTGGAGACACTGAGGGCACACGGGAAACGCGAAAGATTTCAAATTAACGTAC
CCAAACGCGAAAGCTTGCGCAGCATACACTCGAAGCGAACATCCCGAACCATCG
AGAGGCGGAGAGCGATAAGTCTTTCACGCTGCGAAGTGTTGCGACGGCTGCGCC
GCTGCACTGTGAATTGGGCGCCAATATTGCATCCTAGGCCTGACGCGCCTCCTG
CAGAACGCGAGACACTGGGATATGTAGAGCCAAGGGGGAAACCTTCGAACTCTC
GAATGTCTTCTCTGACAAGAATCATATTTCCATCAGTTCTGTCAGATTTTCAAATGG
CGACCTGCAGAGGCCTGCTTCCTCCCTGTGCGCTCTTCGAAGGGGCTTTCTGTC
GCGCAGGGTCACCTCGTCCCCGAAGGGGGTGTTTGCCTTCTGGTAAATGGGGAT
GTCAAGTTGAATGGATTGATGGACGCGGGTTTTAGAGCTAGAAATAGCAAGTTAA
AATAAGGCTAGTCCGTTATCAACTTGAAAAAGTGGCACCGAGTCGGTGCTTTTTTT
TTCTTTT

*Tg*EPCS

ATGTTGGAGACACTGAGGGCACACGGGAAACGCGAAAGATTTCAAATTAACGTAC
CCAAACGCGAAAGCTTGCGCAGCATACACTCGAAGCGAACATCCCGAACCATCG
AGAGGCGGAGAGCGATAAGTCTTTCACGCTGCGAAGTGTTGCGACGGCTGCGCC
GCTGCACTGTGAATTGGGCGCCAATATTGCATCCTAGGCCTGACGCGCCTCCTG
CAGAACGCGAGACACTGGGATATGTAGAGCCAAGGGGGAAACCTTCGAACTCTC
GAATGTCTTCTCTGACAAGAATCATATTTCCATCAGTTCTGTCAGATTTTCAAATGG

CGACCTGCAGAGGCCTGCTTCCTCCCTGTGCGCTCTTCGAAGGGGCTTTCTGTC
GCGCAGGGTCACCTCGTCCCCGAAGGGGGTGTTTGCCTTCTGGTAAATGGGGAT
GTCAAGTTGGAGGAACTCTGCACACTGGGTTTTAGAGCTAGAAATAGCAAGTTAA
AATAAGGCTAGTCCGTTATCAACTTGAAAAAGTGGCACCGAGTCGGTGCTTTTTTT
TTCTTTT

pTUB-YFP-mAID-HA-HXGPRT (Partially)

Serve as template for PCR-based mAID-insertional tagging.

AGATCCCGCTAAGCCGCCTGCCAAGGCCCAGGTGGTTGGCTGGC
CCCCGGTTAGGAGTTACCGCAAGAACGTGATGGTCTCTTGCCAGA
AGTCTAGTGGTGGCCCTGAGGCGGCGGCATTCGTTAAAGTCTCCA
TGGACGGAGCGCCGTACCTGCGAAAGATTGATTTGCGAATGTATAA
AAGTGGCGGCGGCGGCTCTTACCCGTACGACGTCCCGGACTACG
CTGGCTATCCCTATGATGTGCCCGATTATGCGTATCCTTACGATGT
TCCAGATTATGCCTAACCCGGGCATATGTAGAAAAGTTGTAACGTT
AGTAAACGTAACACACGGGTATAATAGCCATTTAATGGCGCCGTAT
ATTTTTCACTCCCCCTCTCCGATAGGAGGAAGAAAGACGATCCGTC
TGCGAATGTATATTACATCGACCGGCCATAGTACGAGAAGTGGTGC
CGGTATTGTTCTGTCCGGGGGGTGTACCATCCTATTTTTTGTATATG
TCGTTCTTGTCGGGGAGCAACAGCCCATCTTCCGGCTATTGTCTCG
TATCAGTTGTGAAACAGACTGCGTTTTGCCGAAAATGAGTCCTATG
TCCGATGGCTATTTGTACCGCTTCGTACCATTTCGCTTGTCAGCTG
TAATCAACCGAATTCATTTGGCGAGACATGATTCCGATTAAATTCTT
TACTGCGCGTGCTCGGATCCACTAGTTCTACTCGAGGTCGACGGT
ATCGATAAGCTTATAACTTCGTATAGCATACATTATACGAAGTTATC
AGCACGAAACCTTGCATTCAAACCCGCCCGCGGAAGATCCGATCTT
GCTGCTGTTCGCAGTCCCAGTAGCGTCCTGTCGGCCGCGCCGTCT
CTGTTGGTGGGCAGCCGCTACACCTGTTATCTGACTGCCGTGCGC
GAAAATGACGCCATTTTTGGGAAAATCGGGGAACTTCATTCTTTAAA
AGTATGCGGAGGTTTCCTTTTTCTTCTGTTCGTTTCTTTTTCTCGGG
TTTGATAACCGTGTTCGATGTAAGCACTTTCCGTCTCTCCTCCGTG
CTTTGTTCGACATCGAGACCAGGTGTGCAGATCCTTCGCTTGTCGA
TCCGGAGACGCGTGTCTCGTAGAACCTTTTCATTTTACCACACGGC
AGTGCGGAGCACTGCTCTGAGTGCAGCAGGGACGGGTGAAGTTTC
GCTTTAGTAGTGCGTTTCTGCTCTACGGGGCGTTGTCAGATCCAGC
AAAATGGCGTCCAAACCCATTGAAGACTACGGCAAGGGCAAGGGC
CGTATTGAGCCCATGTATATCCCCGACAACACCTTCTACAACGCTG
ATGACTTTCTTGTGCCCCCCCACTGCAAGCCCTACATTGACAAAAT
CCTCCTCCCTGGTGGATTGGTCAAGGACAGAGTTGAGAAGTTGGC

GTATGACATCCACAGAACTTACTTCGGCGAGGAGTTGCACATCATT
TGCATCCTGAAAGGCTCTCGCGGCTTCTTCAACCTTCTGATCGACT
ACCTTGCCACCATACAGAAGTACAGTGGTCGTGAGTCCAGCGTGC
CCCCCTTCTTCGAGCACTATGTCCGCCTGAAGTCCTACCAGAACGA
CAACAGCACAGGCCAGCTCACCGTCTTGAGCGACGACTTGTCAAT
CTTTCGCGACAAGCACGTTCTGATTGTTGAGGACATCGTCGACACC
GGTTTCACCCTCACCGAGTTCGGTGAGCGCCTGAAAGCCGTCGGT
CCCAAGTCGATGAGAATCGCCACCCTCGTCGAGAAGCGCACAGAT
CGCTCCAACAGCTTGAAGGGCGACTTCGTCGGCTTCAGCATTGAA
GACGTCTGGATCGTTGGTTGCTGCTACGACTTCAACGAGATGTTCC
GCGACTTCGACCACGTCGCCGTCCTGAGCGACGCCGCTCGCAAAA
AGTTCGAGAAGTAAACCCTGCATAGCCCACAGAAGCTGCCCGTCT
CTCGTTTTCCTCTCTTTTCGGAGGGATCAGGGAGAGTGCCTCGGAT
CGGAGAGAGCTGACGAGGGGGTGCCAGAGACCCCTGTGTCCTTTA
TCGAAGAAAAGGGATGACTCTTCATGTGGCATTTCACACAGTCTCA
CCTCGCCTTGTTTTCTTTTTGTCAATCAGAACGAAAGCGAGTTGCG
GGTGACGCAGATGTGCGTGTATCCACTCGTGAATGCGTTATCGTTC
TGTATGCCGCTAGAGTGCTGGACTGTTGCTGTCTGCCCACGACAG
CAGACAACTTTCCTTCTATGCACTTGCAGGATGGTGCAGCGCAAAC
GACGGAGAGAAAGGAGCACCCTCTCAGTTTCCCTACGATGTGCTG
TCAGTTTCGACTCTTCACCGCGAACGATTGGCGATACGTCTCTGTT
GACTTGTTAGGCTCCGACCACGAAGCTCCCTTAACTAGATAAGCCG
CGACACCTAAGTGTACACCATTTGCAGATCGATAATCTGCGACCGC
TGAATCCGTCCAGATCAGTAAAACCGCACCACCTAAGTGTAAACCT
TGTTTAGGTCGATAAAATGCTACCAACCCCCACCCACAATCGAGCC
TTGAGCGTTTCTGCGCACGCGTTGGCCTACGTGACTTGCTGATGC
CTGCCTCTGGCCATTCATGCCAGTCAGTGCGCATAAAAATGTGGAC
ACAGTCGGTTGACAAGTGTTCTGGCAGGCTACAGTGACACCGCGG
TGGAGGGGGATCATTGAAATAACTTCGTATAGCATACATTATACGA
AGTTAT

pLinker-AID-HA-DHFR-TS (Partially)

Serve as template for PCR-based AID-insertional tagging.

ATGGGCAGTGTCGAGCTGAATCTGAGGGAGACTGAGCTGTGTCTT
GGTCTTCCCGGTGGAGATACAGTGGCTCCGGTAACCGGAAACAAG
AGAGGGTTCTCAGAGACGGTTGATCTGAAGCTAAATCTGAATAATG
AGCCTGCAAACAAGGAAGGATCTACGACTCATGACGTCGTGACTTT
TGATTCCAAGGAGAAGAGTGCTTGTCCTAAAGATCCAGCCAAACCT

CCGGCCAAGGCACAAGTTGTGGGATGGCCACCGGTGAGATCATAC
CGGAAGAACGTGATGGTTTCCTGCCAAAAATCAAGCGGTGGCCCG
GAGGCGGCGGCGTTCGTGAAGGTATCAATGGACGGAGCACCGTA
CTTGAGGAAAATCGATTTGAGGATGTATAAAAGCTACGATGAGCTT
TCTAATGCTTTGTCCAACATGTTCAGCTCTTTTACCATGGGCAAACA
TGGAGGAGAAGAAGGAATGATAGACTTCATGAATGAGAGGAAATTG
ATGGATTTGGTGAATAGCTGGGACTATGTTCCCTCTTATGAAGACA
AAGACGGTGATTGGATGCTCGTCGGCGACGTTCCTTGGCCAATGT
TCGTCGATACATGCAAGCGTTTACGTCTCATGAAAGGATCGGATGC
CATTGGTCTCGCTCCGAGGGCGATGGAGAAGTGCAAGAGCAGAGC
TGGGCGCGCCGGCTCTGGCGGCGGCGGCGGCGGCTCTTACCCGT
ACGACGTCCCGGACTACGCTGGCTATCCCTATGATGTGCCCGATTA
TGCGTATCCTTACGATGTTCCAGATTATGCCTAACCCGGGCATATG
TAGAAAAGTTGTAACGTTAGTAAACGTAACACACGGGTATAATAGC
CATTTAATGGCGCCGTATATTTTTCACTCCCCCTCTCCGATAGGAG
GAAGAAAGACGATCCGTCTGCGAATGTATATTACATCGACCGGCCA
TAGTACGAGAAGTGGTGCCGGTATTGTTCTGTCCGGGGGGTGTAC
CATCCTATTTTTTGTATATGTCGTTCTTGTCGGGGAGCAACAGCCCA
TCTTCCGGCTATTGTCTCGTATCAGTTGTGAAACAGACTGCGTTTTG
CCGAAAATGAGTCCTATGTCCGATGGCTATTTGTACCGCTTCGTAC
CATTTCGCTTGTCAGCTGTAATCAACCGAATTCATTTGGCGAGACAT
GATTCCGATTAAATTCTTTACTGCGCGTGCTCGGATCCACTAGTTCT
ACTCGAGGTCGACGGTATCGATTCTAGAGAATTCGAGCTCGGTACC
CATAACTTCGTATAGCATACATTATACGAAGTTATAAGCTTCGCCAG
GCTGTAAATCCCGTGAGTCGTCCTCACAAATCATCAAGCAGGTGTC
CTCAGGGAGACTGCCTGACTGAGTTATGCTAATTCCTTTCTACTTTG
GCGTGGTAACGGGCGCGCCGGATCCTTAATTAAGTCTAGCATGTC
ATTCGATTTTCACCCCCCGCGTAGTTCCTGTGTGTCATTCGTTGTC
GAGACAACTCTGTCCCGCCCCGGTGCTGTTCCATATGCGTGACTTT
CCCGCAATTTTTTCAGACTTTCAGGAAAGACAGGCTCCGGAACGAT
CTCGTCCATGACTGGTAAATCCACGACACCGCAATGGCCCCCAGC
ACCTCTATCTCTCGTGCCAGGGGACTAACGTTGTATGCGTCTGCGT
CTTGTCTTTTTGCATTCGCTTTCCAAAAAAGAGAGCCATCCGTTCCC
CCGCACATTCAACGCCGCGAGTGCGGTTTTTGTCTTTTTTGAGTGG
TAGGACGCTTTTCATGCGCGAACTACGTGGACATTAAGTTCCATTC
TCTTTTTCGACAGCACGAAACCTTGCATTCAAACCCGCCCGCGGAA
GATCCGATCTTGCTGCTGTTCGCAGTCCCAGTAGCGTCCTGTCGG
CCGCGCCGTCTCTGTTGGTGGGCAGCCGCTACACCTGTTATCTGA
CTGCCGTGCGCGAAAATGACGCCATTTTTGGGAAAATCGGGGAAC
TTCATTCTTTAAAAGTATGCGGAGGTTTCCTTTTTCTTCTGTTCGTTT
CTTTTTCTCGGGTTTGATAACCGTGTTCGATGTAAGCACTTTCCGTC
TCTCCTCCGTGCTTTGTTCGACATCGAGACCAGGTGTGCAGATCCT
TCGCTTGTCGATCCGGAGACGCGTGTCTCGTAGAACCTTTTCATTT
TACCACACGGCAGTGCGGAGCACTGCTCTGAGTGCAGCAGGGAC

GGGTGAAGTTTCGCTTTAGTAGTGCGTTTCTGCTCTACGGGGCGTT
GTCGTGTCTGGGAAGATGCAGAAACCGGTGTGTCTGGTCGTCGCG
ATGACCCCCAAGAGGGGCATCGGCATCAACAACGGCCTCCCGTGG
CCCCACTTGACCACAGATTTCAAACACTTTCGTCGTGTGACAAAAA
CGACGCCCGAAGAAGCCAGTCGCCTGAACGGGTGGCTTCCCAGG
AAATTTGCAAAGACGGGCGACTCTGGACTTCCCTCTCCATCAGTCG
GCAAGAGATTCAACGCCGTTGTCATGGGACGGAAAAACTGGGAAA
GCATGCCTCGAAAGTTTAGACCCCTCGTGGACAGATTGAACATCGT
CGTTTCCTCTTCCCTCAAAGAAGAAGACATTGCGGCGGAGAAGCCT
CAAGCTGAAGGCCAGCAGCGCGTCCGAGTCTGTGCTTCACTCCCA
GCAGCTCTCAGCCTTCTGGAGGAAGAGTACAAGGATTCTGTCGAC
CAGATTTTTGTCGTGGGAGGAGCGGGACTGTACGAGGCAGCGCTG
TCTCTGGGCGTTGCCTCTCACCTGTACATCACGCGTGTAGCCCGC
GAGTTTCCGTGCGACGTTTTCTTCCCTGCGTTCCCCGGAGATGACA
TTCTTTCAAACAAATCAACTGCTGCGCAGGCTGCAGCTCCTGCCGA
GTCTGTGTTCGTTCCCTTTTGTCCGGAGCTCGGAAGAGAGAAGGA
CAATGAAGCGACGTATCGACCCATCTTCATTTCCAAGACCTTCTCA
GACAACGGGGTACCCTACGACTTTGTGGTTCTCGAGAAGAGAAGG
AAGACTGACGACGCAGCCACTGCGGAACCGAGCAACGCAATGAGC
TCCTTGACGTCCACGAGGGAGACAACTCCCGTGCACGGGTTGCAG
GCTCCTTCTTCGGCCGCAGCCATTGCCCCGGTGTTGGCGTGGATG
GACGAAGAAGACCGGAAAAAACGCGAGCAAAAGGAACTGATTCGG
GCCGTTCCGCATGTTCACTTTAGAGGCCATGAAGAATTCCAGTACC
TTGATCTCATTGCCGACATTATTAACAATGGAAGGACAATGGATGA
CCGAACGGGCGTTGGTGTCATCTCCAAATTCGGCTGCACTATGCG
CTACTCGCTGGATCAGGCCTTTCCACTTCTCACCACAAAGCGTGTG
TTCTGGAAAGGGGTCCTCGAAGAGTTGCTGTGGTTCATTCGCGGC
GACACGAACGCAAACCATCTTTCTGAGAAGGGCGTGAAGATCTGG
GACAAGAATGTGACACGCGAGTTCCTCGATTCGCGCAATCTCCCC
CACCGAGAGGTCGGAGACATCGGCCCGGGCTACGGCTTCCAGTG
GAGACACTTCGGCGCGGCATACAAAGACATGCACACAGACTACAC
AGGGCAGGGCGTCGACCAGCTGAAGAATGTGATCCAGATGCTGAG
AACGAATCCAACAGATCGTCGCATGCTCATGACTGCCTGGAATCCT
GCAGCGCTGGACGAAATGGCGCTGCCGCCTTGTCACTTGTTGTGC
CAGTTCTACGTGAACGACCAGAAGGAGCTGTCGTGCATCATGTATC
AGCGGTCGTGCGATGTCGGCCTCGGCGTCCCCTTCAACATCGCTT
CCTATTCGCTTTTGACGCTCATGGTTGCACACGTCTGCAACCTAAA
ACCTAAGGAGTTCATTCACTTCATGGGGAACACGCATGTCTACACG
AACCATGTCGAGGCTTTAAAAGAGCAGCTGCGGAGAGAACCGAGA
CCGTTCCCCATTGTGAACATCCTCAACAAGGAACGCATCAAGGAAA
TCGACGATTTCACCGCCGAGGATTTTGAGGTCGTGGGCTACGTCC
CGCACGGACGAATCCAGATGGAGATGGCTGTCGGTGACGAGCTGT
ACAAGTAGATGGAGATGGCTGTCGGTGACGAGCTGTACAAGTAAG
CTGAGCATAACTTCGTATAGCATACATTATACGAAGTTATCGGAAAT

ACAGAAGCTGCCCGTCTCTCGTTTTCCTCTCTTTTCGGAGGGATCA
GGGAGAGTGCCTCGGGTCGGAGAGAGCTGACGAGGGGGTGCCAG
AGACCCCTGTGTCCTTTATCGAAGAAAAGGGATGACTCTTCATGTG
GCATTTCACACAGTCTCACCTCGCCTTGTTTTCTTTTTGTCAATCAG
AACGAAAGCGAGTTGCGGGTGACGCAGATGTGCGTGTATCCACTC
GTGAATGCGTTATCGTTCTGTATGCCGCTAGAGTGCTGGACTGTTG
CTGTCTGCCCACGACAGCAGACAACTTTCCTTCTATGCACTTGCAG
GATGGTGCAGCGCAAACGACGGAGAGAAAGGAGCACCCTCTCAGT
TTCCCTACGATGTGCTGTCAGTTTCGACTCTTCACCGCGAACGATT
GGCGATACGTCTCTGTTGACTTGTTAGGCTCCGACCACGAAGCTCC
CTTAACTAAATAAGCCGCGACACCTAAGTGTACACCATTTGCAGAT
CGATAATCTGCGACCGCTGAATCCGTCCAGATCAGTAAAACCGCAC
CACCTAAGTGTAAACCTTGTTTAGGTCGATAAAATGCTACCAACCC
CCACCCACAATCGAGCCTTGAGCGTTTCTGCGCACGCGTTGGCCT
ACGTGACTTGCTGATGCCTGCCTCTGGCCATTCATGCCAGTCAGTG
CGCATAAAAATGTGGACACAGTCGGTTGACAAGTGT

pQE-60-*Tg*PIS

For functional test of *Tg*PIS in *E.coli* M15, mutation site highlighted

AAATCATAAAAAATTTATTTGCTTTGTGAGCGGATAACAATTATAATA
GATTCAATTGTGAGCGGATAACAATTTCACACAGAATTCATTAAAGA
GGAGAAATTAACCATGGGAGGATCCAGATCTATGGCGGGGACTTC
TGCAAGCCGCGAGGACAGCCAGTCTCCCGCTGTTCGACAGAGAGT
GGGCAGCGCTTCTGGAGGCAAAAGTGTCCAAGCGGCGTCAGATTC
TGACCTTTCTCATGAACAAAAATGGGCGCGGGAGTTGAAAGTTTTC
CTCTACGTGCCAAACATCATTGGATACGTTCGTATCGCGCTGCTGT
TGGCCGCTGCATTTGCGTGGCGAGAAGCGTACACTTCTCTTTTCTT
TGTTTCTTATGTTACATCGCAATGCCTGGACGCAGTCGATGGCGCT
GCCGCACGCCGTCTGGGCCAAGTTTCCATTGTCGGCGCCTGTCTC
GACCAAGTTGTCGACCGGCTTTCAACATGTCTACTGTATGTTCTGA
ACGCCTCGGTCTACCCTGACTTTGCTTTCGCGTTTTTCATCGCGCT
TTTTCTGGACATGGGTGGCCACTGGGTCCACTTCTTCGCCGCGGC
CGTCGTTGGCGCAAAGTCTCACAAAACGATGGATCCGGAAGTGAA
TGCCATTCTCTCCGTCTACTACCGTTCTCGCCCGGTCATGTTTTCG
GCGATCGTGGGCTTCGAGGGGTTCTTCATGTGCCTTCTTCTTTTGG
CATCGCCGGTCGTCCAGGCTTCAGCTGCCTCGCTGTCCTCGGCAC
TCCTCGTCATTGTCTACGTCACTTCTCCCCTGATGATCTTCAAGACG

CTGACGAATCTCCTCCAAGGACTGTACGGAGCCAGGCGCTTGGTT
GCGTGCGACATTTTTGGTGCGCCCTCGTCGCATCACCATCACCATC
ACTAA

Construction of pQE-60-*Tg*PIS (mutation)

*Tg*PIS^{D91A}: GAC->GCC
*Tg*PIS^{D94A}: GAT->GCT
*Tg*PIS^{Q103G}:CAA->GGA
*Tg*PIS^{D112AQ113G}:GACCAA->GCCGGA
*Tg*PIS^{D116AR117G}:GACCGG->GCCGGG

N-Terminal-truncated (*Tg*PIS$^{49-258}$):

~~ATGGCGGGGACTTCTGCAAGCCGCGAGGACAGCCAGTCTCCCGCT~~
~~GTTCGACAGAGAGTGGGCAGCGCTTCTGGAGGCAAAAGTGTCCAA~~
~~GCGGCGTCAGATTCTGACCTTTCTCATGAACAAAAATGGGCGCGG~~
~~GAGTTGAAA~~GTTTTCCTCTACGTGCCAAACATCATTGGATACGTTC
GTATCGCGCTGCTGTTGGCCGCTGCATTTGCGTGGCGAGAAGCGT
ACACTTCTCTTTTCTTTGTTTCTTATGTTACATCGCAATGCCTGGAC
GCAGTCGATGGCGCTGCCGCACGCCGTCTGGGCCAAGTTTCCATT
GTCGGCGCCTGTCTCGACCAAGTTGTCGACCGGCTTTCAACATGT
CTACTGTATGTTCTGAACGCCTCGGTCTACCCTGACTTTGCTTTCG
CGTTTTTCATCGCGCTTTTTCTGGACATGGGTGGCCACTGGGTCCA
CTTCTTCGCCGCGGCCGTCGTTGGCGCAAAGTCTCACAAAACGAT
GGATCCGGAAGTGAATGCCATTCTCTCCGTCTACTACCGTTCTCGC
CCGGTCATGTTTTCGGCGATCGTGGGCTTCGAGGGGTTCTTCATGT
GCCTTCTTCTTTTGGCATCGCCGGTCGTCCAGGCTTCAGCTGCCTC
GCTGTCCTCGGCACTCCTCGTCATTGTCTACGTCACTTCTCCCCTG
ATGATCTTCAAGACGCTGACGAATCTCCTCCAAGGACTGTACGGAG
CCAGGCGCTTGGTTGCGTGCGACATTTTTGGTGCGCCCTCGTCG

Enzymes		CDP-alcohol-phosphotransferase motif (DX$_3$DGX$_2$ARX$_{8/9}$GX$_3$DX$_3$D)	GenBank No.
Phosphatidylinositol Synthase (PIS)	Apicomplexans	***Tg*PIS** ..DAVDGAAARRL-GQVSIVGACLDQVVDDR..	KX017549
		*Nc*PIS ..DAVDGEAARRL-GQVSVVGACLDQVVDDR..	XP_003879813
		*Ef*PIS ..DSVDGFAARSL-KQASVFGACLDQLTDDR..	KX785375
		*Pf*PIS ..DALDGWTARKF-NQTSVFGQILDQITDDR..	XP_002809014
	Kinetoplastids	*Tb*PIS ..DAVDGMVARRF-GQCTQFGAILDMLTDDR..	CAG29793
		*Tc*PIS ..DAADGMVARLM-DQCSHFGAIFDMLTDDR..	XP_811459
		*Lm*PIS ..DAADGMAARAL-DQCSNFGAILDMLTDDR..	XP_001684255
	Algae	*Cm*PIS ..DAADGYAARLL-GQSSAFGAVLDMLTDDR..	BAM80990
		*Cr*PIS ..DELDGRFARMF-NQTSTFGAVLDMVTDDR..	EDP06395
		*Ot*PIS ..DAIDGACARAF-EQSSTFGAALDMITDDR..	CAL56685
	Plants	*At*PIS ..DAVDGWVARRF-NQVSTFGAVLDMVTDDR..	Q8LBA6
		*Os*PIS ..DGLDGWFARKF-NQASTFGAVLDMVTDDR..	CAC37011
		*Zm*PIS ..DGVDGWFARKF-NQASTFGAVLDMVTDDR..	NP_001105559
	Fungi	*Cg*PIS ..DALDGTMARKY-NQVSRLGAVLDMVTDDR..	KTB24417
		*Sc*PIS ..DALDGTMARKY-NQVSSLGAVLDMVTDDR..	AAA34876
		*Sp*PIS ..DAFDGWAARKL-HQATNFGAILDMVTDDR..	Q10153
	Animals	*Dm*PIS ..DAVDGQAARAF-NQSTRFGAMLDQLTDDR..	AAF48491
		*Dr*PIS ..DAFDGHAARAL-NQGTKFGAMLDMLTDDR..	AAT68039
		*Mm*PIS ..DAFDGHAARAL-NQGTRFGAMLDMLTDDR..	Q8VDP6
Choline/Ethanolamine Phosphotransferase (CEPT)	Apicomplexans	*Tg*CEPT1 ..DAVDGKQARRT-NSSTPLGQLFDHGCDS..	EPR63017
		*Tg*CEPT2 ..DAIDGKHARRN-GLSSPLGQLFDHGCDI..	EPR62697
		*Tg*CEPT3 ..DNVDGKQARRL-RQCTAGGDFLDHSSDS..	EPR59237
		*Nc*CEPT1 ..DAVDGKQARRT-NSSTPLGQLFDHGCDS..	XP_003883203
		*Nc*CEPT2 ..DAIDGKHARRN-SLSSPLGQLFDHGCDI..	XP_003882816
		*Nc*CEPT3 ..DNVDGKQARRL-RQCTAGGDFLDHSSDS..	XP_003880256
		*Ef*CEPT1 ..DAVDGKQARRT-NTATPLGQLFDHGCDS..	KX785376
		*Ef*CEPT2 ..DATDGKHARRL-GLSSPLGQLMDHGCDI..	KX785377
		*Ef*CEPT3 ..DNIDGKQARRL-GLCSAGGDFFDHSSDS..	KX785378
		*Pf*CEPT ..DALDGKQARRT-NTSSPLGQLFDHGCDS..	XP_966266
		*Cp*CEPT1 ..DAADGKHARRL-KISSPLGQLLDHGLDS..	XP_625864
		*Cp*CEPT2 ..DNLDGKQARRL-GVSSNSGEFIDHAIDS..	XP_625646
	Kinetoplastids	*Tb*CEPT ..DAIDGKQARRT-NTGSPLGELFDHGCDV..	XP_823114
		*Tc*CEPT ..DAVDGKQARRT-QTCGPLGELFDHGCDA..	EKG04257
		*Lm*CEPT ..DAIDGKQARRT-GTGSPLGELFDHGCDA..	XP_001687178
	Algae	*Gs*CEPT1 ..DNLDGRQARRT-NSSSPLGHLFDHGCDA..	EME27119
		*Gs*CEPT2 ..DNLDGRQARRT-NSSSPLGHLFDHGCDA..	EME32110
		*Ot*CEPT1 ..DGMDGKQARRT-KSGSPLGEVIDHACDG..	XP_003080347
		*Ot*CEPT2 ..DGIDGKQARRT-KSGSPLGEVVDHGCDA..	CEF97354
	Plants	*At*CEPT1 ..DAVDGKQARRT-NSSSPLGELFDHGCDA..	O82567
		*At*CEPT2 ..DAVDGKQARRT-NSSSPLGELFDHGCDA..	O82568
		*Zm*CEPT1 ..DAVDGKQARRT-SSSSPLGELFDHGCDA..	XP_008649197
		*Zm*CEPT2 ..DAVDGKQARRT-NSSSPLGELFDHGCDA..	AFW69854
	Fungi	*Cg*CEPT1 ..DGCDGIHARLT-GQSGPLGELFDHSIDA..	KTB18544
		*Cg*CEPT2 ..DACDGMHARRT-GQSSPLGELFDHCIDS..	KTB25778
		*Sc*CEPT1 ..DGCDGVHARRI-NQSGPLGELFDHSIDA..	P22140
		*Sc*CEPT2 ..DACDGMHARRT-GQQGPLGELFDHCIDS..	AAA63571
	Animals	*Dm*CEPT ..DGMDGKQARRT-GTSGPLGELFDHGLDS..	NP_609149
		*Dr*CEPT ..DAIDGKQARRT-NSSSPLGELFDHGCDS..	NP_001103187
		*Mm*CEPT ..DAIDGKQARRT-NSCSPLGELFDHGCDS..	NP_001140162
Phosphatidylserine Synthase (PSS)	Bacteria	*Bs*PSS ..DFFDGMAARKL-NAVSDMGRELDSFADL..	BAA07225
		*Hp*PSS ..DGLDGRVARLT-NTTSKFGIEFDSLADV..	AAC45587
		*Mt*PSS ..DGLDGRVARIL-DAQSRMGAEIDSLADA..	GAA44221
	Fungi	*Cg*PSS ..DFFDGRVARLR-NRSSLMGQELDSLADL..	KTB22122
		*Sc*PSS ..DFLDGRVARLR-NRSSLMGQELDSLADL..	BAA00121
		*Sp*PSS ..DFLDGKVARWR-GKSSLMGQELDSLADL..	O94584
Phosphatidylglycerol Phosphate Synthase (PGPS)	Bacteria	*Ec*PGPS ..DNFDGFIARRW-NQSTRFGAFLDPVADK..	AAA98754
		*Hp*PGPS ..DLLDGYIARSY-KAKSRFGEIFDPVADK..	EIE30130
	Algae	*Cm*PGPS ..DWLDGYIARRL-NVSSVWGAFLDPVADK..	BAM80263
		*Cr*PGPS ..DYFDGYIARKL-KIATVFGAFLDPVADK..	EDO97733
	Plants	*At*PGPS1 ..DWLDGYIARKM-RLGSAFGAFLDPVADK..	O80952
		*At*PGPS2 ..DWLDGYIARKM-RLGSEFGAFLDPVADK..	Q9M2W3
		*Os*PGPS ..DWLDGYIARKM-QLGTPFGAFLDPVADK..	XP_015630365
Cardiolipin Synthase (CLS)	Algae	*Cm*CLS ..DVLDGYIARKY-QKVTTLGSILDPVADK..	BAM81296
		*Cr*CLS ..DWLDGWIARRL-GASSVFGSYLDPLADK..	XP_001699073
		*Ot*CLS ..DYLDGFIARRW-KQQTILGSYLDPVADK..	XP_003082955
	Plants	*At*CLS ..DWLDGYVARRM-KINSVVGSYLDPLADK..	Q93YW7
		*Os*CLS ..DWLDGFIARKM-GINSVFGSYLDPLADK..	Q5N9A1
	Fungi	*Cg*CLS ..DFLDGYIARRY-NMKSDAGTILDPMADK..	KTB14470
		*Sc*CLS ..DFMDGYIARKY-GLKTIAGTILDPLADK..	NP_010139
		*Sp*CLS ..DLVDGYIARKF-DLGSIAGTVLDPLADK..	CAB16578
	Animals	*Dm*CLS ..DLLDGQIARRWPSQASKFGSFLDPMADK..	NP_651418
		*Dr*CLS ..DLLDGYIARNWPNQKSALGSALDPLADK..	NP_998096
		*Mm*CLS ..DLLDGFIARNWANQKSALGSALDPLADK..	AAH48702

Table.S1: Sequence alignment of CDP-alcohol-phosphotransferase motifs from representative proteins across the tree of life identifies the signature residues of PtdIns synthases. Conserved motifs of indicated sequences were predicted by Simple Modular Architecture Research Tool and then aligned by the CLC workbench. Proteins were chosen based on the CDP-alcohol-phosphotransferase motif shown in the top row. Organism abbreviations in the order of presentation are: *Tg, Toxoplasma gondii; Nc, Neospora caninum; Ef, Eimeria falciformis; Pb, Plasmodium berghei; Pf, Plasmodium falciparum; Tb, Trypanosoma brucei; Tc, Trypanosoma cruzi; Lm, Leishmania major; Cm, Cyanidioschyzon merolae; Cr, Chlamydomonas reinhardtii; Ot, Ostreococcus tauri; At, Arabidopsis thaliana; Os, Oryza sativa; Zm, Zea mays; Cg, Candida glabrata; Sc, Saccharomyces cerevisiae; Sp, Schizosaccharomyces pombe; Dm, Drosophila melanogaster; Dr, Danio rerio; Hs, Homo sapiens; Cp, Cryptosporidium parvum; Gs, Galdieria*

sulphuraria; Bs, Bacillus subtilis; Hp, Helicobacter pylori; Mt, Mycobacterium tuberculosis; Ec, Escherichia coli.

Protein names	Species	Accession Number
*Tb*ECT	*Trypanosoma brucei*	*Tb*927.11.14140
*Tc*ECT	*Trypanosoma cruzi*	*Tc*CLB.511727.120
*Lm*ECT	*Leishmania major*	*Lmj*F.32.0890
*Ef*ECT	*Eimeria falciformis*	*Efa*B_PLUS_7742.g777
*Pf*ECT	*Plasmodium falciparum*	*Pf*3D7_1347700
*Tg*ECT	*Toxoplasma gondii*	*Tg*GT1_310280
*Mm*ECT	*Mus musculus*	Q922E4 (Uniprot)
*Hs*ECT	*Homo sapiens*	Q99447 (Uniprot)
*Tb*ECT	*Trypanosoma brucei*	*Tb*927.10.12810)
*Tc*CCT	*Trypanosoma cruzi*	*Tc*CLB.509805.220
*Lm*CCT	*Leishmania major*	*Lmj*F.18.1330
*Ef*CCT	*Eimeria falciformis*	*Efa*B_PLUS_6035.g580
*Pf*CCT	*Plasmodium falciparum*	*Pf*3D7_1316600
*Tg*CCT	*Toxoplasma gondii*	*Tg*GT1_216930
*Mm*CCT	*Mus musculus*	P49586 (Uniprot)
*Hs*CCT	*Homo sapiens*	P49585 (Uniprot)

Table.S2: Sequence alignment of CCT/ECTs from representative proteins across the tree of life identified the conserved motifs of cytidylyltransferase in hypothetical *Tg*CCT/ECT. Sequences of protozoan parasites were obtained from EuPathDB, while the sequences of model organisms were extracted by using uniport. Conserved motifs of indicated sequences were predicted by InterProScan and then aligned by the CLC sequence viewer.

List of conferences and publications

Publications

Bingjian Ren and Nishith Gupta, Taming Parasites by Tailoring Them, ***Front Cell Infect Microbiol***. 2017 Jul 6;7:292

Holger Erler, **Bingjian Ren**, Nishith Gupta, and Eric Beitz, The Intracellular Parasite Toxoplasma gondii Harbors Three Druggable FNT-Type Formate and L-Lactate Transporters in the Plasma Membrane, ***Journal of Biological Chemistry.*** 2018 doi:10.1074/jbc.RA118.003801

Bingjian Ren, Pengfei Kong, Fatima Hedar,Jos Brouwers and Nishith Gupta, A novel Golgi-dwelling phosphatidylinositol synthase dependent on exogenous myo-inositol and endogenous CDP diacylglycerol is essential for the lytic cycle of Toxoplasma gondii, ***in submission***

Conferences

2017	The 14th Toxoplasma gondii research community biennial meeting, Tomar, Portugal **Poster,** Apicomplexan parasites, *Toxoplasma gondii* and *Eimeria falciformis*, induce and co-opt a master transcription factor c-Fos in the mammalian host cell
2018	14th International Congress of Parasitology (ICOPA), Daegu, Korea 1th **Oral presentation**, Transcription factor c-Fos is co-operated during infection of Apicomplexan *Eimeria falciformis* and *Toxoplasma gondii* 2nd **Oral presentation,** Identification of a novel phosphatidylinositol synthase in *Toxoplasma gondii*
2018	28th Annual Meeting of the German Society for Parasitology, Berlin, Germany

	Poster, Apicomplexan parasites, *Toxoplasma gondii* and *Eimeria falciformis*, induce and co-opt a master transcription factor c-Fos in the mammalian host cell
2019	The 15th Toxoplasma gondii research community biennial meeting, Quimbaya, Columbia
	Oral Presentation, CDP-ethanolamine pathway for PtdEtn biogenesis is required for sphingolipid synthesis

Acknowledgements

First of all, I would like to thank my supervisor Dr. Nishith Gupta, for offering me the chance to work together in his group and all the help and support during my Ph.D. It was a great pleasure to do the research with him and in his group. I would also express my thankfulness to Prof. Dr. Richard Lucius, for reviewing my dissertation and offering me the chance to come and join the Department of Molecular Parasitology after an enjoyable interview.

I want to thank Prof. Dr. Jos Brouwers, for reviewing my thesis and for being extremely patient in helping our conducting the lipidomic analysis. And the gratitude goes to Jeroen Jansen as well, for his expertise and assistance to finish the lipidomic analysis. I am grateful to Prof. Kai Matuschewski and Prof. Bang Shen for being part in my thesis committee, as well as their kindly suggestions and comments in different occasions, not only limited to the scientific research, but also concerning my future career. And to my dearest colleagues in MolPara, it was a great pleasure to be a member of you guys and work in the team. Special thankfulness to our technician Grit Meusel, Manuel Rauch and secretary Désirée Dzomo for being extremely helpful. Thank you Pengfei, Özlem, Xiaohan, Matthias, Richard, Arun, KimChi, Kai, Laura and Alex, for sharing the lab together with me. As a supervisor, I learnt a lot from my supervised students Annica, Annika, Anna, Beatrice, Florian, Julie and Ruben. It has been a great honor to share several months with you and thank you for being helpful to our projects. Thanks for Sonnenfeld-Stiftung for financial supporting for me to complete the Ph.D work.

I wish to express my deepest gratitude to my parents, for their unconditional supporting and understanding of my work. My faraway home has always been a warm shelter for me, and I believe it will still be. Last, I am expressing my thankfulness to Yi Li, for being my moonlight and tree at every cloudy night. This work described here can never be done without her. Thank you for always being with me.

Selbständigkeitserklärung

Hiermit erkläre ich an Eides statt, die vorliegende Dissertation selbstständig und angefertigt und keine anderen als die angegebenen Hilfsmittel verwendet zu haben.

Ort, Datum Unterschrift